

TURUN YLIOPISTON JULKAISUJA
ANNALES UNIVERSITATIS TURKUENSIS

SARJA - SER. A I OSA - TOM. 392

ASTRONOMICA - CHEMICA - PHYSICA - MATHEMATICA

**TAUTOMERISM AND FRAGMENTATION
OF BIOLOGICALLY ACTIVE HETERO
ATOM (O, N)-CONTAINING ACYCLIC
AND CYCLIC COMPOUNDS UNDER
ELECTRON IONIZATION**

by

Olli Martiskainen

TURUN YLIOPISTO
Turku 2009

From: Department of Chemistry
University of Turku
Turku, Finland

Supervisor: Professor (Emeritus) Kalevi Pihlaja
Department of Chemistry
University of Turku
Turku, Finland

Custos: Professor (Emeritus) Kalevi Pihlaja
Department of Chemistry
University of Turku
Turku, Finland

Reviewers: Professor Pirjo Vainiotalo
Department of Chemistry
University of Joensuu
Joensuu, Finland

Dr Pentti Oksman
Department of Chemistry
University of Oulu
Oulu, Finland

Opponent: Professor Dietmar Kuck
Faculty of Chemistry
Bielefeld University
Bielefeld, Germany

ISBN 978-951-29-3863-6 (PRINT)

ISBN 978-951-29-3864-3 (PDF)

ISSN 0082-7002

Painosalama Oy – Turku, Finland 2009

CONTENTS

Preface	5
Abstract	7
List of original publications	8
Abbreviations	9
1. INTRODUCTION	10
2. AIMS OF THE STUDY	12
3. TAUTOMERISM AND FRAGMENTATION MECHANISMS UNDER EI	13
3.1 Prototropic and non-prototropic tautomerism	13
<i>3.1.1 Prototropic tautomerism</i>	13
<i>3.1.2 Annular tautomerism</i>	14
<i>3.1.3 Non-prototropic tautomerism</i>	14
3.2 Other types of tautomerism	16
<i>3.2.1 Ring-chain tautomerism</i>	16
<i>3.2.2 Valence tautomerism</i>	17
3.3 Keto-enol tautomerism	17
<i>3.3.1 Some notes on keto-enol tautomerism and NMR</i>	17
<i>3.3.2 Some notes on substituent effects on keto-enol tautomerism</i>	18
<i>3.3.3 Keto-enol tautomerism in 2-phenacylpyridines [I] and 2-phenacylquinolines [VI]</i>	20
<i>3.3.4 Hammett substituent constants</i>	22
<i>3.3.5 Hammett substituent constants and quantitative structure–activity relationships</i>	24
<i>3.3.6 Biologically active heterocycles and pharmaceutical effects</i>	24
3.4 Fragmentation mechanisms in EIMS	27
<i>3.4.1 General aspects</i>	27
<i>3.4.2 Rearrangements in EIMS</i>	29
<i>3.4.2.1 Metastable ions and fragmentation pathways</i>	29
<i>3.4.2.2 Distonic ions</i>	30
<i>3.4.2.3 Rearrangements</i>	31
<i>3.4.3 CO-loss under EI</i>	32
<i>3.4.4 Retro-Diels-Alder fragmentation</i>	36
3.5 Mass spectrometry and keto-enol-tautomerism	38
<i>3.5.1 Some notes on MS and tautomerization</i>	38
<i>3.5.2 The tautomerization of molecular ions</i>	40
3.6 Materials and methods	42
<i>3.6.1 MS measurements</i>	42
<i>3.6.2 NMR measurements</i>	43
<i>3.6.3 Linear fits and structures of molecules</i>	43
<i>3.6.4 The compounds studied</i>	44
4. RESULTS AND DISCUSSION	45
4.1 2-Phenacylpyridines 1a–n [I] and 2-phenacylquinolines 2a–h [VI]	45

4.1.1	General fragmentations	45
4.1.2	Ions related to tautomers	50
4.1.3	Correlations with Hammett substituent constants for 2-phenacylpyridines 1a–n	52
4.1.4	Correlations with Hammett substituent constants for 2- phenacylquinolidines 2a–h	54
4.1.5	Comparison of the results for 1a–n and 2a–h	57
4.1.6	The CO loss from 2-phenacylpyridines 1a–n and 2-phenacylquinolines 2a–h	58
4.2	8-Aryl-3,4-dioxo-2H,8H-6,7-dihydroimidazo[2,1-c][1,2,4]tri- azines 3a–j [II]	60
4.3	Pyrrolo- and isoindoloquinazolinones 4–17 [III]	64
4.3.1	Structures and base peaks	64
4.3.2	Non-RDA-related stereospecific fragmentations	67
4.3.3	RDA related fragmentations	
4.4	Aryl- and benzyl-substituted 2,3-dihydroimidazo[1,2-a]pyrimi- dine-5,7-(1H,6H)-diones 18–21 [IV]	73
4.5	Naphthoxazine, naphthpyrrolo-oxazinone and naphthoxazino- benzoxazine derivatives 22–29 [V]	79
4.5.1	General fragmentations	79
4.5.2	Comparison of regioisomers	85
4.5.3	Effects of substituents	87
4.5.4	Fragmentations of 1-(α -aminobenzyl)- and 1-aminomethyl- 2-naphthol derivatives	88
5.	CONCLUSIONS	90
6.	REFERENCES	92

Preface

This thesis is based on work carried out at the Laboratory of Organic Chemistry and Chemical Biology, Department of Chemistry, University of Turku, since early 2005. The experimental work was carried out using mass spectrometer available at the Instrument Centre of the Department of Chemistry.

First I would like to thank my supervisor Professor Emeritus Kalevi Pihlaja for providing me the opportunity to work in the interesting field of mass spectrometry and structural chemistry and for guidance and support.

I also want to thank our collaborators Prof. Ryszard Gawinecki, Prof. Dariusz Matosiuk, Prof. (Emeritus) Géza Stájer and Prof. Ferenc Fülöp and their research groups in Poland and Hungary for synthesizing and providing the compounds studied.

I am grateful for the reviewing and constructive criticism provided by Prof. Pirjo Vainiotalo and Dr. Pentti Oksman.

I would like to thank the staff of the Instrument Center, Docent Petri Ingman, Kirsti Wiinamäki and Jaakko Hellman for nice work atmosphere and coffee company, and also other researchers and students from the University of Turku, Åbo Akademi and from other universities. Kirsti also helped in recording mass spectra and always provided the consumables for mass spectrometry, thank you for these years. I want to thank Doc. Vladimir Ovcharenko for first teaching me the basics of mass spectrometry. Also Markku Reunanen from Åbo Akademi has also given many useful tips regarding mass spectrometers. Also the technical staff of the Chemistry Department is greatly appreciated; special thanks go to Kari Loikas and Mauri Nauma for keeping the instruments and computers alive.

Doc. Jari Sinkkonen, Doc. Petri Tähtinen and Dr. Henri Kivelä have always been helpful in issues related to NMR and computational chemistry. We have also shared many

Preface

scientific and/or humorous discussions. Henri also recorded and analyzed the NMR spectra of some compounds.

I am thankful to Prof. Juha-Pekka Salminen and my “room-mate” Dr. Maarit Karonen, who have given many valuable practical tips. Also the company and friendship of other PhD students, Jaana Liimatainen, Anu Tuominen, Johanna Moilanen, Matti Vihakas and the former members of “Team Pihlaja”, is greatly appreciated. Thanks go also to other former and present personnel and students in the Laboratory of Organic Chemistry and Chemical Biology.

I am deeply grateful for funding from Magnus Ehrnrooth foundation, and for the financial support from Prof. Emeritus Kalevi Pihlaja, Prof. Harri Lönnberg and Doc. Petri Ingman for finishing the thesis. I am also grateful for travel funding from Palomaa-Erikoski foundation, and Graduate School of Organic Chemistry and Chemical Biology.

I would like to thank “Team Utö” and “Minigolf & Bowling Buddies” and other friends. I want to thank also my mother Marja-Leena, for supporting and believing in me all these years.

Turku, March 2009

Olli Martikainen

Abstract

In this thesis a total of 86 compounds containing the hetero atoms oxygen and nitrogen were studied under electron ionization mass spectrometry (EIMS). These compounds are biologically active and were synthesized by various research groups. The main attention of this study was paid on the fragmentations related to different tautomeric forms of 2-phenacylpyridines, 2-phenacylquinolines, 8-aryl-3,4-dioxo-2H,8H-6,7-dihydroimidazo-[2,1-c][1,2,4]triazines and aryl- and benzyl-substituted 2,3-dihydroimidazo[1,2-*a*]pyrimidine-5,7-(1*H*,6*H*)-diones. Also regio/stereospecific effects on fragmentations of pyrrolo- and isoindoloquinazolinones and naphthoxazine, naphthpyrrolo-oxazinone and naphthoxazino-benzoxazine derivatives were screened. Results were compared with NMR data, when available.

The first part of thesis consists of theory and literature review of different types of tautomerism and fragmentation mechanisms in EIMS. The effects of tautomerism in biological systems are also briefly reviewed.

In the second part of the thesis the own results of the author, based on six publications, are discussed. For 2-phenacylpyridines and 2-phenacylquinolines the correlation of different Hammett substituent constants to the relative abundances (RA) or total ion currents (% TIC) of selected ions were investigated. Although it was not possible to assign most of the ions formed unambiguously to the different tautomers, the linear fits of their RAs and % TICs can be related to changing contributions of different tautomeric forms. For dioxoimidazotriazines and imidazopyrimidinediones the effects of substituents were rather weak.

The fragmentations were also found useful for obtaining structural information. Some stereoisomeric pairs of pyrrolo- and isoindoloquinazolines and regiomeric pairs of naphthoxazine derivatives showed clear differences in their mass spectra. Some mechanisms are suggested for their fragmentations.

List of original publications

This thesis is based on the following publications that are referred to in the text by their Roman numerals. Some unpublished results are also presented in the text.

[I]. Olli Martiskainen, Ryszard Gawinecki, Borys Ośmiałowski and Kalevi Pihlaja. “Electron ionization mass spectra and tautomerism of 2-phenacylpyridines”, *Eur. J. Mass Spectrom.*, 2006; **12**: 25–29.

[II]. Olli Martiskainen, Krzysztof Sztanke, Dariusz Matosiuk and Kalevi Pihlaja. “Electron ionization mass spectra of 8-aryl-3,4-dioxo-2*H*,8*H*-6,7-dihydroimidazo[2,1-*c*][1,2,4]triazines. Do they exhibit tautomerism in the gas phase?”, *Rapid Commun. Mass Spectrom.*, 2006; **20**: 2548–2552. *ERRATUM Rapid Commun. Mass Spectrom.*, 2006; **20**: 3163.

[III]. Kalevi Pihlaja, Olli Martiskainen and Géza Stájer. “Does the electron ionization induced fragmentation of partly saturated stereoisomeric pyrrolo- and isoindoloquinazolinones show stereospecificity?” *Rapid Commun. Mass Spectrom.*, 2007; **21**: 653–660.

[IV]. Olli Martiskainen, Henri Kivelä, Dariusz Matosiuk, Elzbieta Szacon, Marzena Rzadkowska and Kalevi Pihlaja. “Electron ionization mass spectra of aryl- and benzyl-substituted 2,3-dihydroimidazo[1,2-*a*]pyrimidine-5,7(1*H*,6*H*)-diones”, *Rapid Commun. Mass Spectrom.*, 2007; **21**: 3891–3897.

[V]. Olli Martiskainen, Ferenc Fülöp, István Szatmári and Kalevi Pihlaja. “Electron Ionization Mass Spectra of Naphthoxazine, Naphthpyrrolo-oxazinone and Naphthoxazinobenzoxazine Derivatives”, *ARKIVOC*, 2009; (iii): 115–129.

[VI]. Olli Martiskainen, Ryszard Gawinecki, Borys Ośmiałowski, Kirsti Wiinamäki and Kalevi Pihlaja. “Electron ionization mass spectra and tautomerism of substituted 2-phenacylquinolines”, *Rapid Commun. Mass Spectrom.*, 2009; **23**: 1075–1084.

Article [I], Copyright © 2006 IM Publications, reprinted with permission. Articles [II], [III], [IV], [VI], Copyrights © 2006, 2007, 2009, respectively, John Wiley & Sons Ltd, reproduced with permission. Article [V], Copyright © 2009 Arkat USA Inc., reprinted with permission.

Abbreviations

Ar	aryl group
CID	collision induced dissociation
DMSO	dimethyl sulfoxide
DNA	deoxyribonucleic acid
EI	electron ionization
EIMS	electron ionization mass spectrometry
FFR	field-free region
GC	gas chromatography
IR	infrared
KER	kinetic energy release
MIKE	mass-analyzed ion kinetic energy
MS	mass spectrometry
NOESY	nuclear Overhauser effect
NMR	nuclear magnetic resonance
Ph	phenyl group
Py	pyridine
QET	quasi-equilibrium theory
QSAR	quantitative structure–activity relationship
Qui	quinoline
RA	relative abundance
RDA	retro-Diels-Alder
RNA	ribonucleic acid
TIC	total ion current
UV	ultraviolet

1. INTRODUCTION

The structural properties of various heterocyclic compounds have been subjected to under extensive study at the University of Turku for a considerable time. This structural information is needed during the investigation of biochemical reactions or in searches for new compounds with pharmaceutical properties.

Theoretical calculations, nuclear magnetic resonance (NMR), gas chromatography (GC), high-performance liquid chromatography (HPLC), ultraviolet (UV) and infrared (IR) spectroscopies and mass spectrometry (MS) all give information about the structures of organic molecules. Stereoisomeric and regioisomeric fragmentations are important in the MS analysis of organic compounds, e.g. when synthesized molecules are to be identified, or the purity of isomeric samples is to be determined.

MS methods can be applied to the study of tautomerism in the gas phase. Tautomers are interconvertible structural isomers. Tautomerism should not be confused with resonance; resonance structures differ in the positions of electrons, whereas tautomerism involves the movement of H or another atom and may result in changes in molecular geometry. Tautomerism can affect chemical reactions; as an example, the oxidation of a ketone by a strong oxidizing agent can proceed via tautomerization to the enol [1]. In solution, enolization is enhanced by acid or base catalysis. Tautomeric equilibria can be shifted to favor one of the tautomers through the use of different substituents with electron-donating or electron-accepting properties. Tautomerism can be important in biochemical reactions, even though the relative amount of the reactive tautomer may be small, an example being the base pairing in deoxyribonucleic acid (DNA) or ribonucleic acid (RNA) [2,3]. Different tautomers may also have different pharmaceutical effects.

The amounts of the distinct tautomers can vary appreciably in the different states. Tautomeric equilibria can be studied with the aid of X-ray diffraction, UV and IR spectroscopy in the solid state, and NMR and UV spectroscopic methods in solution or in the liquid state. Theoretical calculations can be applied to calculate the heats of formation

and hence compare the stabilities of different tautomers in the gas phase. One useful method with which to gain information about tautomerism in the gas phase is electron ionization MS (EIMS). If the tautomeric system is transferred into the gas phase, external factors such as solvents and intermolecular interactions can be excluded and the process becomes unimolecular [4].

2. AIMS OF THE STUDY

The aim of this study was to apply EIMS to obtain information on the tautomeric equilibria and structures of heterocyclic or acyclic compounds containing the hetero atoms O and N in the gas phase. Attention was paid in particular to the effects of different substituents and various competitive fragmentation routes. The compounds studied possess potential pharmacological activity.

3. TAUTOMERISM AND FRAGMENTATION MECHANISMS UNDER EI

3.1 Prototropic and non-prototropic tautomerism

3.1.1 Prototropic tautomerism

Prototropic tautomerism involves the relocation of an H atom and a double bond. One example of prototropic tautomerism is that between keto and enol forms (Fig. 1). The keto tautomer possesses a CO group, while the enol form has a vinylic alcohol structure. Increasing acidity of the α -H affects this tautomerism, favoring the enol form. Conjugated double bonds and intramolecular H-bonds can also stabilize the enol form.

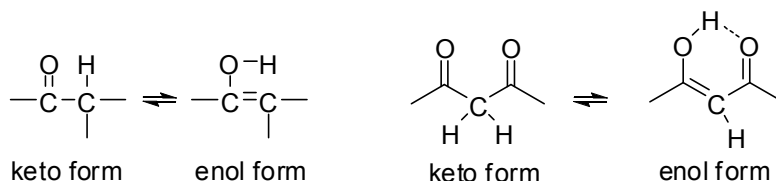


Figure 1. Keto-enol tautomerism and stabilization of the enol form through the intramolecular H-bonding.

Other types of prototropic tautomerism are amine-imine tautomerism (e.g. in adenines [5], amide-imidic acid tautomerism (related to asparagine-linked glycosylation [6]) and, as a special case, lactam-lactim tautomerism (present in uracil and thymine [7]) (Fig. 2).

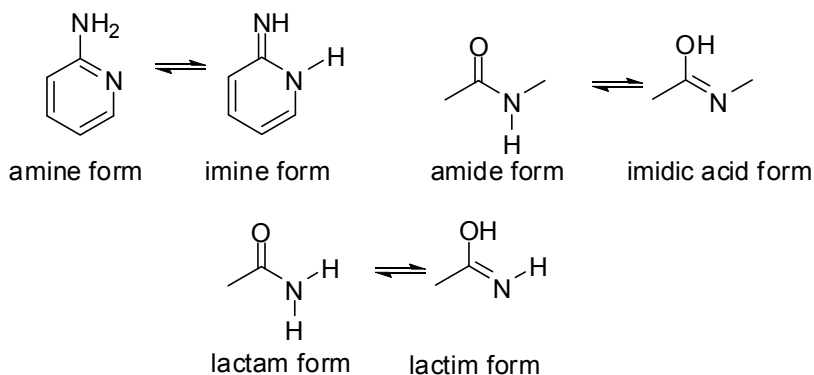


Figure 2. Other types of prototropic tautomerism.

Prototropic tautomerism can be studied by MS if the fragmentation patterns of the tautomers are different [4,8]. The tautomeric studies in this work are limited to prototropic tautomerism.

3.1.2 Annular tautomerism

This is a special case of prototropic tautomerism, where an H can occupy two or more possible locations in a heterocyclic system, e.g. indazole, which can have $1H$ and $2H$ tautomers. (Fig. 3) [9,10].

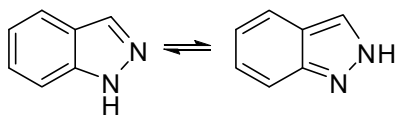


Figure 3. $1H$ and $2H$ tautomers of indazole.

3.1.3 Non-prototropic tautomerism

Non-prototropic tautomerism involves the relocation of a substituent other than H, e.g. the tautomerism of 1- and 2- $(N,N$ -disubstituted aminomethyl)benzotriazoles (Fig. 4) [11].

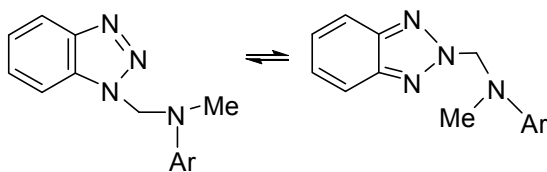


Figure 4. Non-prototropic tautomerism between 1- and 2-(*N,N*-disubstituted aminomethyl)benzotriazoles.

Other forms of non-prototropic tautomerism include acylotropism (transfer of acyl group), methylotropism (transfer of a Me group) and aroylotropism (transfer of an Ar group), transfer of N groups and elementotropism (transfer of halogens and metals).

Elementotropism includes chlorotropism (transfer of a Cl), and metallotropism (transfer of a metal atom or a metal-containing group) [12,13].

Elementotropic migrations are very fast, which is often indicated by narrow averaged signals in the ^1H NMR spectra. Differentiation of these tautomers by MS is therefore usually impossible. However, the slow migration of substituents on C atoms can make it possible to differentiate non-prototropic tautomers. One example where MS has been successfully applied is the isomerization of mercaptotetrazole to aminothiatriazole (Fig. 5) [14].

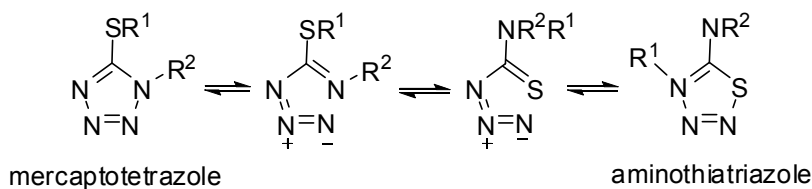


Figure 5. Isomerization of mercaptotetrazole to aminothiatriazole.

3.2 Other types of tautomerism

3.2.1 Ring-chain tautomerism

In ring-chain tautomerism, a structural change occurs between an open-chain form and a ring form through an H-transfer. This is an important process for monosaccharides such as sugars. Glucose is a well-known example (Fig. 6), which can exist in five different tautomeric forms in solution. Ring-chain tautomerism was first discovered by Emil Fischer in the 1890s.

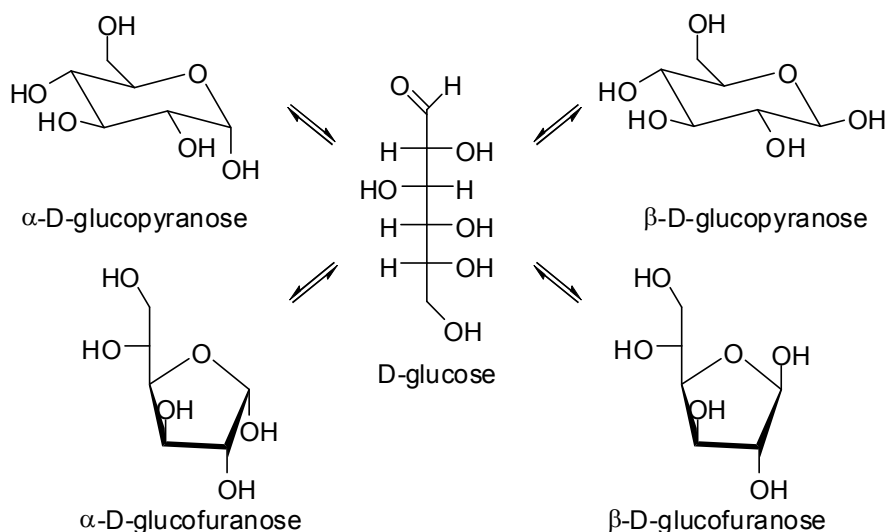


Figure 6. The open-chain and ring tautomers of glucose.

Mass spectrometry has proved to be a relatively successful method for identification of the ring and open-chain tautomers of organic compounds, because the fragmentations of the molecular ions of the different tautomers often differ considerably [4]. The ring-chain tautomerism of 1,3-*O,N*-heterocycles has been studied quite extensively with EIMS [15a-g].

3.2.2 Valence tautomerism

Valence tautomerism involves the reorganization of bonding electrons, which results in changes in molecular geometry. A classical example is the tautomerism between 1,3,5-cyclo-octatriene and bicyclo[4.2.0]octa-2,4-diene (Fig. 7) [16]. Another example of valence tautomerism is bullvalene, with 1,209,600 possible tautomers [17,18]. The rapid Cope rearrangements of bullvalene cause all the H atoms and all the C atoms to be

equivalent and only one line is seen in the high-temperature ^1H NMR spectrum [19]. A further example of valence tautomerism is azide-tetrazole tautomerism [20]. The latter has been studied by EIMS with varying success [21].

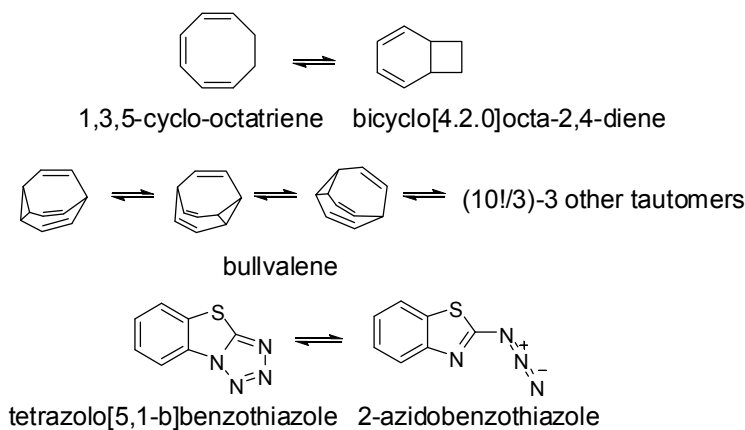


Figure 7. Examples of valence tautomerism.

3.3 Keto-enol tautomerism

3.3.1 Some notes on keto-enol tautomerism and NMR

Although the studies involved the use of EIMS, the results were compared with information obtained with NMR, which necessitates a brief discussion of the identification of tautomers via NMR methods.

Calculation of the relative amounts of keto and enol tautomers are based on the integral intensities of the signals of H atoms α to CO group (-CH₂-CO). For 2-phenacylpyridines and 2-phenacylquinolines, the hydrogen exchange in solution is slow because in one of the tautomers the H is bound to a neutral C atom. However, the hydrogen exchange is not too slow to enable the differentiation of tautomers through the ¹⁵N and ¹³C chemical shifts [22a,23,24].

In the case of fast H transfer between the individual tautomers, each nucleus gives only one averaged signal. If the tautomers contain strongly electronegative basic centers such as O and N, integration of the ¹H NMR signals with a view to estimating the amounts of tautomers is useless [25].

In 8-aryl-3,4-dioxo-2*H*,8*H*-6,7-dihydroimidazo[2,1-*c*][1,2,4]triazines, the occurrence of amide-imidol tautomerism can be expected, but this requires H transfer between two basic centers. The ¹H NMR signal for an enolic/imidic H is slightly broadened, and the signal at 11.42-11.89 ppm for this rather acidic H indicates that the equilibrium in solution favors the 3-oxo form rather than the 3-hydroxy form [26].

3.3.2 Some notes on substituent effects on keto-enol tautomerism

The acidity of an H α to the CO group is an important factor in keto-enol tautomerism. The keto form is usually more favored and the enol form is rapidly tautomerized back to the keto form. The more acidic the H, the more the equilibrium favors the enol form. The solvent polarity also strongly affects the keto-enol equilibrium [27], polar solvents generally favoring the keto form and apolar solvents the enol form. If the H is α to two CO groups, the enol form becomes more favored because of the inductive electron withdrawal of the two CO groups (Fig. 8).

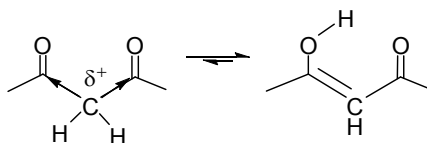


Figure 8. The inductive electron-withdrawal of two CO groups.

The tautomerism also depends on changes in π -electron conjugation. Conjugated double-bonds help to stabilize the enol form. Another stabilizing factor is the formation of internal H-bonds [28]. Steric crowding between the CO group and the substituents may affect the relative amounts of the tautomers, as does the electrostatic repulsion between two polar functionalities. This was observed in the tautomeric equilibria of cyclic α -nitro ketones [29].

Electron-accepting groups destabilize the keto form and stabilize the enol form by electron delocalization. This is seen, for example, in the enolization of 3-nitrobutan-2-one

in comparison with 2-butanone [30]. The substituents attached to aromatic groups affect the conjugated system with resonance and inductive effects by repelling (electron-donating groups or electron donors) or attracting electrons (electron-accepting groups or electron acceptors) (Fig. 9).

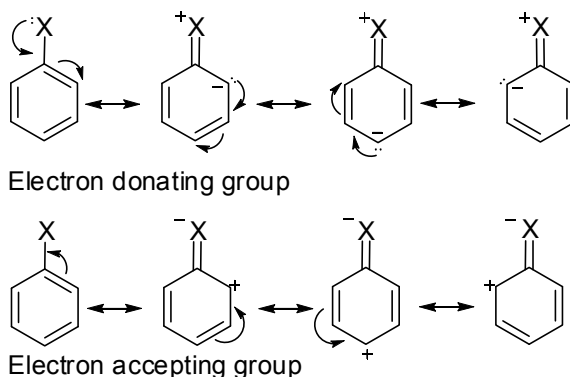


Figure 9. Effect of electron donating and electron accepting groups on the aromatic ring.

3.3.3 Keto-enol tautomerism in 2-phenacetylpyridines [II] and 2-phenacetylquinolines [VI]

The two series of compounds studied which most probably exhibit keto-enol tautomerism were 2-phenacetylpyridines and 2-phenacetylquinolines.

2-Phenacetylpyridines (**K**, ketimine form) are in equilibrium with (*Z*)-2-(2-hydroxy-2-phenylvinyl)pyridines (**O**, enolimine form). The third possible tautomer (**E**, enamionone form) is not detected in CDCl₃ solution [23] or in aqueous solution [31,32]. The presence of an intramolecular H-bond stabilizes form **O** [33]. With different substituents the amount of form **K** in CDCl₃ solution varies from the 99% for electron-donating substituents to 7.8% for electron-accepting substituents [23]. This wide range makes 2-phenacetylpyridines ideal for a study in the gas phase, because at least the compounds containing the strongest electron-donating or accepting groups may be expected to furnish different mass spectrometric fragmentations.

In the presence of a strong electron-donating substituent in the aromatic ring form **K** of 2-phenacetylpyridines or -quinolines can attain the mesomeric form **K'** besides form **K** form (**K**↔**K'**) Similarly, forms **E** and **O** have mesomeric forms **E'** and **O'**, respectively (Fig. 10) [23]. However, the increased stabilization of forms **E'** and **O'** by H-bonding is contrasted by the lost aromaticity of both the benzene ring and the pyridine (Py) ring (in 2-phenacetylpyridines) or the quinoline (Qui) ring (in 2-phenacetylquinolines). In form **K'** the Py and Qui rings remain aromatic [34]. Form **E** which has no possibility for an internal H-bonding (e.g. in 2-ketomethylquinolines [35]) is usually less stable than form **K**. Electron-accepting substituents make the methylene H atoms adjacent to the CO group more acidic and their transfer to *aza* atoms becomes more favorable [34].

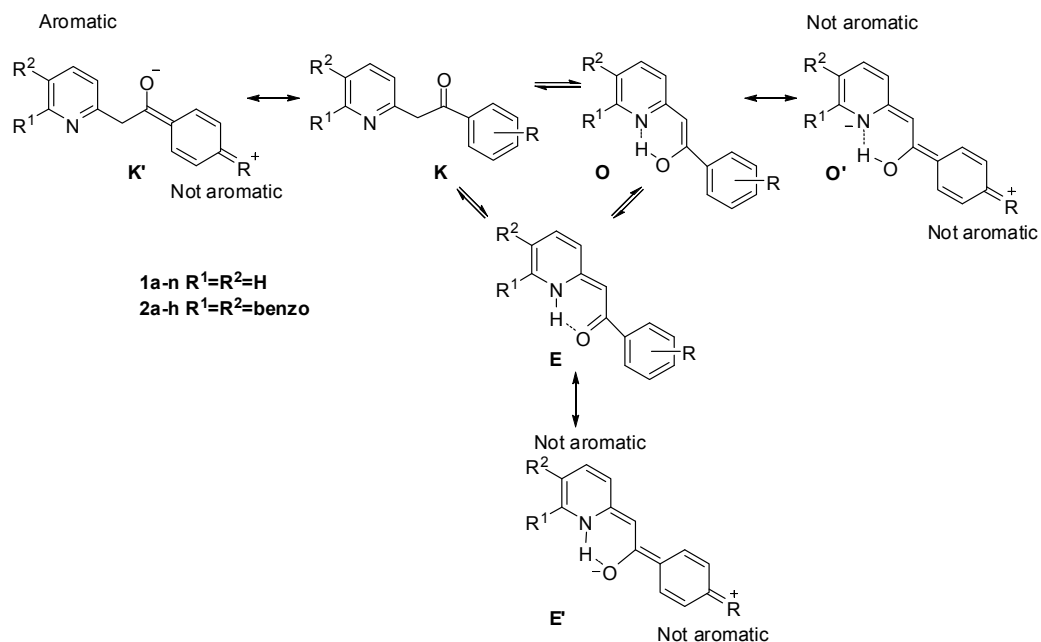


Figure 10. The stabilizing effect of the electron-donating substituent on ketimine form **K** and its destabilizing effect on enaminone forms **E'** and **O'**.

On the other hand, benzo-annelated 2-phenacylquinolines do not prefer tautomer **K** since its amount in solution is clearly less than for 2-phenacylpyridines, the maximum value being 39.3% for the *p*-N(CH₂)₄-substituted compound (in CDCl₃ solution, 303 K) [24]. X-ray crystallographic studies reveal only the presence of form **E** in the solid state [22a]. The effect of an intramolecular H-bond on form **E** stronger than that of an electron-donating substituent on form **K**. Although the intramolecular H-bonding in form **E** is weaker than that in form **O**, the π -electron delocalization is more effective in the former [34].

The theoretical heats of formation of forms **E** and **K**, based on AM1 calculations [22b] for some of the 2-phenacylquinolines studied [22a], are valid for isolated molecules in the gas phase. Thus, the *p*-F-, *p*-Cl-, *m*-F- and *p*-CF₃-substituted 2-phenacylquinolines prefer form **E** in the gas phase. AM1 calculations reveal that form **K** has a lower heat of formation than that of form **E** in the cases of the *p*-NMe₂, *p*-OMe, *p*-Me and *m*-Me

derivatives [22a]. Form **E** is therefore expected to be present in compounds with electron-accepting substituents under mass spectrometric conditions.

3.3.4 Hammett substituent constants

The Hammett constants σ were first obtained from the ionization of organic acids in solution. They are defined as:

$$\sigma = \log K - \log K_0$$

where K_0 is the ionization constant of benzoic acid and K is the corresponding constant for *m*- (σ_m) or *p*-substituted benzoic acid (σ_p). These constants have been successfully used to compare the electronic effects of substituents on the rates and equilibria of organic reactions [36]. Taft extended these principles to polar, steric and inductive and resonance effects [37-40].

The substituents may push or pull electrons inductively or by resonance. The substituent constants σ_p and σ_m can be split into field/inductive (σ_I) and resonance (σ_R) components [38]:

$$\sigma_p = \sigma_I + \sigma_R$$

The field effect is the phenomenon that a charge separation will influence the energy associated with the development of charge elsewhere in the molecule as a result of through-space electrostatic interactions. The inductive effect means a transmission of bond dipoles through the intervening bonds by successive polarization of each bond. The field and inductive effects together are regarded as polar effects, expressed by substituent constant σ_F [41]. However, the field effect outweighs the inductive effect [42,43]. Accordingly, σ_I is mainly due to the field effect component [44].

There are various ways to establish σ_I , such as the use of ionization constants for bicyclo-octane carboxylic acids [45] or quinuclidines [46]. The tabulated σ_I ($\equiv F$) values are calculated from the results of the above two methods [47].

For the resonance effect parameter R ($\equiv \sigma_R$), Swain and Lupton [48] made the assumption that

$$\sigma_p = \alpha\sigma_I + \sigma_R$$

The coefficient α does not differ much from 1 [47], and thus the resonance effect parameter σ_R can be expressed as

$$\sigma_R = \sigma_p - \sigma_I$$

This definition of σ_R applies only to *para* substituents. The difference between σ_m and σ_p for a given substituent is due to the possible difference between inductive (σ_I) and resonance (σ_R) effects. The sensitivity to resonance effects is much larger for *para* than for *meta* substituents [48]. Resonance contributions are present mainly with *ortho* and *para* substituents, but *ortho* substituents are excluded from the Hammett treatment because of steric effects [41]. Despite the fact that in general the resonance effects cannot be taken as equal to zero, the constants for *meta* substituents are close to the field/inductive parameters ($\sigma_m \approx \sigma_I$).

Other contributions to the Hammett substituent constants are made by polarizability (σ_a) and electronegativity (σ_e) effects [49]. However, in this work only the resonance and field/inductive effects on tautomerism will be discussed.

When substituents are conjugated with a reaction center, the correlations with σ_p are poor. σ^+ constants were developed therefore for better representation of electrophilic reactions where strong resonance occurs between electron-donating substituents and positively charged reaction centers [50]. The positive charge may be located in the aromatic ring and the conjugated substituent helps to delocalize the charge. Correspondingly σ^- constants are used for reactions where the substituent delocalizes the negative charge. In literature the σ_p^- constants differ from σ_p only for substituents that can accept electrons by resonance (such as NO_2 and CN) and conversely σ_p^+ constants differ only for electron donating substituents (such as NH_2 or OMe) [48].

The σ_p^+ and σ_p^- values can be used to define resonance constants R^+ and R^- . However the R^- values for strong π -donating substituents are questionable as a result of strong conjugation with electron-rich reaction centers [47]. Also for strong π -electron-accepting groups with π -electron deficient centers R^+ values are uncertain [49].

3.3.5 Hammett substituent constants and quantitative structure–activity relationships (QSARs)

Hammett functions are among the variables used to study QSARs. In some cases, the constants σ have been correlated with biological activity. The biological activity of benzenesulfonamides against *Escherichia coli* and *Mycobacterium smegmatis* proved to be correlated with σ [51], as was that of 2-hydroxy-6-methyl-7-arylamino-1,7-dihydropurin-8-one against *Agrobacterium tumefaciens* and *Arthobacter globiformis* [52]. For diethyl phenyl phosphates, a correlation was found between the inhibition of insect cholinesterase and σ [53]. However, in general problems arise with the application of Hammett-type relationships to biological systems. This is because biological systems are also affected by other factors, one of the most important being lipophilicity [54a]. Lipophilicity is predicted by $\log P$, where P is the partition coefficient, i.e. the ratio of the concentration of a compound as a neutral molecule in a hydrophobic organic solvent (octanol) to its concentration in the aqueous phase [54b].

3.3.6 Biologically active heterocycles and pharmaceutical effects

In many biological and enzymatic processes, the rate-determining step is H-transfer [55]. Thus, the minor tautomeric forms of natural bases may play an important role in substitution mutagenesis during DNA replication, i.e. the mutation caused by the pairing of wrong base pairs [56,57]. This “rare tautomer hypothesis” is strengthened by the experimental evidence of a direct correlation between the tautomeric constant ($K_T = [\text{amino}]/[\text{imino}]$) and the preferred nucleotide incorporation by the Klenow polymerase [58]. Theoretical calculations on a base-pair analog *N*-methyl-P (6-methyl-3,4-dihydro-

8*H*-pyrimido[4,5-*c*][1,2]oxazin-7-one) additionally point to the role of rare tautomers in mutagenesis during DNA replication [59].

Enaminones (i.e. β -enaminones, compounds containing the conjugated system N-C=C-C=O), which are possible pro-drugs [60-62] and therefore important intermediates in organic synthesis, have also been reported to possess biological activity [63,64]. They are interesting model compounds, with two basic centers and three possible tautomers. Some 2-phenacylpyridines have been noted to have anti-bacterial properties [65]. Enaminones are used as intermediates in the synthesis of biologically active compounds, such as oxytocin antagonists or compounds with anti-epileptic, molluscicidal or larvicidal activities [66,67]. In this work, two series of compounds, phenacylpyridines and phenacylquinolines, with possible enaminone and enolimine tautomers were subjected to an EI study.

Fused imidazoline ring systems containing dioxo groups have been found to exert analgesic opioid-like action without narcotic analgesic side-effects. The presence of two polar CO groups and one hydrophobic moiety has been suggested to be responsible for serotonergic activity, reducing the “head twitch” episodes in mice after 5-hydroxytryptophan administration [68]. In the 8-aryl-3,4-dioxo-2*H*,8*H*-6,7-dihydroimidazo[2,1-*c*][1,2,4]triazines studied in this work, amido-imido tautomerism is possible. The tautomeric equilibrium has been observed to affect pharmacological activity. In aqueous solution the *p*-Cl-substituted compound favors the enol form, and the *m*-Cl-substituted one the keto form [26]. The *p*-Cl compound displays a serotonergic effect and also acts on the opioid receptors. On the other hand, the *m*-Cl compound has an antinociceptive effect, i.e. it reduces sensitivity to painful stimuli (Fig. 11). The *p*-Cl compound exists mainly in the 3-hydroxy form, and accordingly transformation of the 3-oxo group to a 3-hydroxy group is the main factor affecting the activity [26]. This conflicts with the earlier model of the two oxo groups influencing the serotonergic receptors, and means that the models for opioid and serotonergic activity require adjustment.

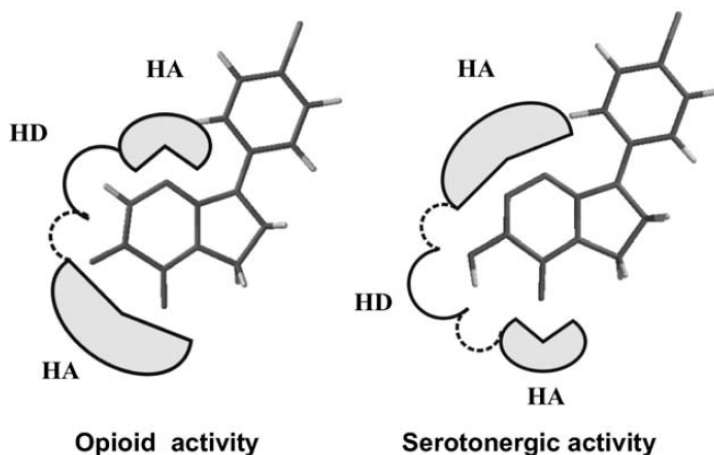


Figure 11. Possible H-bond-acceptor (HA) and donor (HD) interaction sites for opioid activity and serotonergic activity of 8-(4-chlorophenyl)-3,4-dioxo-2*H*,8*H*-6,7-dihydroimidazo[2,1-*c*][1,2,4]triazine [69]. Copyright © Elsevier 2004, reproduced with permission.

The 8-aryl-3,4-dioxo-2*H*,8*H*-6,7-dihydroimidazo[2,1-*c*][1,2,4]triazines also have other possible pharmaceutical applications. The *p*-Cl derivative displays high potency for the inhibition of LS180 human Caucasian colon adenocarcinoma cells, HeLa Negroid cervix epitheloid carcinoma and A549 human Caucasian lung cancer cells. The *m*-Cl derivative inhibits HeLa cancer cells relatively strongly, but is completely inactive against LS180 and A549 cells. These differences are suggested to arise from the more lipophilic ($\log P = 1.28$) nature of the electron-withdrawing substituent *p*-Cl [69].

Ar- and benzyl-substituted 2,3-dihydroimidazo[1,2-*a*]pyrimidine-5,7(1*H*,6*H*)-diones [70] are structural modifications resembling 8-aryl-3,4-dioxo-2*H*,8*H*-6,7-dihydro-imidazo[2,1-*c*][1,2,4]triazines. The *o*-MeO substituent has been observed by X-ray diffraction to exist only as the 5-oxo/7-OH tautomer in the solid state [71]. These compounds may also have pharmacological effects.

Cyclohexane/ene-fused pyrimido[2,1-*a*]isoindol-6-ones are of pharmacological importance because their starting synthons and analogs exhibit biological effects and are

applicable in therapy. Quinazolinone derivatives may have hypnotic and sedative properties, and may be useful as analgesics, sedatives and hypertensives [72,73].

3.4 Fragmentation mechanisms in EIMS

3.4.1 General aspects

The formation of molecular ions follows the Franck-Condon principle [74], i.e. the ionization is a fast vertical process. When an electron transition caused by an electron beam or a photon beam occurs, the time for the transition is extremely short compared to the vibration between the atoms, and therefore the structure of the molecule does not change during the ionization.

Mass spectral fragmentations are well explained by the quasi-equilibrium theory (QET), at least when the impact energy is sufficiently higher than the appearance energy or the molecules are not very small [75]. The fragmentation takes a longer time than the redistribution of energy to the different degrees of freedom. It requires the conversion of internal electronic energy acquired during ionization into vibrational and rotational energies [76a]. When the oscillating molecular ion has a sufficient amount of energy it undergoes the fragmentation reaction. The fragments may have sufficient energy to dissociate through a similar sequence of events, and the rearrangements of bonds may also occur [76b]. Another theory similar to the QET, but for neutral molecules, is the Rice-Ramsperger-Kassel-Marcus theory of unimolecular gas reactions in which the rate at which the energized reactant molecule breaks down is treated as a function of the energy that it contains, and the normal-mode vibrations and rotations too are taken into account [77].

The EI fragmentation of the molecular ion produces a positively charged ion and a neutral fragment (radical or molecule). Typical EI fragmentations result from a single-bond cleavage where a radical is lost from the molecular ion via a σ -bond, homolytic or

heterolytic cleavage. In an odd-electron ion the σ -bond cleavage can also lead to two sets of ion-radical products:



According to Stevenson's rule the positive charge will preferably stay at the fragment with lowest ionization energy. The fragment with higher ionization energy will be the less abundant ion in the spectrum. The lowest-energy ion is most stable and therefore most abundant [78]. One of the exceptions to this rule is the loss of the largest alkyl radical at a reactive site i.e. the site of ionization, which may result in the least stable, but abundant ions. Such fragmentations can be observed for aliphatic hydrocarbons with the loss of large alkyl radicals (Fig. 12) [79a].

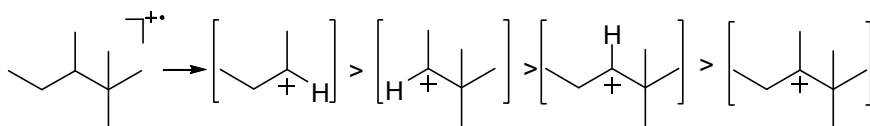


Figure 12. The favored fragmentations of 2,2,3-trimethylpentane, which do not obey Stevenson's rule.

In the homolytic cleavage of a molecular ion, an electron from a pair between two atoms moves to form a pair with the odd electron. The atom that possesses the charge will retain the charge after ionization, and a radical is lost. A special case of homolytic cleavage is α -cleavage (radical-site-driven cleavage), where the unpaired electron forms a new bond to an adjacent atom and another bond to this atom is cleaved. The new bond formed compensates the cleaved bond energetically (Fig. 13) [76a].

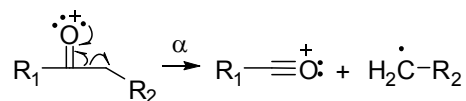


Figure 13. A special case of homolytic cleavage in a ketone (α -cleavage).

Heterolytic cleavage (charge-site-driven or inductive cleavage) involves the movement of a pair of bonding electrons to the charged site. As a result, the charged site moves to the adjacent atom. A radical is lost as a result of fragmentation (Fig. 14) [76a,80].

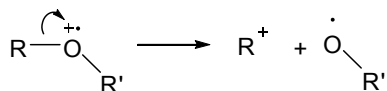


Figure 14. Heterolytic cleavage in an ether.

If a favorable product site exists for the unpaired electron, this can make the reaction pathway more important. Radical stabilization is improved by delocalization (allyl radical), increased branching (*t*-Bu radical) or electronegative sites such as O (alkoxyl radical). The neutral products may also be small molecules, such as H₂, CH₄, H₂O, C₂H₄, CO, NO, CH₃OH, H₂S, HCl, CH₂CO or CO₂ [79a]. The loss of neutral molecules occurs via direct dissociations or rearrangements.

3.4.2 Rearrangements in EIMS

3.4.2.1 Metastable ions and fragmentation pathways

Typical fragmentations of ions occur in the ion source within 10⁻⁷ s after their formation. Metastable ions dissociate after leaving the ion source and before arriving at the detector. Metastable ions can be detected in the field-free regions (FFRs) of the MS instrument. The typical dissociation time of a metastable ion is 10⁻⁴–10⁻⁶ s.

Metastable ions can offer information on fragmentation pathways. In the normal mass spectra, metastable ions were originally observed as small wide peaks at an apparent mass m^* :

$$m^* = \frac{m_2^2}{m_1}$$

where m_1 = mass of the precursor ion and m_2 = mass of the product ion. The ions are presumed to have a single charge ($z_1 = z_2 = 1$). In theory, m^* can be used to calculate the masses for product ions. However, the abundance of metastable ions is often too low to be seen in the normal mass spectra, so pathways are nowadays solved by using better methods.

For a double-focusing mass spectrometer, the metastable transitions can be utilized by linked scans. The product ions formed from a selected precursor ion can be identified by keeping the ratio of the magnetic field B and the electrostatic field strength E constant; this experiment is known as a linked scan at constant B/E [81a]. Similarly, the precursor ions of selected product ions can be identified with a linked scan at constant B^2/E [81a]. The fragmentation of precursor ions can be made more efficient and variable by increasing the internal energy with a collision cell in the FFRs by introducing a collision gas, such as He. This method is called collision-induced dissociation (CID) [81b].

3.4.2.2 Distonic ions

Distonic radical ions are odd electron ions in which the radical and charge sites are separated. They are important intermediates and products in dissociation reactions of organic molecules. Distonic ions result from rearrangements, such as H-migration. They can also be formed via ring opening. X- and γ -ray radiation too have been observed to produce distonic radical cations [82a]. Some simple routes to distonic ions are presented in Fig. 15 [82a].

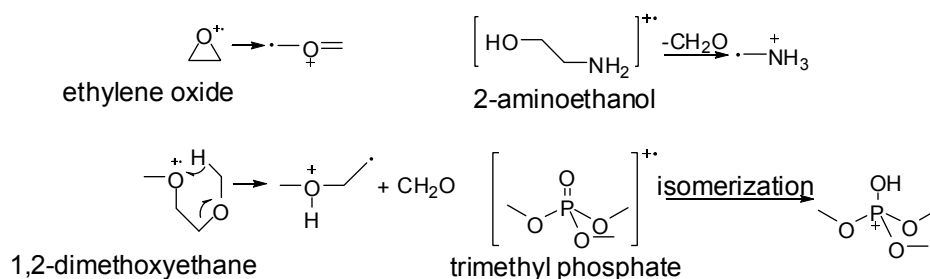


Figure 15. Examples of formation of distonic ions.

3.4.2.3 Rearrangements

Rearrangement reactions make the mass spectra more complex to interpret, but they may also yield information on stereochemical and structural problems. Gas-phase radical cations that have low internal energy often dissociate via rearrangement processes. Rearrangements tend to be reactions with low activation energies, while simple cleavages require higher energies [83a-b]. The ions from rearrangements can be very abundant in EI spectra, because of their low activation energies [83c]. Rearrangements are usually associated with multiple-bond cleavages and the formation of new bonds, which requires a favorable conformation. Due to the large negative activation entropies, the rearrangement reactions are slower than simple cleavage reactions [83b-c], and they may therefore occur in the metastable ion time frame.

There are numerous types of rearrangements, and only some of them can be discussed here as examples. The most common and best-understood rearrangements are H-rearrangements [79b]. Typically, an H atom moves away to another location within the ion. One bond is broken and another bond is formed. An example of an H-rearrangement is the McLafferty rearrangement (Fig. 16) [84a,b]. The H atom is transferred to a radical cation site via a six-membered cyclic intermediate. A distonic radical cation is formed, where the charge site and radical site are separated. The rearrangement is then followed by charge- or radical-site-driven cleavage.

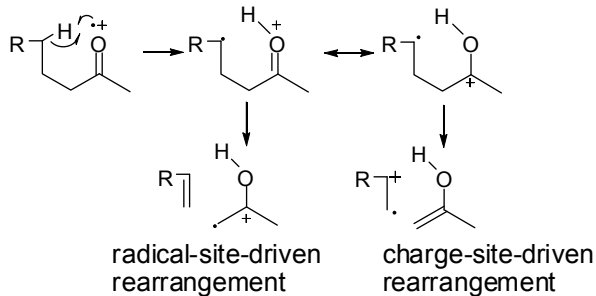


Figure 16. McLafferty rearrangement.

Displacement reactions are energetically favored since one bond is formed in compensation for the one cleaved [79b]. The displacement arrangements may involve the loss of halogen or alkyl radicals, resulting in cyclic cations (Fig. 17).

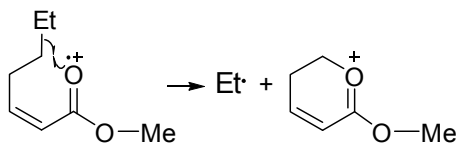


Figure 17. A displacement reaction of methyl (2Z)-2-heptenoate.

Elimination reactions involve the migration of H or some functional group with the elimination of small stable neutrals. One example of an elimination with H-transfer is the 1,4-elimination of water from an alcohol and another is alkenyl radical elimination from the dimethyl ester of cyclopentanediol (Fig. 18) [85a].

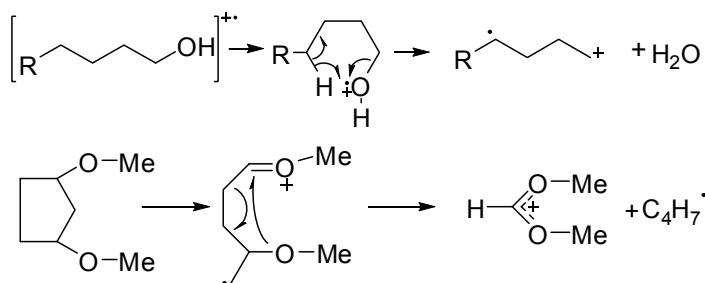


Figure 18. 1,4-Elimination of water from an alcohol and elimination of an alkenyl radical from the dimethyl ester of cyclopentanediol.

3.4.3 CO loss under EI

The loss of a CO molecule under EI is often observed in the mass spectra of diketones, phenols, acetamides, esters, aromatic epoxides and chalcones. The ion $[M-CO]^{+\bullet}$ has variable relative abundances (RAs), ranging from very low to high. The loss of CO from acyclic molecular ions containing a CO group (acyclic ketones) requires rearrangements and/or cyclic intermediates.

Acetylacetone ($\text{CH}_3\text{COCH}_2\text{COCH}_3$) has been observed to exhibit the loss of CO, with a RA of 10% [86]. This fragmentation requires the migration of a Me group. In comparison, benzoylacetone ($\text{C}_6\text{H}_5\text{COCH}_2\text{COCH}_3$) does not exhibit CO loss, but the presence of the tropylium ion indicates some phenyl migration [86]. For 2,2-dimethyl-3,5-hexanedione, the migration of a *t*-Bu group involving an intermediate ion/neutral complex has been suggested as the mechanism of CO loss [87].

2,3-Pentanediones, 2,3-butanediones and 3,4-hexanediones have been observed to lose CO. This fragmentation has been suggested to occur via a stable transition state, which has been confirmed by the energies of the minima and the transition states and geometrical optimizations calculated at the B3-LYP/6-31+G(d) level of theory, where the 2-butanone ion is bound electrostatically to CO (Fig. 19). The rearrangement involves an energy barrier, but the production of the low-energy CO molecule makes the decarbonylation process able to compete with other fragmentation processes [88].

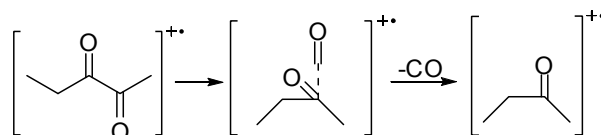


Figure 19. Formation of $[\text{M}-\text{CO}]^{+\bullet}$ from 2,3-pentanedione.

Phenol exhibits a strong CO loss (RA 40%) [89a]. Phenol has been suggested to lose CO via tautomerization of the enol form to the keto form (Fig. 20) [89b]. The 1,3-H shift requires excess energy for activation. The resulting ions are isolated, so the excess energy cannot be transferred through collision, and the kinetic energy is transferred to the decarbonylation step. A high kinetic energy release (KER) has been observed by mass-analyzed ion kinetic energy (MIKE) spectrometry [89c].

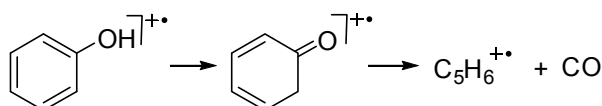


Figure 20. Decarbonylation of phenol radical cation.

o-, *m*- and *p*-anisoyl fluorides lose CO requiring F atom migration via a three-membered transition state. *m*-Anisoyl fluoride also forms *para* or *ortho* isomers via a four-membered transition state via H-transfer (Fig. 21). However, for anisoyl chloride no CO loss was observed [90,91].

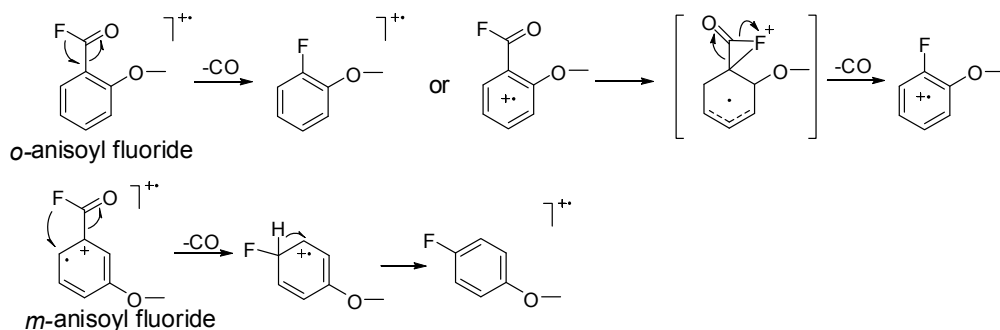


Figure 21. Proposed mechanisms for the loss of CO from *o*-anisoyl fluoride and *m*-anisoyl fluoride with formation of the *para* isomer from the latter [90, 91].

The loss of CO from ionized acetamide ($\text{CH}_3\text{CONH}_2^+$) has been suggested to occur via an H-bonded complex (Fig. 22). It is interesting to note that tautomerization of the acetamide molecular ion to the enol radical cation ($\text{H}_2\text{C}=\text{C}(\text{OH})\text{NH}_2^+$) is prevented by substantial energy barrier, and thus tautomerization does not affect the CO loss [92].

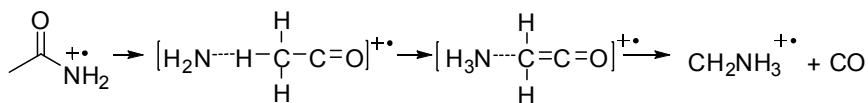


Figure 22. The loss of CO from acetamide via an H-bonded complex.

Dimethyl malonate has been proposed to lose CO via an H-bridged structure (Fig. 23). This mechanism has been studied via the MIKE spectra, KER values and thermochemistry [93].

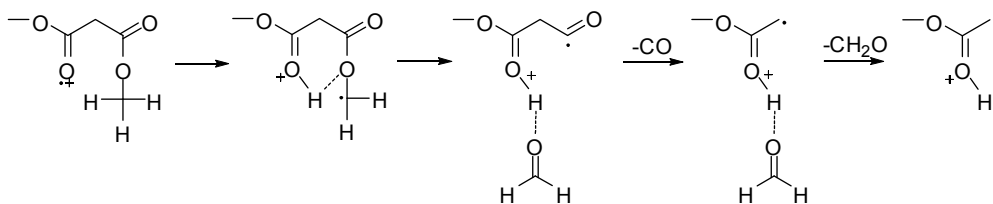


Figure 23. Proposed mechanism of CO loss from dimethyl malonate [93].

Aromatic epoxides, such as *trans*-stilbene oxide, have been found to undergo skeletal rearrangements, making CO or CHO losses possible [94,95] (e.g. Fig. 24).

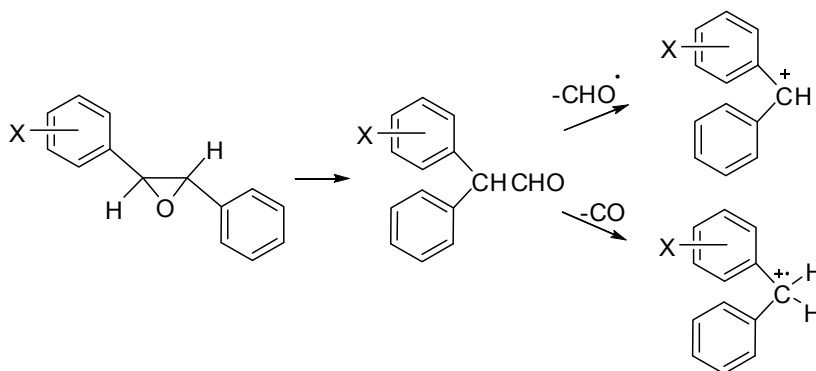


Figure 24. CO and CHO[•] loss from *trans*-stilbene oxide.

The molecular ions, [M-H]⁺ and [M-CH₃]⁺ of chalcones have been observed to undergo ring formation and structural rearrangement, which permits fragmentation pathways that may eventually lead to the loss of CO [96,97a,b], e.g. Fig. 25.

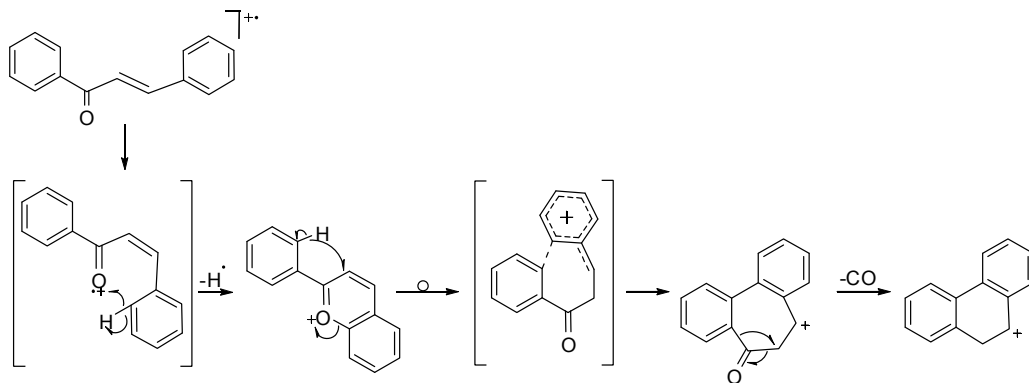


Figure 25. Loss of CO from [M-H]⁺ ion of chalcone.

3.4.4 Retro-Diels-Alder (RDA) fragmentations

RDA fragmentations occur with compounds containing a cyclohexene ring and produce neutral molecules or odd-electron product ions of dienes and alkenes. The different mechanisms and energies of RDA reactions are widely discussed in the literature [98a,b]. Suggested mechanisms for the concerted RDA fragmentation of cyclohexene [98a] and the stepwise RDA fragmentation of 4-vinylcyclohexene [98b] are shown in Fig 26.

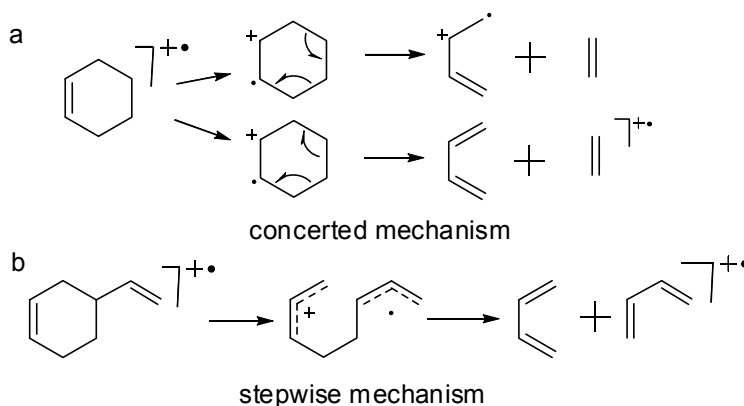


Figure 26. **a:** Concerted RDA mechanism for cyclohexene; **b:** stepwise mechanism for 4-vinylcyclohexene.

RDA fragmentation may give different RAs of ions for *cis*- and *trans*-fused ring systems. However, the stereochemical effects affecting the mechanisms of RDA fragmentation are difficult and perhaps impossible to generalize [99]. The stereospecificity of an RDA fragmentation is defined by the following equation ($m/z \geq 40$) [100]:

$$\frac{\% \sum_{40} RDA_{cis} - \% \sum_{40} RDA_{trans}}{\% \sum_{40} RDA_{cis} + \% \sum_{40} RDA_{trans}} \cdot 100$$

where RDA_{cis} and RDA_{trans} are the RAs of ions formed from either the *cis* or the *trans* isomer, respectively, in RDA-related fragmentations. Similarly, on the basis of the normalized difference of the intensities I (\equiv % total ion current, i.e. % TIC) of the same RDA ions produced from either isomer [101]:

$$\frac{I_{cis} - I_{trans}}{I_{cis} + I_{trans}}$$

There have been attempts to explain EI-induced RDA reactions by comparing the degrees of substitution at the bonds cleaved in the fragmentation. Compounds can be classified as involving low, medium or high degrees of substitution (Fig. 27) [100]. The degree of substitution is related to the critical energy of RDA fragmentation. The definition of substitution is somewhat blurred, but the critical energy differences of *cis* and *trans* isomers can still be used to explain RDA stereospecificity [100,101]. The critical energy differences between *cis* and *trans* isomers cause the medium-substituted compounds to give stereospecific RDA fragmentations, while the low and high-substituted compounds exhibit low stereospecificity. When the degree of substitution is high, the critical energies for RDA are low for both the *cis* and *trans* isomers, and when the degree of substitution is low, the critical energies are high. For medium-substituted compounds, the critical energy for *trans* isomers increases relative to that for *cis* isomers, leading to stereospecific RDA fragmentations [100].

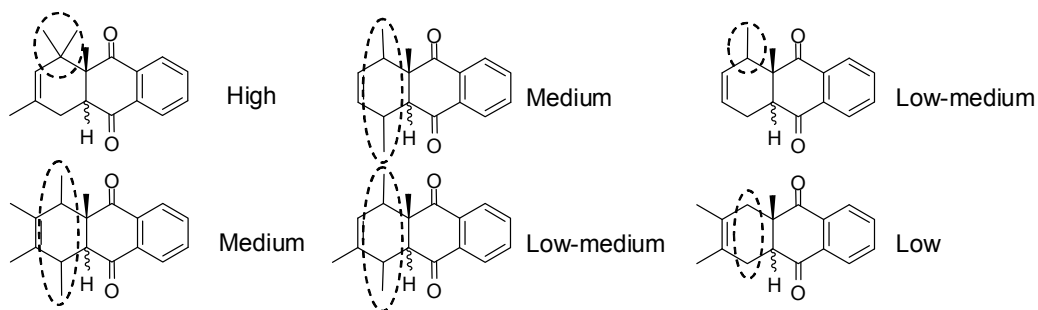


Figure 27. Examples of fused cyclohexene systems with high, medium or low degrees of substitution [100]. The sites mostly defining the classification are highlighted.

There are also results which indicate that the stereospecificity of an RDA process may depend more on the molecular geometry (*cis* vs *trans* annelation) rather than the substitution in the cyclohexene ring being cleaved [101]. Moreover, the stereospecificity of the RDA reaction indicates a concerted single-step fragmentation mechanism [102].

RDA fragmentations may involve H-transfers. The even-electron dienophile cations resulting from RDA fragmentations accompanied by H transfer are referred to either as

(RDA+H) or as (RDA–H), corresponding to the addition of H to or the removal of H from the dienophile, respectively [101]. The RDA+/-H processes and also RDA+2H or RDA–2H are multi-step processes and often stereospecific [103,104].

In addition to the purely MS processes, RDA fragmentations may also occur via thermal decomposition. Thermal decomposition may be problematic for methods requiring vaporization of the sample by heating prior to ionization. Fast-atom bombardment or liquid secondary ion MS methods may be more useful than EI for the study of regio- and stereospecific RDA fragmentations because the samples are ionized at ambient temperatures [105].

3.5 MS and keto-enol tautomerism

3.5.1 Some notes on MS and tautomerization

Although MS methods have long been used for structural investigations of organic compounds, their application for the study of tautomerism in the gas phase has only recently been recognized. The keto-enol tautomerism of β -diketones was the first case studied by this means [87,106-109].

Different ionization energies and inlet temperatures were used to investigate their effects on fragmentations related to keto-enol tautomerism of variously substituted β -diketones [110]. The intensities I of the peaks (i.e. RA or % TIC) originating from the pure keto and enol forms were presumed to obey the modified van't Hoff equation $\ln K = -\frac{\Delta H}{RT} + C$:

$$\ln \frac{I_{enol}}{I_{keto}} = \ln \frac{[enol]}{[keto]} + a = \ln K + a = -\frac{\Delta H}{RT} + (C + a)$$

where K is the equilibrium constant for keto-enol equilibria, ΔH is the enthalpy difference between the enol and keto forms, T is the absolute temperature, R is the gas constant, and C and a are constants [110].

The source temperature affects the tautomer ratio. At higher source temperatures for 2-pentanone, it was observed that the amount of the enol tautomer increased [111]. Another noteworthy fact was that the peak intensities depended not only on the tautomerism but also on the differences in bond strengths [110].

In studies of tautomerism with MS, two important facts should be born in mind [11]:

1. The assignments of mass spectral fragmentations should be tautomer-specific, since the corresponding abundance ratios should correlate to the keto/enol contents.
2. Ionization in the ion source is postulated to have no effect on the position of the equilibrium, so that the results reflect the tautomer contents in the gas phase prior to ionization.

The identification of peaks formed exclusively from either the keto or the enol form is necessary to permit conclusions relating to the tautomerism [11]. The EI fragmentations of β -ketoesters have been studied by GC-MS in an attempt to separate the tautomers, but the problem was the non-negligible interconversion of the tautomers inside the column [112]. However, the enol and keto forms of methyl and ethyl acetoacetate could be separated by making use of GC retention times and mass spectra. It was seen that the intermolecular stabilization of the enol form was higher for α -chloromethyl and α -chloroethyl acetoacetate, which resulted in more enol form being present in the gas phase; this indicates the effect of the electron accepting Cl substituent on the tautomeric equilibria [112].

It is assumed that the equilibrium established at a certain temperature in the inlet system will not be changed in the ion source, as the vapor pressure inside the mass spectrometer is too low for the molecules to take part in collisions [110]. The energy barrier of unimolecular isomerization from ketone to enol is high. Once formed, therefore, the tautomer should retain its original structure in the gas phase, irrespective of the relative stabilities of the isomers [113]. However, the radical cations may have sufficient energy for tautomerization.

The degree of enolization of ketones of the type $R_1(C=O)CHR_2R_3$ is generally favored by the increase of the steric effect exerted by the substituent at the position α to the CO group. In general, the loss of OH from the molecular ion is assigned to the enol form and the loss of R to the keto form, where R is the radical moiety that participates in the enolization process next to the CO group (CHR_2R_3). Ion RA ratios $[(M-R)^+]/[(M-OH)^+]$ of selected ketones have been correlated with semi-empirical AM1 MO calculations of the approximate equilibrium constants of enolization [114]. However, the stabilization of the enol form by conjugation may lead to the absence of $[M-R]^+$.

The loss of OH can also be used for the identification of other prototropic tautomers. For example, supportive fragmentations and rearrangements have been found for imidol forms of amides and their sulfur analogs, thioamides, such as the loss of H, OH/SH, H_2O/SH_2 , and the double H (McLafferty+1)-type rearrangement [115.] For lactones or their sulfur analogs the OH/SH loss indicates the presence of the enol form, and the loss of CX or CX_2 ($X = O$ or S) that of the keto form [116].

3.5.2 The tautomerization of molecular ions

Some mechanisms for the interconversion of molecular ions of the tautomers have been observed.

Radical cations of phenol can tautomerize if they are sufficiently activated to undergo CO loss [89]. The molecular ion of phenol, $M^{+\bullet}$, can acquire sufficient excess energy, with ionization energies of 50-70 eV, whereas $[M-CO]^{+\bullet}$ vanishes at energies < 15 eV [117a]. As mentioned earlier the excess energy from ionization is changed to kinetic energy when CO is lost, and this compensates the energy required for the tautomerization reaction.

KER measurements on sterically crowded triaryl-substituted enols show that the enol radical cations isomerize to excited ketones in a rate-determining step prior to fragmentation (Fig. 28). This is achieved by a greater KER from the enol than from the keto form [118].

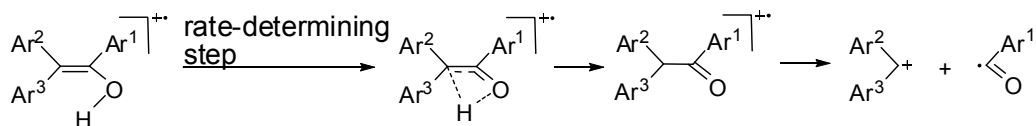


Figure 28. The tautomerization of a triaryl-substituted enol radical cation.

The single and double McLafferty (or McLafferty+1) rearrangement have been studied using deuterium-labeled ketones [117b]. It has been stated that the McLafferty rearrangement of aliphatic ketones can produce enolic radical cations rather than keto ions [117a,b] (Fig. 29). The enolization is simultaneous with the loss of alkene.

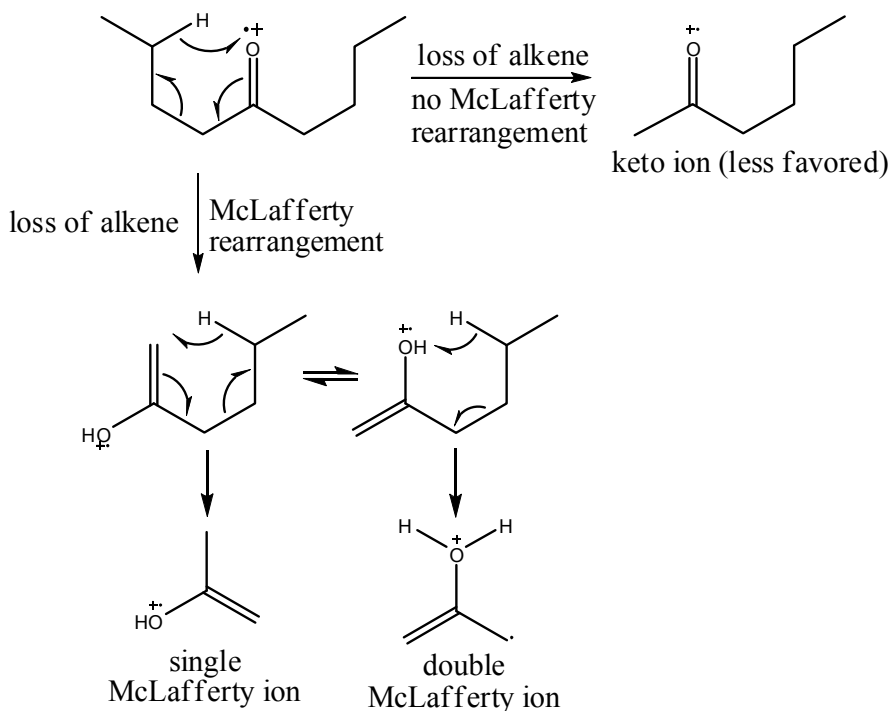


Figure 29. The mechanisms for fragmentation of a ketone with a single McLafferty rearrangement with a consecutive double McLafferty rearrangement [117a].

In general, the tautomerization of radical cations is quite rare, and the tautomerization of neutral molecules is more important than that of radical cations. For example, the ion abundances of lactones and related compounds have been correlated with the differences in heats of formation between the keto and enol forms of the neutral molecules [116].

This means that the impact of radical cations on tautomerization is at its minimum for lactones and their sulfur analogs.

It would seem that the interpretation of MS results is not as straightforward as was once believed. Although the effects of solvents and intermolecular interactions can be avoided, new variables such as the source temperature and ionization energy appear together with reactions of radical cations. Despite this MS can yield important information in studies of tautomerism in the gas phase, especially when the results are compared with those of theoretical semiempirical calculations.

3.6 Materials and methods

3.6.1 MS measurements

All measurements were made in the Instrument Centre in the Department of Chemistry at the University of Turku between 2003 and 2008. The EI mass spectra were recorded on a VG ZABSpec oaTOF mass spectrometer (VG Analytical, Division of Fisons, Manchester, UK) equipped with the Opus V3.3X program package (Fisons Instruments, Manchester, UK). The ionization energy was 70 eV and the source temperature was 160 °C. The acceleration voltage was 8 kV and the usual trap current was 200 μ A. Perfluorokerosine was used for calibration of the mass scale. A small amount of solid sample dissolved in MeOH was placed into a quartz capillary tube and the MeOH was evaporated off with hot air. Thereafter, the sample was transferred into the ionization chamber via the solid inlet. The probe was sometimes heated in order to evaporate the samples.

The fragmentation pathways were solved on the basis of B/E -linked scans (first field-free region, i.e. FFR1) and in some cases also B^2/E . The low-resolution spectra and B/E scans were measured with a resolving power of 3000 (10% valley definition). The accurate masses were determined by voltage scanning, at a resolving power of 6,000–10,000 for small m/z values and $> 10,000$ for the larger values. Also collision induced dissociation

(CID) was used to inspect the fragmentation pathways; He was applied as collision gas in the FFR1. The gas flow was adjusted so that the beam transmission was 50%. Orthogonal acceleration time-of-flight (oaTOF) measurements were made in some cases.

3.6.2 NMR measurements

Most of the compounds have been characterized earlier with NMR methods. However, the NMR spectra for 2,3-dihydroimidazo[1,2-*a*]pyrimidine-5,7(1*H*,6*H*)-diones were recorded and analyzed in our department by Dr. Henri Kivelä [IV]. The latter spectra were acquired with a Bruker Avance 500 NMR spectrometer (Bruker BioSpin Scandinavia AB, Taby, Sweden) operating at 500.13 MHz for ^1H and at 125.77 MHz for ^{13}C , equipped with a vendor-provided 5-mm direct or inverse detection Z-gradient probe (BBO-5mm-Zgrad or BBI-5mm-Zgrad-ATM, respectively), the probe temperature set at 298 K. Because of some solubility problems in CDCl_3 , deuterated dimethyl sulfoxide (DMSO-*d*₆) was used as solvent. The ^1H spectra were referenced to internal SiMe_4 (0.00 ppm) and the ^{13}C spectra to the middle resonance line of the DMSO solvent signal (39.40 ppm). A standard one-dimensional (1D) ^1H NMR spectrum and a ^{13}C spectrum with broad-band proton decoupling were run on each sample, supplemented by 2D gradient-selected correlation spectroscopy (COSY), nuclear overhauser enhancement spectroscopy (NOESY), multiplicity-edited heteronuclear single quantum correlation (HSQC) and heteronuclear multiple bond correlation (HMBC) experiments for selected samples to help with the assignment of signals. Vendor-provided pulse sequences were used throughout the work. For NOESY, a mixing time of 0.3 s was employed, and the heteronuclear experiments were optimized for a one-bond C,H coupling of 145 Hz and a long-range coupling of 8–10 Hz.

3.6.3 Linear fits and structures of molecules

The linear functions for 2-phenacylpyridines were calculated by using linear regression on the Origin 6.0 package (Microcal Software, Inc., Northampton, MA, USA).

The linear functions for 2-phenacylquinolines were calculated by using linear regression on the Origin 8 SR1 package (OriginLab Corporation, Northampton, MA, USA). As default Origin 8 gives the coefficient of determination as adjusted R^2 . The value of adjusted R^2 increases only if the new term improves the model more than would be expected by chance.

The structures of molecules in sections 4.3.2 and 4.5.2 have been drawn with the ChemOffice Ultra 10.0 package (Cambridgesoft Corporation, Cambridge, Massachusetts, USA) using Chem3D Pro 10.0 for MM2 energy minimizations.

3.6.4 The compounds studied

The compounds studied were obtained from different research groups. 2-Phenacylpyridines **1a–n** [**I**] (Scheme 1, p. 45) and 2-phenacylquinolines **2a–h** [**VI**] (Scheme 2, p. 46) were received from Prof. Ryszard Gawinecki (Department of Chemistry, University of Technology and Life Sciences, Bydgoszcz, Poland), 8-aryl-3,4-dioxo-2*H*,8*H*-6,7-dihydroimidazo[2,1-*c*][1,2,4]triazines **3a–j** [**II**] (Scheme 6, p. 60) and Ar- and benzyl-substituted 2,3-dihydroimidazo[1,2-*a*]pyrimidine-5,7(1*H*,6*H*)-diones **18–21** [**IV**] (Scheme 10, p. 73) from Prof. Dariusz Matosiuk (Department of Synthesis and Chemical Technology of Pharmaceutical Substances, Professor Feliks Skubiszewski Medical University, Lublin, Poland), pyrrolo- and isoindolo-quinazolinones **4–17** [**III**] (Scheme 8, p. 65, and Table 8, p. 66) from Prof. (Emeritus) Géza Stájer (Institute of Pharmaceutical Chemistry, University of Szeged, Hungary), and naphthoxazine, naphthpyrrolo-oxazinone and naphthoxazino-benzoxazine derivatives **22–29** [**V**] (Scheme 11, p. 79, and Table 14, p. 80) from Prof. Ferenc Fülöp (Institute of Pharmaceutical Chemistry, University of Szeged, Hungary).

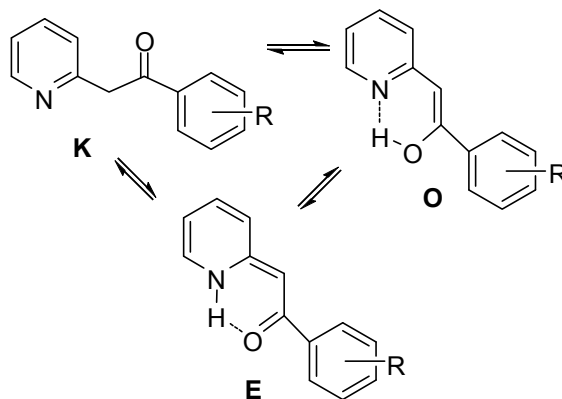
The syntheses have been published for **1a–n** [119,120], **2a–h** [125], **3a–j** [26,121], **4–17** [122], **18–21** [70] and **22–29** [123,124].

4. RESULTS AND DISCUSSION

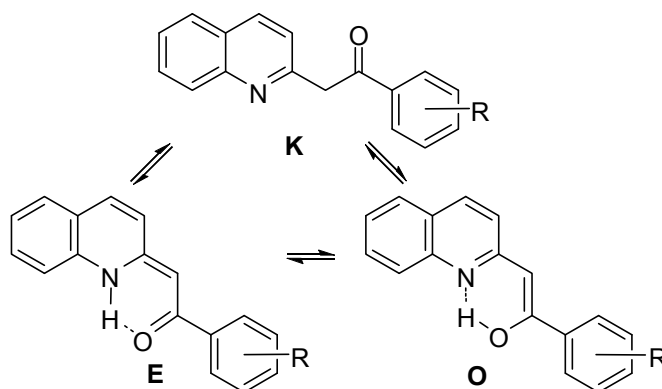
4.1 2-Phenacetylpyridines **1a–n** [I] and 2-phenacetylquinolines **2a–h** [VI]

4.1.1 General fragmentations

2-Phenacetylpyridines **1a–n** (Scheme 1) and 2-phenacetylquinolines **2a–h** were selected for study because strong effects of the substituents on the tautomeric equilibria were expected to be seen in the gas phase as different fragmentations or different abundances of ions for forms **K**, **O** and **E**. The results were also thought to give information about the presence of internal hydrogen bonding in the gas phase. For 2-phenacetylpyridines form **E** is theoretically possible, but only forms **K** and **O**, i.e. (*Z*)-2-(2-hydroxy-2-phenylvinyl)pyridine, have been observed. 2-Phenacetylquinolines **2a–h** (Scheme 2) resemble the 2-phenacetylpyridines, but instead of form **O** the other tautomer besides form **K** is **E**, i.e. (*Z*)-2-benzoyl-methylene-1,2-dihydroquinoline. For 2-phenacetylpyridines form **E** and for 2-phenacetylquinolines form **O** are not detected in solvents or in the solid state.



Scheme 1. Structures and possible tautomers of 2-phenacetylpyridines **1a–n**: R = **a**: H, **b**: *m*-Me, **c**: *p*-Me, **d**: *p*-NH₂, **e**: *m*-F, **f**: *p*-F, **g**: *p*-OMe, **h**: *p*-Cl, **i**: *p*-N(Me)₂, **j**: *p*-NO₂, **k**: *p*-CF₃, **l**: *p*-N(CH₂)₄, **m**: *p*-Br, **n**: *m*-Br. **K** = 2-phenacetylpyridine (ketimine), **O** = (*Z*)-2-(2-hydroxy-2-phenylvinyl)pyridine (enolimine), **E** = (*Z*)-1,2-dihydro-2-benzoylmethylenepyridine (enaminone).



Scheme 2. 2-Phenacylquinolines **2a–h** and their possible tautomers. R = **a**: $p\text{-N}(\text{CH}_2)_4$, **b**: $p\text{-NMe}_2$, **c**: $p\text{-OMe}$, **d**: $p\text{-Me}$, **e**: $m\text{-Me}$, **f**: $p\text{-Cl}$, **g**: $p\text{-Br}$, **h**: $p\text{-CF}_3$. **K** = 2-phenacylquinoline (ketimine), **E** = (*Z*)-1,2-dihydro-2-benzoylmethylenequinoline (enaminone), **O** = (*Z*)-2-(2-hydroxy-2-phenylvinyl)quinoline (enolimine).

Common fragment ions with their RAs are presented for **1a–n** in Table 1 [**I**] and for **2a–h** in Table 2 [**VI**], and their typical fragmentation pathways are illustrated in Schemes 3 and 4, respectively.

Table 1. Common ions for compounds **1a–n** and their RAs [I].

M ⁺	<i>m/z</i> (RA%)									
	[M–H] ⁺	[M–OH] ⁺	[M–CO] ⁺	[M–HCO] ⁺	PyCH ₂ CO ⁺	ArCO ⁺	Ar ⁺	PyCH ₂ ⁺	C ₃ H ₅ ⁺	
1a	197(26)	196(34.5)	180(2)	169(47)	168(33)	120(9)	105(100)	77(61)	92(11.5)	65(10)
1b	211(22)	210(28.5)	194(3.0)	183(51)	182(34)	120(10.5)	119(100)	91(60)	92(10.5)	65(26)
1c	211(13)	210(20)	194(1)	183(39.5)	182(20)	120(4.5)	119(100)	91(49)	92(10.5)	65(20)
1d	212(14.5)	211(3.5)	195(0.5)	184(14.5)	183(3)	120(100) ^a	120(100) ^a	92(22)	92(22)	65(17)
1e	215(45.5)	214(42)	198(3)	187(55)	186(43.5)	120(18)	123(100)	95(60)	92(20)	65(14)
1f	215(9)	214(11)	198(1)	187(24.5)	186(14)	120(3.5)	123(100)	95(42)	92(5.5)	65(5)
1g	227(7)	226(5.5)	210(0.5)	199(24)	198(4.5)	120(0.5)	135(100)	107(5)	92(14.5)	65(4)
1h	231/233(19)	230/232(23.5)	214/216(2.5)	203/205(39)	202/204(26)	120(6.5)	139/141(100)	111/113(39)	92(9)	65(9)
1i	240(24)	239(2)	223(1)	212(2)	211(1)	120(0.5)	148(100)	120(4)	92(3)	65(3.5)
1j	242(100)	241(57)	225(3.5)	214(50.5)	213(58)	120(32)	150(46)	122(+)	92(48.5)	65(22)
1k	265(72)	264(75)	248(4.5)	237(54.5)	236(52)	120(27.5)	173(100)	145(69)	92(28)	65(18)
1l	266(23)	265(2)	249(+)	238(1.0)	237(0.5)	120(+)	174(100)	146(4)	92(1)	65(3)
1m	275/277(46)	264/276(40.5)	258/260(2.8)	247/249(58.5)	246/248(35)	120(10.5)	183/185(100)	155/157(37.5)	92(14)	65(13)
1n	275/277(62.5)	274/276(43.5)	258/260(4.5)	247/249(62.5)	246/248(55)	120(24.5)	183/185(96.5)	155/157(51)	92(23)	65(20)

RAs are corrected for ¹³C, RAs of halogen isotope-containing ions are summed, and those of **1h**, **1m** and **1n** have been renormalized. RAs are rounded to the nearest half per cent.

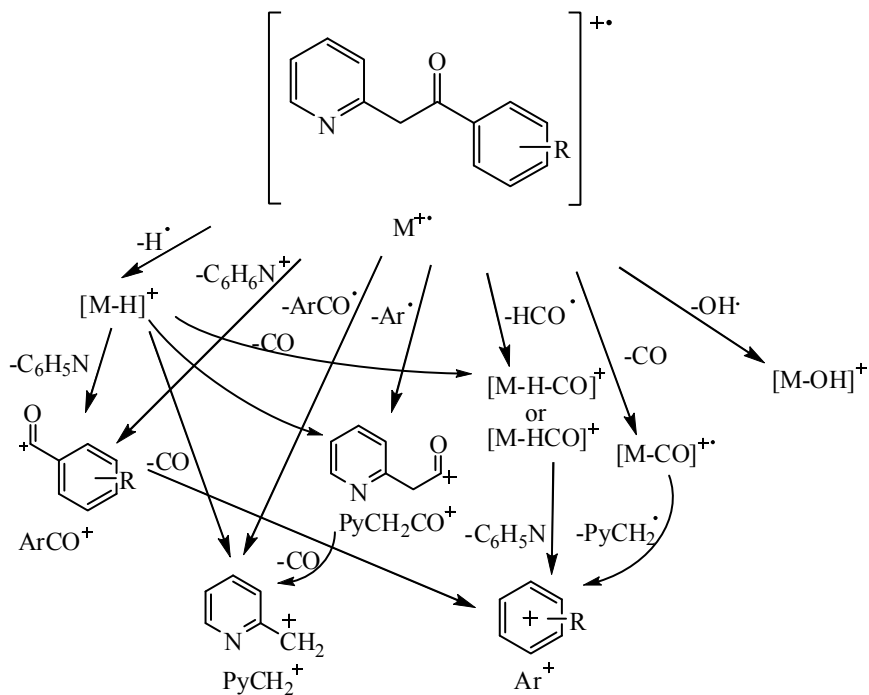
^a Elemental composition C₇H₆NO⁺.

Table 2. Common ions for compounds **2a–h** and their RAs [VI]

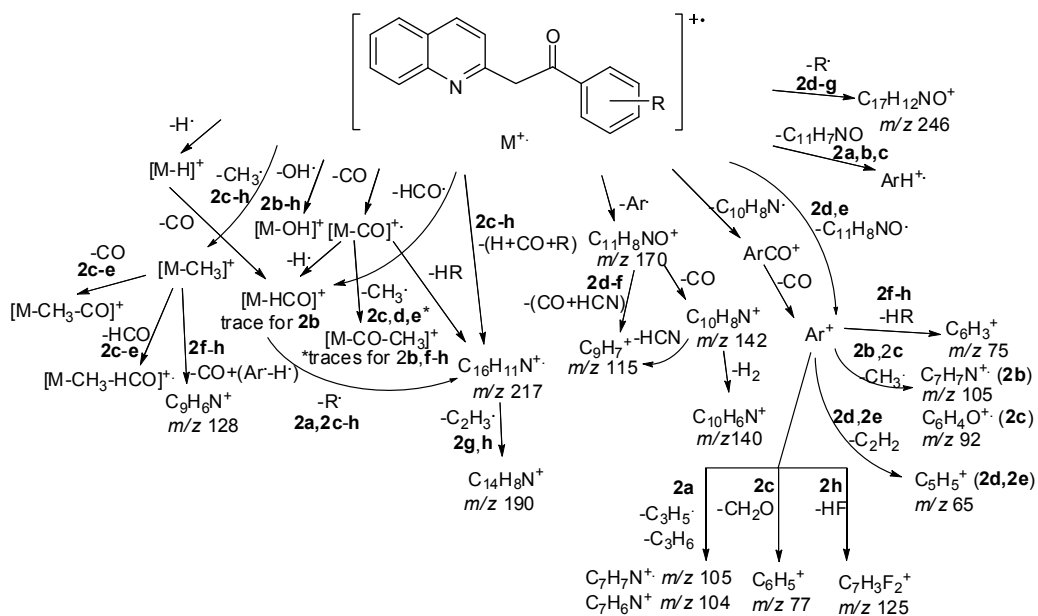
	m/z (RA%)								
	M ^{•+}	[M–H] ⁺	[M–CO] ^{•+}	[M–H–CO] ⁺	[M–Ar] ⁺	ArCO ⁺	C ₁₀ H ₈ N ⁺	Ar ⁺	C ₉ H ₇ ⁺
2a	316(45)	315(3.5)	288(2)	-	170(3)	174(100)	142(3.5)	146(5) ^a	115(3)
2b	290(48)	289(4)	262(3)	261(0.5)	170(1)	148(100)	142(3)	120(3) ^a	115(2.5)
2c	277(58)	276(28.5)	249(47)	248(7.5)	170(10)	135(100)	142(8)	107(4) ^a	115(7.5)
2d	261(74)	260(55)	233(60.5)	232(25)	170(27.5)	119(100)	142(16.5)	91(41)	115(15.5)
2e	261(79)	260(43)	233(62.5)	232(32.5)	170(38)	119(100)	142(19.5)	91(52.5)	115(17.5)
2f	281/283(100)	280/282(58.5)	253/255(40.5)	252/254(27)	170(32.5)	139/141(61.5)	142(18.5)	111/113(26)	115(14.5)
2g	325/327(100)	324/326(48)	297/299(40)	296/298(23)	170(27.5)	183/185(55)	142(16.5)	155/157(20)	115(14)
2h	315(100)	314(53.5)	287(31.5)	286(35.5)	170(46)	173(37.5)	142(24)	145(27.5)	115(16.5)

RAs are corrected for ¹³C, RAs of halogen isotope-containing ions are summed, and those of **2f**, **2g** and **2h** have been renormalized. RAs are rounded to the nearest half per cent.

^a Also ArH^{•+}: **2a** 147(11), **2b** 121(16.5) and **2c** 108(1.5).



Scheme 3. The general fragmentation pathways of **1a-n**.



Scheme 4. The general fragmentation pathways of **2a-h**.

All compounds studied gave clear M^+ peaks; for the *p*-NO₂-substituted compound **1j** and the halogen-substituted **2f–h** this was the base peak. It is worth mentioning that the substituent effects of the NO₂ group are different for benzophenone-type molecular ions, due to the possible alteration in the structure of the NO₂ substituent in which the oxygen atom becomes attached to the same carbon atom to which the nitrogen had earlier been attached (Fig. 30) [126].

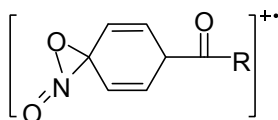


Figure 30. The alteration in the structure of the NO₂ substituent.

4.1.2 Ions related to tautomers

There were fragmentations indicating tautomerism for 2-phenacylpyridines **1a–n**. The RAs of $[M-OH]^+$ were slightly higher for compounds with stronger electron acceptors, i.e. for the compounds most likely to exhibit form **O**, but in general they were quite low (RA <7%). For 2-phenacylquinolines **2a–h** $[M-OH]^+$ was observed (RA <5%) for all compounds except **2a**, and $[M-OH]^+$ was again slightly more favored with electron-withdrawing substituents. Only traces of $[M-OH]^+$ were observed for compounds with strong electron-donating groups. Since the OH loss can in general be assigned to the enol form [114,116], and since the fragmentation cannot occur from form **K**, this fragmentation may indicate the presence of form **O** or **E**.

For 2-phenacylpyridines **1a–n** and 2-phenacylquinolines **2a–h**, the ion Ar^+ was found to be more abundant for electron-withdrawing substituents as were $[M-ArCO]^+$, $[M-Ar]^+$, $[M-H]^+$ and M^{++} . The ions Ar^+ and $[M-Ar]^+$ may be formed from both tautomers, but $[M-Ar]^+$ should have different structures (Fig. 31). Although the RA of $ArCO^+$ was 100% for most compounds, its % TIC decreased for stronger electron-withdrawing substituents, possibly as an indication of an increased contribution of form **O** or **E**. This can be

explained by the dissociation of the bond α to the CO group, which is easier for the σ -bond of form **K** than for the double bond of form **O** (Fig. 31).

Forms **O** and **E** seem to favor the formation of $[M-Ar]^+$, and form **K** that of $ArCO^+$. The intramolecular H-bond may make the formation of $ArCO^+$ from form **O** (and also form **E**) less favorable. The ion ArH^{2+} from **1i,l** and **2a-c** may be specific for form **K**.

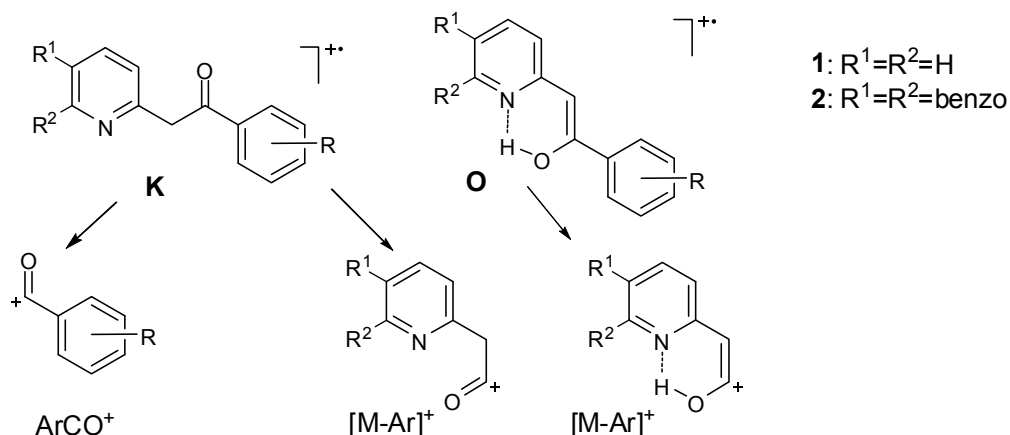


Figure 31. The formation of $ArCO^+$ from form **K** and the formation of $[M-Ar]^+$ from forms **K** and **O**.

The RAs of ions $[M-CO]^+$ and $[M-HCO]^+$ were greater for compounds with electron acceptors. These two losses were weak for the compounds most likely to exist in form **K**, i.e. for the compounds **1d,i,l** and **2a,b** with the most negative substituent constants. Therefore, the structure of form **O** or **E** is favorable for (H)CO loss. The formation of ions $[M-CO]^+$ and $[M-HCO]^+$ requires rearrangements. CO and HCO losses were observed for 2-phenacylpyridines **1a-n** and 2-phenacyl-quinolines **2a-h**; the suggested mechanism is discussed in section 4.1.6. It should be noted that, for **2b-e**, $[M-CO]^{2+}$ was present with RAs of 4 to 8%.

Comparisons of compounds presumed to exhibit the keto form have been made with EI data recorded in the US National Institute of Standards and Technology database [89].

The carbon analogs of 2-phenacylpyridines, e.g. 1,2-diphenylethan-1-one, 1-(4-bromophenyl)-2-phenylethanone and diphenylethanedione, give very weak molecular peaks and no $[M-H]^+$ or $[M-CO]^{+*}$ is noted. None of these compounds contains an internal H-bond that would stabilize the enol form, and thus only the keto tautomer is present in the gas phase.

The RAs of the molecular ions for **1j** and **2f–2h**, with the strongest electron acceptors, were 100%. Increase of the molecular ion may be another indication of the increasing form **E** or **O**. The molecular ion of a stable enol form is often more abundant than that of the keto form [112,127,128]. The reason for this behavior may be that the positive enol ions are thermodynamically more stable than the corresponding keto ions [129].

4.1.3 Correlations with Hammett σ for 2-phenacylpyridines 1a–n

Hammett σ_p or σ_m functions were used to correlate the RAs and % TICs of ions. Even better correlations were obtained by omitting the inductive parameter from the calculations and using the resonance effect parameter σ_R . The best correlations are presented in Table 3, and the linear fit of $ArCO^+$ (% TIC vs σ_p or σ_m) is depicted in Fig. 32. The presence of the ion $ArCO^+$ seems to be related to form **K**, and that of the ions $[M-H]^+$, $[M-CO]^{+*}$, $[M-HCO]^+$ and $[M-Ar]^+$ ions to form **O**.

Dual-substituent parameter analysis of the equilibrium constant K_T , based on the NMR results, has shown that the resonance substituent effect predominates over the inductive effect [23]. The better correlations of the ion RAs with σ_R than with σ_p or σ_m indicate that the substituents of 2-phenacylpyridines may affect the tautomerism mainly by resonance in the gas phase.

Table 3. RAs or % TICs of the ions from **1a–n** which correlate with the Hammett constants σ (σ_m or σ_p) or σ_R and the parameters for the linear fits.

Parameters for $y = a + bx$						
Ion	y	x	$a \pm \text{error}$	$b \pm \text{error}$	R	Notes
ArCO ⁺	% TIC	σ_m or σ_p	26.2±1.2	-(23.1±2.8)	-0.926	
ArCO ⁺	% TIC	σ_R	18.2±2.0	-(30.3±4.4)	-0.924	
[M–H] ⁺	% TIC	σ_m or σ_p	5.44±0.45	5.7±1.0	0.859	
[M–H] ⁺	% TIC.	σ_R	7.9±0.5	8.5±1.1	0.943	
[M–CO] ⁺	RA	σ_m or σ_p	38.7±3.0	34.0±6.8	0.834	
[M–CO] ⁺	RA	σ_R	49.0±3.1	45.7±6.8	0.922	
[M–HCO] ⁺	RA	σ_m or σ_p	27.4±2.4	39.6±5.5	0.907	
[M–HCO] ⁺	RA	σ_R	49.0±3.2	45.7±6.8	0.922	
[M–HCO] ⁺	% TIC	σ_m or σ_p	5.5±0.4	5.3±0.9	0.876	
[M–HCO] ⁺	% TIC	σ_R	7.2±0.4	7.5±0.8	0.961	
PyCH ₂ CO ⁺	% TIC	σ_m or σ_p	1.6±0.2	4.0±0.6	0.912	1d and 1i excluded
PyCH ₂ CO ⁺	% TIC	σ_R	3.0±0.3	5.5±1.0	0.920	1d and 1i excluded
Ar ⁺	RA	σ_R	57.4±2.8	53.4±9.1	0.966	1g and 1j excluded
[M–H] ⁺	log ₁₀ (RA)	σ_R	1.62±0.05	1.44±0.11	0.978	
[M–HCO] ⁺	log ₁₀ (RA)	σ_R	1.61±0.07	1.60±0.13	0.974	

1l values are excluded because of missing σ values for the pyrrolidino substituent.

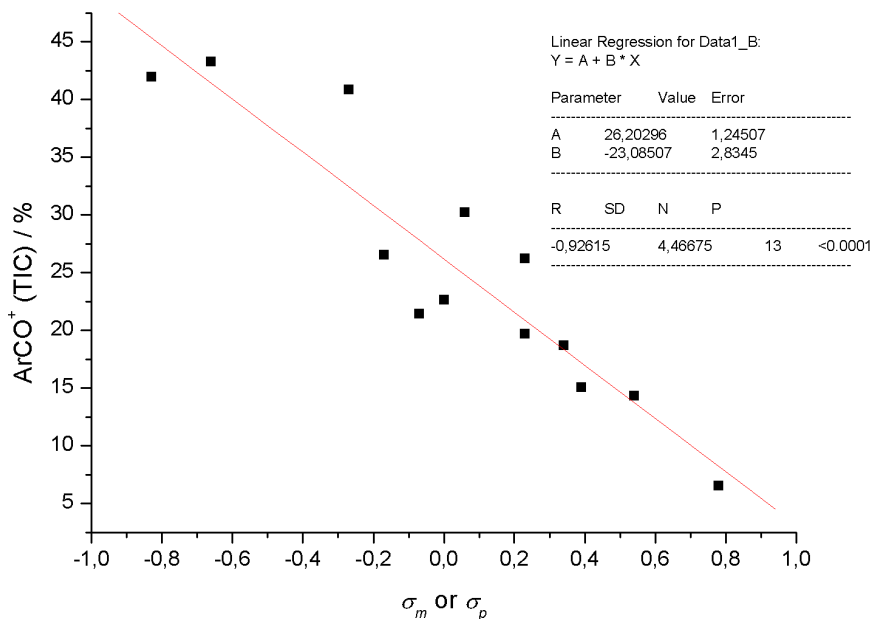


Figure 32. ArCO⁺ (% TIC) vs σ_m or σ_p for 2-phenacylpyridines **1a–n** excluding **1l**.

4.1.4 Correlations with Hammett σ for 2-phenacylquinolines **2a–h**

For the 2-phenacylquinolines the RAs and % TICs correlated with the Hammett substituent constants σ_m , σ_p , σ_R and σ^+ and resonance constant R^+ (Tables 4 and 5). Pyrrolidino-substituted **2a** was excluded from the calculations, since its σ values in the literature were obtained by using a different method [130]. In fact, the σ_p or σ_R values of pyrrolidino are slightly smaller than those of NMe₂. The RAs of common ions from **2a** and **2b** were generally similar. The linear fit of ArCO⁺ (% TIC) vs σ_m or σ_p is presented in Fig. 33.

Table 4. RAs or % TICs of the ions from **2b–h** which correlate with the Hammett constants σ (σ_m or σ_p) or σ_R and the parameters for the linear fits.

Fragment ion	Parameters for $y = a + bx$				Adjusted R ²
	y	x	a±error	b±error	
[M–H] ⁺	RA	σ	43±5	37±10	0.690
[M–H] ⁺	RA	σ_R	58±5	50±10	0.819
[M–H] ⁺	% TIC	σ	7.7±0.6	5.9±1.5	0.734
[M–H] ⁺	% TIC	σ_R	10±1	7.4±1.8	0.777
[M–HCO] ⁺	RA	σ	23±3	24±7	0.653
[M–HCO] ⁺	RA	σ_R	30±2	32±4	0.951
[M–HCO] ⁺	% TIC	σ	3.9±0.4	4.2±0.9	0.806
[M–HCO] ⁺	% TIC	σ_R	5.3±0.3	5.4±0.5	0.962
ArCO ⁺	% TIC	σ	16±1	-22±3	0.935
ArCO ⁺	% TIC	σ_R	8.2±1.9	-28±4	0.911
C ₁₀ H ₈ N ⁺	RA	σ	16±2	15±3	0.796
C ₁₀ H ₈ N ⁺	RA	σ_R	21±1	19±2	0.971
C ₁₀ H ₈ N ⁺	% TIC	σ	2.8±0.2	2.2±0.3	0.922
C ₁₀ H ₈ N ⁺	% TIC	σ_R	3.6±0.2	2.7±0.4	0.931
C ₉ H ₇ ⁺	RA	σ	13±2	10±4	0.594
C ₉ H ₇ ⁺	RA	σ_R	16±1	14±2	0.921
C ₉ H ₇ ⁺	% TIC	σ	2.3±0.2	1.4±0.3	0.800
C ₉ H ₇ ⁺	% TIC	σ_R	2.8±0.1	1.8±0.2	0.941
[M–Ar] ⁺	RA	σ	28±3	31±8	0.733
[M–Ar] ⁺	RA	σ_R	37±3	40±5	0.947
[M–Ar] ⁺	% TIC	σ	4.7±0.4	5.3±0.9	0.854
[M–Ar] ⁺	% TIC	σ_R	6.5±0.4	6.6±0.8	0.937

2a is excluded because of missing σ values for the pyrrolidino substituent.

σ_R values available only for *para* substituents.

ArCO⁺ seems to be related to form **K**, while [M–H]⁺, [M–HCO]⁺ and [M–Ar]⁺ are related to form **E** or **O**. In contrast with the situation in 2-phenacylpyridines (presumed to attain form **O**), the RA of [M–CO]⁺ did not correlate with the substituent constants for 2-phenacylquinolines (form **E**), even when the RAs of [M–CO]²⁺ were included. This may be due to the different conjugation of form **E** relative to that of form **O**.

Table 5. RAs or % TICs of the ions from **2b–h** which correlate with the Hammett constants σ^+ (σ_m^+ or σ_p^+) and R^+ (only for *para* substituents) and the parameters for the linear fits.

Fragment ion	Parameters for $y = a + bx$				
	y	x	$a \pm \text{error}$	$b \pm \text{error}$	Adjusted R^2
[M–H] ⁺	RA	σ^+	48±4	23±5	0.793
[M–H] ⁺	RA	R^+	58±5	27±5	0.862
[M–H] ⁺	% TIC	σ^+	8.3±0.7	4.5±0.9	0.743
[M–H] ⁺	% TIC	R^+	10±1	4.0±0.9	0.821
[M–HCO] ⁺	RA	σ^+	26±2	16±3	0.825
[M–HCO] ⁺	RA	R^+	30±2	17±2	0.952
[M–HCO] ⁺	% TIC	σ^+	4.4±0.3	2.6±0.3	0.926
[M–HCO] ⁺	% TIC	R^+	5.2±0.3	2.9±0.3	0.965
ArCO ⁺	% TIC	σ^+	13±1	-13±1	0.983
ArCO ⁺	% TIC	R^+	8.3±1.5	-15±2	0.946
C ₁₀ H ₈ N ⁺	RA	σ^+	18±1	9.1±1.1	0.918
C ₁₀ H ₈ N ⁺	RA	R^+	20±1	10±1	0.968
C ₁₀ H ₈ N ⁺	% TIC	σ^+	3.1±0.1	1.3±0.2	0.946
C ₁₀ H ₈ N ⁺	% TIC	R^+	3.5±0.2	1.4±0.2	0.920
C ₉ H ₇ ⁺	RA	σ^+	14±1	6.6±1.3	0.798
C ₉ H ₇ ⁺	RA	R^+	17±1	7.3±0.8	0.953
C ₉ H ₇ ⁺	% TIC	σ^+	2.5±0.1	0.87±0.09	0.937
C ₉ H ₇ ⁺	% TIC	R^+	2.8±0.1	0.96±0.07	0.975
[M–Ar] ⁺	RA	σ^+	31±2	19±3	0.864
[M–Ar] ⁺	RA	R^+	37±3	21±3	0.933
[M–Ar] ⁺	% TIC	σ^+	5.4±0.3	3.2±0.4	0.925
[M–Ar] ⁺	% TIC	R^+	6.4±0.5	3.5±0.5	0.921

2a is excluded because of the missing σ^+ and R^+ values for the pyrrolidino substituent.

The correlations with σ^+ were generally better than those with σ , indicating conjugation of the Ph substituent to the electron-deficient reaction site. The good correlations of the ion RAs with R^+ and σ_R show that in the gas phase the **E** (or **O**) tautomers of 2-phenacylquinolines containing electron-withdrawing substituents are stabilized mostly by resonance effects, in addition to possible intramolecular H-bonding.

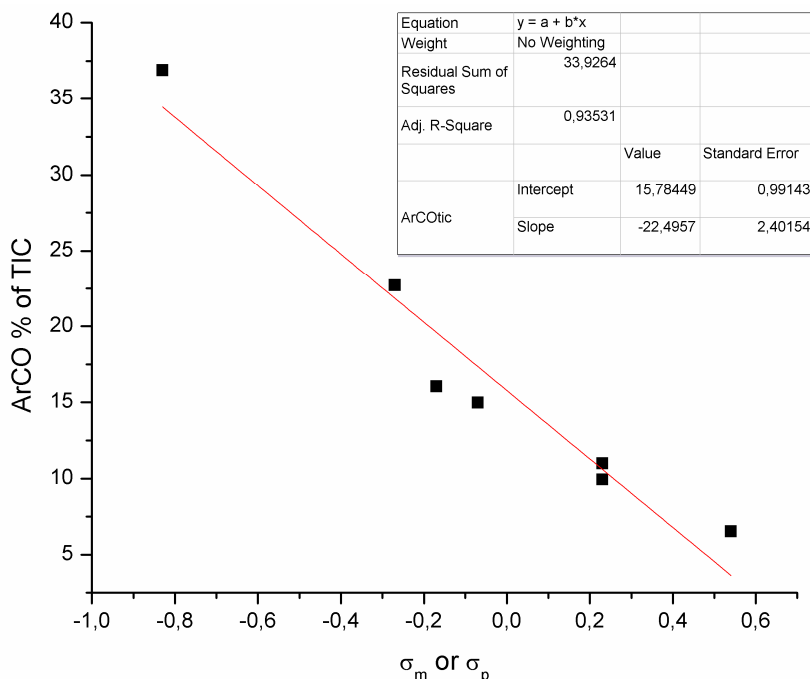


Figure 33. ArCO⁺ (% TIC) vs σ_m or σ_p for 2-phenacylquinolines **2b–h**.

4.1.5 Comparison of results for 1a–n and 2a–h

A comparison of the linear fits of some common ions of 2-phenacylpyridines and 2-phenacylquinolines (Table 6) indicates common trends in the slopes. Those of ArCO⁺ (% TIC) vs σ_R or σ , [M–Ar]⁺ (% TIC) vs σ_R or σ , and [M–H]⁺ (% TIC) vs σ_R or σ are similar within the margins of error. Therefore, the effects of the substituents seem to be similar for **1a–n** and **2a–h**.

The molecular ions were the base peaks of 2-phenacylquinolines with strong electron acceptors **2f–h**. These compounds have less than 2% of form **K** in CDCl₃ solution [22a]. The only molecular ion base peak of the 2-phenacylpyridine was that of **1j**, with 7.8% of form **K** in solution [23]. In general, 2-phenacylquinolines (1–33% form **K** in solution) exhibited more abundant molecular ion peaks for the compounds with electron-donating substituents (RA >45%) than 2-phenacylpyridines (7.8–99% form **K** in solution, RA >7%). The different substituents are therefore not the only cause of the variation in the

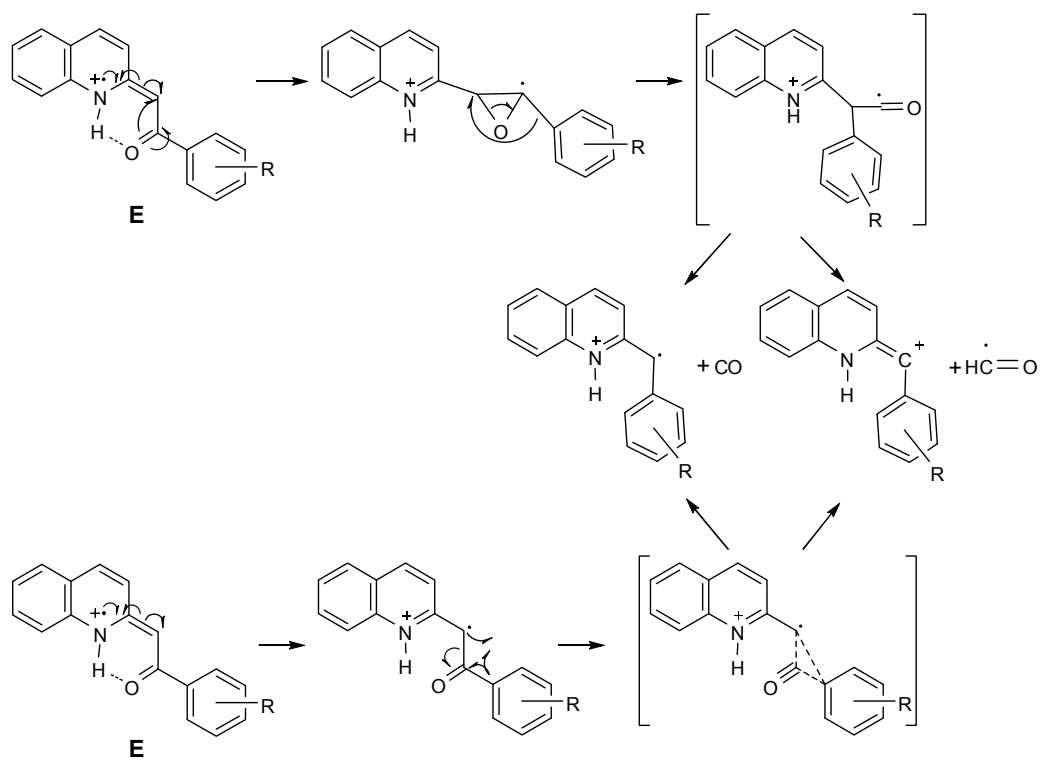
RAs, but the Py and Qui rings also play important roles, as is the case in solution. The molecular ion appears to be stabilized by the intramolecular H-bonding present in the **E** or **O** tautomers in the gas phase.

Table 6. A comparison of the linear correlations for 2-phenacylpyridines **1a–n** and 2-phenacylquinolines **2a–h**.

	Parameters for $y = a + bx$				
	Fragment ion	y	x	a	b
2-phenacylpyridines	ArCO ⁺	% TIC	σ	27±2	-23±2
2-phenacylquinolines	ArCO ⁺	% TIC	σ	16±1	-22±3
2-phenacylpyridines	ArCO ⁺	% TIC	σ_R	18±2	-30±5
2-phenacylquinolines	ArCO ⁺	% TIC	σ_R	8.2±1.9	-28±4
2-phenacylpyridines	[M–Ar] ⁺	% TIC	σ	1.6±0.2	4.0±0.6
2-phenacylquinolines	[M–Ar] ⁺	% TIC	σ	4.7±0.4	5.3±0.9
2-phenacylpyridines	[M–Ar] ⁺	% TIC	σ_R	3.0±0.3	5.5±1.0
2-phenacylquinolines	[M–Ar] ⁺	% TIC	σ_R	6.5±0.4	6.6±0.8
2-phenacylpyridines	[M–H] ⁺	% TIC	σ	5.4±0.5	5.7±1.0
2-phenacylquinolines	[M–H] ⁺	% TIC	σ	7.7±0.6	5.9±1.5
2-phenacylpyridines	[M–H] ⁺	% TIC	σ_R	7.9±0.5	8.5±1.1
2-phenacylquinolines	[M–H] ⁺	% TIC	σ_R	10±1	7.4±1.8

4.1.6 CO loss from 2-phenacylpyridines **1a–n** and 2-phenacylquinolines **2a–h**

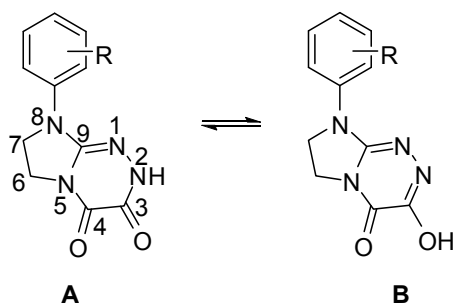
The 2-phenacylpyridines and 2-phenacylquinolines structurally resemble stilbenes and chalcones. The rearrangements for CO loss and HCO loss may therefore be similar to those for chalcones and *trans*-stilbene oxides (see section 3.4.3 *CO loss under EI*). The suggested mechanisms for CO loss and HCO loss from 2-phenacylquinolines are presented in Scheme 5. The CO loss from 2-phenacylpyridines probably occurs by a similar mechanism.



Scheme 5. The possible mechanisms for losses of CO and HCO[•] from form E.

4.2 8-Aryl-3,4-dioxo-2H,8H-6,7-dihydroimidazo[2,1-c][1,2,4]triazines 3a–j [III]

Two tautomers are possible: 8-aryl-2,6,7,8-tetrahydroimidazo[2,1-c][1,2,4]triazine-3,4-dione (the amide form with a 3-oxo group) and 3-hydroxy-8-aryl-7,8-dihydroimidazo[2,1-c][1,2,4]triazin-4(6H)-one (the imidol form with 3-OH group) (Scheme 6).



Scheme 6. Structures of compounds **3a–j** (R = **a**: H, **b**: *o*-Me, **c**: *p*-Me, **d**: *o,m*-diMe, **e**: *o*-OMe, **f**: *p*-OMe, **g**: *o*-Cl, **h**: *m*-Cl, **i**: *p*-Cl, **j**: *m,p*-diCl) and possible tautomeric forms **A/B**. **A** = 8-aryl-3,4-dioxo-2H,8H-6,7-dihydroimidazo[2,1-c][1,2,4]triazine (amide form), **B** = 3-hydroxy-8-aryl-7,8-dihydroimidazo[2,1-c][1,2,4]triazin-4(6H)-one (imidol form). The numbering used for the assignment of NMR signals is depicted for **A**.

As noted in section 3.3.6, the NMR methods demonstrate that the 3-oxo form is favored in solution (DMSO-*d*₆) [26]. With the use of molecular modeling for *m*- and *p*-Cl-substituted compounds it has been calculated that in general the 3-oxo form is more stable than the 3-OH form in the gas phase. However, in the aqueous solution the heats of formation for the 3-oxo and 3-OH tautomers indicate that the *p*-Cl-substituted compound favors the 3-OH form [26], and thus **3i** is the strongest candidate to exhibit fragmentations related to the enol form.

The 3-oxo and 3-OH tautomers were expected to display different fragmentations, such as the loss of two CO groups (**A**) or an OH radical (**B**). The problem arises from the situation that the compounds generally favor the **A** form. Moreover, there is no stabilizing

hydrogen bond even in the **B** form; this also explains why it is less favorable than the **A** form, in contrast to the **E** or **O** tautomers of 2-phenacylpyridines and –quinolines which possess the stabilizing hydrogen bond.

The main ions are listed in Table 7 [III]. The specific fragmentations of Cl-substituted compounds are presented in Scheme 7.

The molecular ions exhibit the base peaks. Common ions for all compounds **3a–j** were $[M-H]^+$, $[M-CO]^+$, $C_9H_9N_4^+$ (corresponding to **3d** ions $C_{10}H_{11}N_4^+$ and **3j** ions $C_9H_9N_4Cl^+$), Ar^+ , $C_3H_4NO^+$, $HOCN^+$ and $C_2H_4N^+$. Generally the RAs of common ions generally varied very little for differently substituted compounds. The RA of $[M-H]^+$ was low for all compounds. No OH loss was detected; this could be an indication of the absence of the 3-OH form. CO losses were observed (RA <15%) for all compounds except for **3b** with *o*-Me substituent. For other *ortho*-substituted compounds the RA of $[M-CO]^+$ was low. For Cl-substituted compounds an Ar group migration to triazine ring after CO loss was observed; this was confirmed by losses of $C_2H_5N_2^+$, $C_3H_4N_2O$ and $C_3H_4N_3O^+$ and further fragmentations of the corresponding product ions (Scheme 7). The fragmentation involving $C_2H_5N_2^+$ loss cannot occur if the Ar group remains in its original position; an H-transfer is also required. Loss of $C_3H_4N_2O$ does not necessarily require H-transfer.

Table 7. Main ions, m/z (%), formed under EI at 70 eV from compounds **3a–j**

Compound	M^{+*}	[M–H] ⁺	[M–CO] ⁺	$C_9H_9N_4^+$	Ar ⁺	$C_3H_4NO^+$	HO CN^{+*}	$C_2H_4N^+$
m/z (%)								
3a (H)	230(100)	229(3)	202(15)	173(5)	77(22)	70(1.5)	43(3)	42(4)
3b (<i>o</i> -Me)	244(100)	243(3)	-	173(9) ^a 187(2.5) ^b	91(33)	70(3)	43(1)	42(9)
3c (<i>p</i> -Me)	244(100)	243(3.5)	216(10.5)	173(8) 187(2.5) ^b	91(12)	70(1)	43(4)	42(5)
3d (<i>o,m</i> -diMe)	258(100)	257(3)	230(0.3)	187(9) ^c	105(11)	70(3)	43(1)	42(7)
3e (<i>o</i> -OMe)	260(100)	259(3)	232(0.3)	173(8) 203(2) ^d	107(1)	70(2)	43(6)	42(5)
3f (<i>p</i> -OMe)	260(100)	259(1.4)	232(2.4)	173(1.4)	107(1)	70(1)	43(8)	42(4)
3g (<i>o</i> -Cl)	266(33) ^e 264(100) ^f	265(trace) 263(0.2)	238(1.2) 236(3.7)	173(12)	113(4) 111(14)	70(4)	43(7)	42(8)
3h (<i>m</i> -Cl)	266(33) ^e 264(100) ^f	265(2) 263(2.2)	238(4.4) 236(13.5)	173(15)	113(5) 111(15)	70(3)	43(2.5)	42(6)
3i (<i>p</i> -Cl)	266(32) ^e 264(100) ^f	265(1) 263(2)	238(3.5) 236(10.6)	173(11)	113(4) 111(13.5)	70(3)	43(2)	42(5)
3j (<i>m,p</i> -diCl)	302(11) ^g 300(66) ^h 298(100) ⁱ	301(1) 299(2.3) 297(1.6)	274(1.6) 272(8.2) 270(12.8)	209(3) ^j 207(8) ^k	149(2) 147(7) 145(12)	70(5)	43(4)	42(8)

^aContains 4% of $C_{10}H_{11}N_3^+$.^b $C_{10}H_{11}N_4^+$.^c $C_{10}H_{11}N_4^+ + C_{11}H_{13}N_3^+ 7:3$.^d $C_{10}H_{11}N_4O^+$.^eIons in this row contain one ³⁷Cl atom.^fIons in this row contain one ³⁵Cl atom.^gIons in this row contain two ³⁷Cl atoms.^hIons in this row contain one ³⁷Cl and one ³⁵Cl atom.ⁱIons in this row contain two ³⁵Cl atoms.^j $C_9H_8N_4^{37}Cl^+ \cdot C_9H_8N_4^{35}Cl^+$.

The fragmentations involving the losses of CO and COCO generally prove the prevalence of the amido form in the gas phase, and the absence of $[M-OH]^+$ is a sign that no relevant amount of the imidol form is present. The minor amounts of $[M-HCO]^+$ (RA 0–2%) may be indicative of the unfavorable imidol form. Due to the lack of H atoms near the OH group and also because of the ring structure, the usual rearrangements and fragmentations, such as the loss of H₂O, that would support the presence of the imidol form cannot occur.

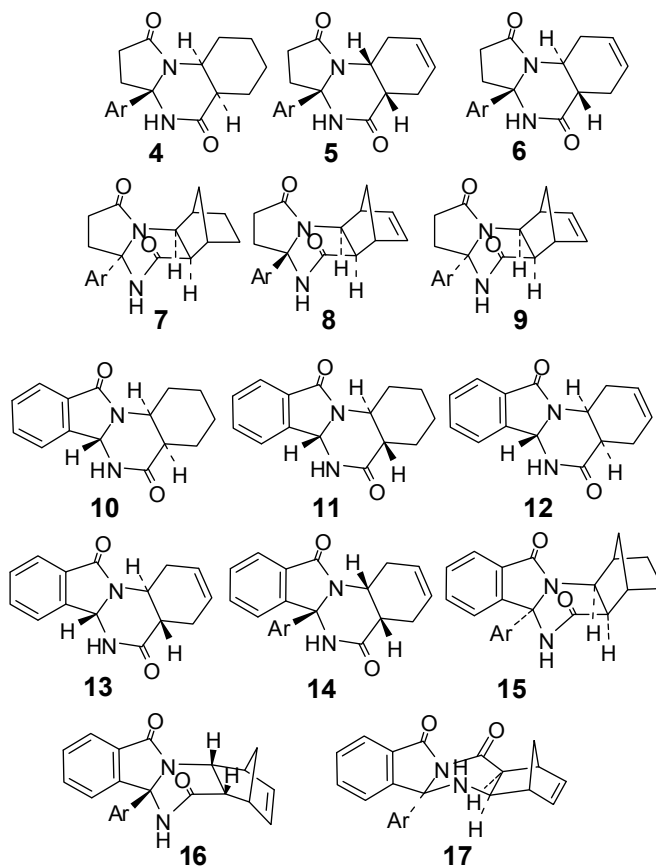
4.3 Pyrrolo- and isoindoloquinazolinones 4–17 [III]

4.3.1. Structures and base peaks

The structures of pyrrolo- and isoindoloquinazolinones **4–17** are shown in Scheme 8 and the names of the compounds are given in Table 8. The set of pyrrolo- and

isoindoloquinazolinones was studied in order to obtain information on the stereochemistry of annulated heterocyclic compounds **5,6,10,11,12** and **13**. The effects of unsaturated rings and of aromatic groups on the fragmentations were additionally investigated. The compounds studied might possibly participate in amide-imidol tautomerism. However, no indication of such tautomerism was detected.

For **6** and **11** the molecular ion, and for **10** $[M-H]^+$ was the base peak. The other common base peaks were due either to RDA-related fragmentations (**8,9,12,13,16** and **17**) or to loss of the Ar group (**7** and **15**). For **4** $[M-C_3H_5O]^+$, for **5** $[M-C_4H_6-C_6H_4Cl]^+$ and for **14** $[M-C_6H_4CH_3-C_4H_6]^+$ were the base peaks. The RAs of the molecular ions were weak for compounds containing fused norbornane or norbornene skeletons (**7,8,9,15,16** and **17**).



Ar = *p*-chlorophenyl (**4-9**) or *p*-tolyl (**14-17**)

Scheme 8. Structures of compounds **4-17**, pyrroloquinazolinones (**4-9**) and isoindoloquinazolinones (**10-17**), or partly saturated pyrroloquinazolinones (**4-6**), benzologs (**10-14**), methylene-bridged derivatives (**7-9**, **15** and **16**) and a bisacyl compound (**17**).

Table 8. Names of compounds 4–17.

4	Pyrrolo[1,2- <i>a</i>]quinazoline-1,5-dione, 3a-(4-chlorophenyl)decahydro-, (3aR,5aR,9aS)-rel-
5	Pyrrolo[1,2- <i>a</i>]quinazoline-1,5-dione, 3a-(4-chlorophenyl)-2,3,3a,4,5a,6,9,9a-octahydro-, (3aR,5aS,9aR)-rel-
6	Pyrrolo[1,2- <i>a</i>]quinazoline-1,5-dione, 3a-(4-chlorophenyl)-2,3,3a,4,5a,6,9,9a-octahydro-, (3aR,5aS,9aS)-rel-
7	6,9-Methanopyrrolo[1,2- <i>a</i>]quinazoline-1,5-dione, 3a-(4-chlorophenyl)decahydro-, (3aR,5aS,6R,9S,9aR)-rel-
8	6,9-Methanopyrrolo[1,2- <i>a</i>]quinazoline-1,5-dione, 3a-(4-chlorophenyl)-2,3,3a,4,5a,6,9,9a-octahydro-, (3aR,5aR,6R,9S,9aS)-rel-
9	6,9-Methanopyrrolo[1,2- <i>a</i>]quinazoline-1,5-dione, 3a-(4-chlorophenyl)-2,3,3a,4,5a,6,9,9a-octahydro-, (3aR,5aS,6S,9R,9aR)-rel-
10	Isoindolo[2,1- <i>a</i>]quinazoline-5,11-dione, 1,2,3,4,4a,6,6a,12a-octahydro-, (4aR,6aS,12aS)-rel-
11	Isoindolo[2,1- <i>a</i>]quinazoline-5,11-dione, 1,2,3,4,4a,6,6a,12a-octahydro-, (4aR,6aR,12aR)-rel-
12	Isoindolo[2,1- <i>a</i>]quinazoline-5,11-dione, 1,4,4a,6,6a,12a-hexahydro-, (4aR,6aS,12aS)-rel-
13	Isoindolo[2,1- <i>a</i>]quinazoline-5,11-dione, 1,4,4a,6,6a,12a-hexahydro-, (4aR,6aR,12aR)-rel-
14	Isoindolo[2,1- <i>a</i>]quinazoline-5,11-dione, 1,4,4a,6,6a,12a-hexahydro-6a-(4-methylphenyl)-, (4aR,6aR,12aS)-rel-
15	1,4-Methanoisoindolo[2,1- <i>a</i>]quinazoline-5,11-dione, 1,2,3,4,4a,6,6a,12a-octahydro-6a-(4-methylphenyl)-, (1R,4S,4aR,6aR,12aS)-rel-
16	1,4-Methanoisoindolo[2,1- <i>a</i>]quinazoline-5,11-dione, 1,4,4a,6,6a,12a-hexahydro-6a-(4-methylphenyl)-, (1R,4S,4aR,6aR,12aS)-rel-
17	6,9-Methanoisoindolo[1,2- <i>b</i>]quinazoline-10,12-dione, 4b,5,5a,6,9,9a-hexahydro-4b-(4-methylphenyl)-, (4bR,5aR,6R,9S,9aS)-rel-

4.3.2 Non-RDA-related stereospecific fragmentations

The loss of an Ar group was observed for cyclohexane-, cyclohexene- and norbornane-fused compounds but not for norbornenes. Of these the cyclohexene derivatives **5** and **14**, in which the Ar group and the annelation H atoms were *cis* to each other, had the least abundant ions $[M-Ar]^+$, with RA = 19% and 30%, respectively.

Stereoisomers **5** and **6** have clearly different EI spectra (Fig. 34, Table 9). The molecular ion and the ion $[M-Ar]^+$ were more abundant for **6**. Other ions differentiating **5** and **6** were $[M-C_7H_8NO]^+$ ($C_{10}H_9NO^{35}Cl^+$), $[M-C_3H_5O]^+$ ($C_{14}H_{12}N_2O_2^{35}Cl^+$), $[M-NH_3CO]^+$ ($C_{16}H_{14}NO^{35}Cl^+$) and $C_4H_7N_2O^+$. The ion $[M-NH_3]^{++}$ was slightly more abundant for **5**. The elemental composition of $[M-NH_3]^{++}$ was confirmed by accurate mass measurements to be $C_{17}H_{14}NO_2^{35}Cl^{++}$, but clarification of the mechanism of its formation would require extensive isotope labeling.

Table 9. Selected EI-induced ions of stereoisomers **5** (*cis*) and **6** (*trans*) and their isotope-corrected RAs.

	M^{++}	$[M-C_6H_4Cl]^+$	$[M-C_7H_8NO]^+$	$[M-C_3H_5O]^+$	$[M-NH_3CO]^+$	$C_4H_7N_2O^+$	$[M-NH_3]^{++}$
5	318(21)	205(19)	196(15)	261(4)	273(8)	99(8)	301(2)
	316(70)		194(50)	259(17)	271(27)		299(6)
6	318(31)	205(58)	196(30)	259(3)	273(2)	99(27)	301(<1)
	316(100)		194(96)		271(5)		299(2)

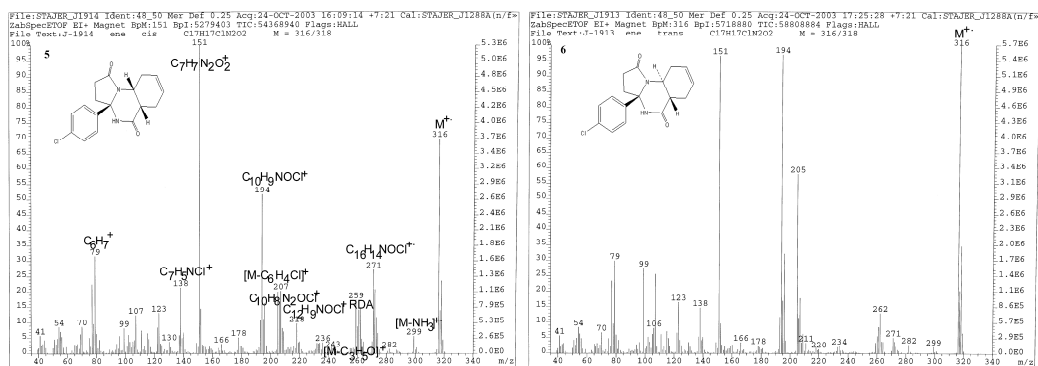


Figure 34. The EI mass spectra of **5** and **6**.

For pyrrolo[2,1-*b*][1,3]oxazin-6-one derivatives [131] with *cis* annelation hydrogens, the loss of $C_3H_5O^{\bullet}$ was more favored than for the *trans* forms. This is suggested to involve a regio-specific H-transfer to the carbonyl oxygen [131]. For **5** and **6**, a corresponding fragmentation mechanism was observed. From the structure in Fig. 35, it can be seen that the *cis* form should favor H-transfer to the carbonyl oxygen more than the *trans*. In fact, a more abundant $[M-C_3H_5O]^+$ is observed for **5** than for **6**. In comparison **4** contains a flexible cycloalkane ring, and $[M-C_3H_5O]^+$ is the base peak. Norbornane-containing compound **7** likewise fragmented by the loss of $C_3H_5O^{\bullet}$. The loss of $C_7H_5O^{\bullet}$ for benzo-fused compounds, corresponding to the loss of $C_3H_5O^{\bullet}$ without benzo-fusion, was missing completely.

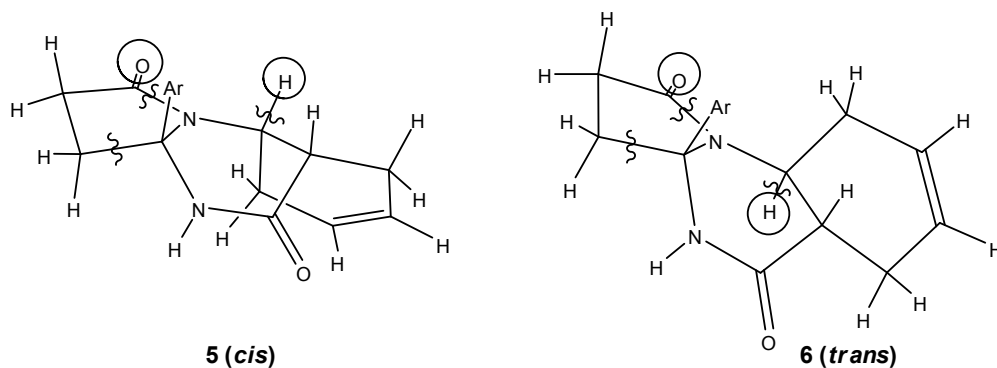


Figure 35. A structural explanation for the stereoselective loss of $C_3H_5O^{\bullet}$ from **5** and **6**. Structures are optimized using MM2 minimum energy calculations.

The structures of **5** and **6** reveal that the cyclohexene ring in **6** causes more steric strain in the C₆H₄Cl group, and as a consequence the ions [M-C₆H₄Cl]⁺ and [M-C₇H₈NO]⁺ are more abundant for the *trans* isomer. These two fragmentations are useful for differentiating stereoisomers.

For benzo-fused compounds, the ion C₈H₇NO⁺⁺ at *m/z* 133, i.e. a possible 2,3-dihydro-1H-isoindol-1-one radical cation (Fig. 36) was observed for **10–13**; for *trans* **11**, this was slightly more favorable than for *cis* **10**. C₈H₇NO⁺⁺ has also been observed for pyrrolo[2,1-*b*][1,3]oxazin-6-ones [131].

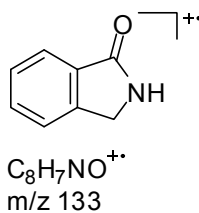


Figure 36. The 2,3-dihydro-1H-isoindol-1-one radical cation (C₈H₇NO⁺⁺).

Stereoisomers **10** and **11** were also distinguishable (Table 10, Fig. 37). The loss of NH₃ from the molecular ion was more abundant for **11** (with *trans* annelation H atoms). The composition of [M-NH₃]⁺⁺ was confirmed (C₁₅H₁₃NO₂⁺⁺) by accurate scans, but the mechanism for its formation is unknown. [M-C₃H₇]⁺ and [M-C₂H₅]⁺ were more abundant for **11**. From the structures of **10** and **11**, it can be seen that the cyclohexane ring in the *cis* form **10** favors the *twist-boat* conformation, whereas the *trans* form **11** favors the *chair* conformation (Fig. 38). This may be the reason for the difference in the RAs of [M-C₃H₇]⁺ and [M-C₂H₅]⁺.

Table 10. Selected EI-induced ions of stereoisomers **10** (*cis*) and **11** (*trans*) and their isotope-corrected RAs.

	M^{+}	$[M-H]^{+}$	$[M-NH_3]^{+}$	$[M-C_2H_5]^{+}$	$[M-C_3H_7]^{+}$
10	256(97.5)	255(100)	239(4.5)	227(6)	213(20)
11	256(100)	255(82)	239(46)	227(23)	213(74)

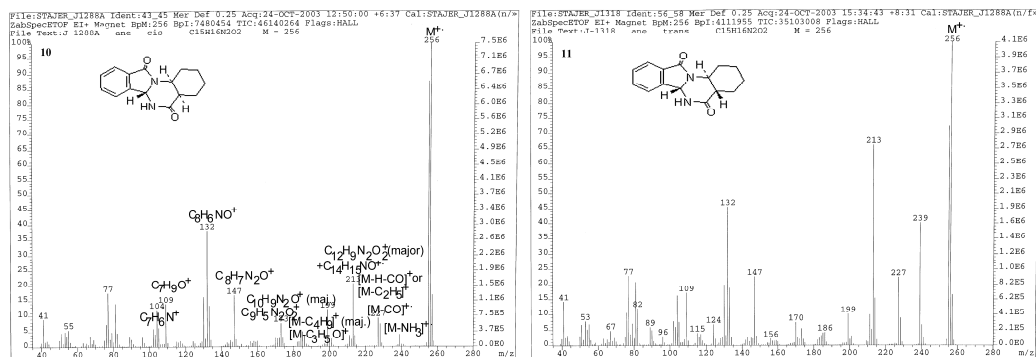


Figure 37. The EI mass spectra of **10** and **11**.

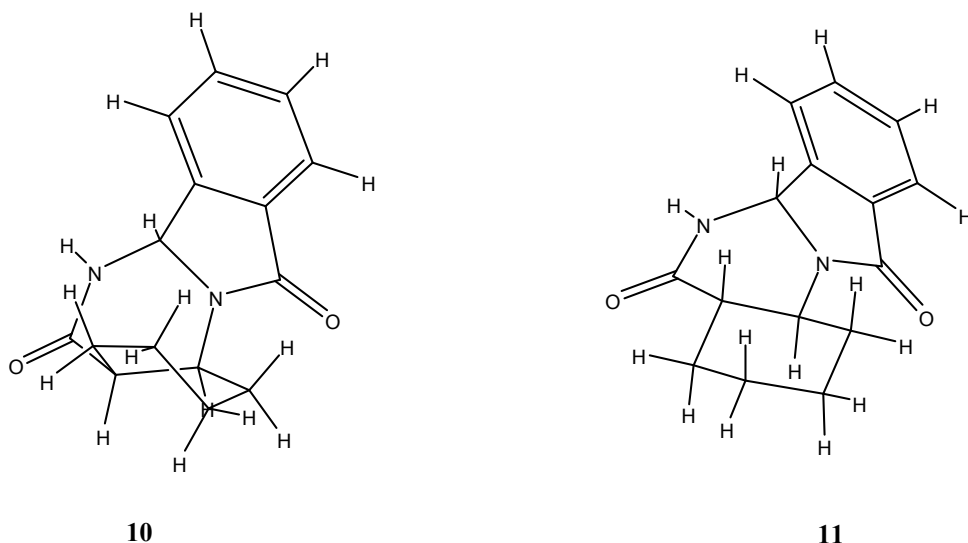


Figure 38. MM2 optimized minimum energy structures of **10** and **11**.

For stereoisomers **12** and **13**, the difference was not so clear. The ions $[M-NH_3]^{++}$ (RA 6% and 1% respectively), $C_{14}H_{11}NO^{++}$ (RA 4% and 1% respectively), and those at m/z 182 ($C_{13}H_{12}N^+$ for **12** 3.5% and $C_{12}H_8NO^+$ for **12** 3%, traces for **13**) were slightly more abundant for **12**, but in general the RAs were very close to each another.

The relative configuration of the Ar group had no effect on the fragmentation of norbornene-fused compounds **8** and **9**.

4.3.3 RDA-related fragmentations

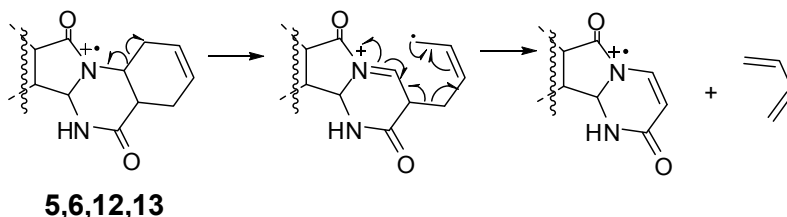
Of the studied compounds, saturated **4,7,10,11** and **15** cannot exhibit RDA-related fragmentations [III]. The RDA fragmentation may be highly stereospecific, and it was therefore considered possible to distinguish the stereoisomers via different RAs of RDA-related fragmentations.

Compounds containing fused cyclohexene rings gave RDA fragments $[M-C_4H_6]^{++}$. The RDA fragmentations for the cyclohexene-fused stereoisomers **5,6** and **12,13** were non-stereospecific. Additionally for **12** and **13** the base peak corresponded to the non-stereospecific (RDA-H)- type fragmentation, leading to the ion $[M-C_4H_7]^+$.

Norbornene-fused compounds exhibit fragment ions $[M-C_5H_5]^+$, resulting from RDA fragmentation with H-transfer (RDA+H). For the stereoisomeric pair **8** and **9**, this fragmentation proved to be non-stereospecific, i.e. the configuration of the Ar group did not cause any stereospecificity. For norbornene-fused 2,3-dihydrothiazolo[3,2-*a*]pyrimidin-5-ones and 3,4-dihydropyrimido[2,1-*b*]thiazin-6-ones RDA+H fragmentations were observed, together with normal RDA fragmentations [132].

It is interesting to note that the RDA fragmentations were highly stereospecific for the pyrrolo[2,1-*b*][1,3]oxazin-6-one derivatives [131], but not for the structurally similar pyrrolo- and isoindoloquinazolinones. This is probably caused by stepwise fragmentation with ring opening involving the CO group (Scheme 9). This ring opening may be similar

to that of *trans*-3,4,4a,5,8,8a-hexahydro-8a-1(2*H*)-naphthalenone (or *trans*- Δ^6 -octalone-1) [98a].

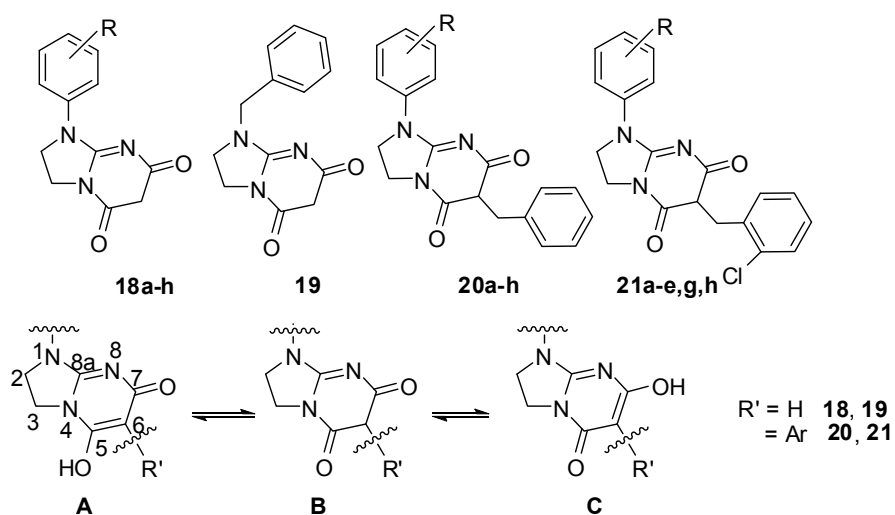


Scheme 9. Possible mechanism for stepwise RDA of pyrrolo- and isoindoloquinazolinones.

The lack of stereospecificity of RDA or related fragmentations suggests a stepwise RDA mechanism, at least for compounds **5**, **6**, **12** and **13**. For the compounds containing a norbornene group, **8** and **9**, RDA+H was more favored than the formation of $[M-R]^+$ ($R = H, C_6H_4CH_3$ or C_6H_4Cl). The molecular ions of bicyclic compounds are not very stable, which is the case for the norbornene and norbornane compounds. The favored RDA-type fragmentations may be caused by the greater release of the ring strain energy of norbornene-fused compounds under fragmentation. As compared with the ring strain energy of cyclohexene, which is estimated to be -1.3 to 10.5 kJ mol^{-1} , the ring strain energy of norbornene is very large: 80.4 – 90.4 kJ mol^{-1} . In comparison, the ring strain of cyclohexane is 0 – 5.7 kJ mol^{-1} and that of the norbornane ring is 60.3 – 69.5 kJ mol^{-1} [133]. The RDA+H process, where the charge remains on the protonated dienophile, seems to be a general feature of bicyclo[2.2.1]heptene compounds with carbonyl, amide, ester or imide substituents at positions 5 and 6 [134,135]. It has been suggested that the driving force for the H-migration for the RDA+H process is the relative stability of the neutral fragment, i.e. the cyclopentadienyl radical [136]. It has further been observed that, for norbornenes RDA-related fragmentations seem to be energetically more favored than the Ar loss. $[M-Ar]^+$ was the base peak for norbornane derivatives **7** and **15**, whereas this ion was missing from norbornene derivatives.

4.4 Aryl- and benzyl-substituted 2,3-dihydroimidazo[1,2-*a*]pyrimidine-5,7-(1*H*,6*H*)-diones 18–21 [IV]

The Ar-substituted pyrimidinediones **18–21** (Scheme 10) were studied by using EIMS and NMR methods [IV]. Compound **20d** was previously has been studied by crystallographic methods; it exists as the 7-hydroxy-5-oxo tautomer in the solid state. This OH-tautomer affects the formation of strong intermolecular resonance-assisted H-bonding, in the solid crystal [71]. However in the gas phase stabilization of the OH-form by intermolecular H-bonding cannot occur. In the gas phase the intermolecular bonds that hold the molecules together in the solid or the liquid state are usually broken during vaporization. No peaks due to dimers or polymers were seen in the EI mass spectra of **18–21**.



Scheme 10. Structures of compounds **18–21** and their possible tautomers **A**, **B** and **C**. **18**: 1-phenyl-2,3-dihydroimidazo[1,2-*a*]-pyrimidine-5,7(1*H*,6*H*)-diones, **19**: 1-benzyl-2,3-dihydroimidazo[1,2-*a*]-pyrimidine-5,7(1*H*,6*H*)-dione, **20**: 6-benzyl-1-phenyl-2,3-dihydroimidazo[1,2-*a*]-pyrimidine-5,7(1*H*,6*H*)-diones, **21**: 6-(*o*-chlorobenzyl)-1-phenyl-2,3-dihydro-imidazo[1,2-*a*]pyrimidine-5,7(1*H*,6*H*)-diones. **18a–h**, **19**, **20a–h** and **21a–e,g,h** (R = **a**: H, **b**: 2-Me, **c**: 4-Me, **d**: 2-OMe, **e**: 4-OMe, **f**: 2-Cl, **g**: 3-Cl, **h**: 4-Cl). The numbering used for the assignment of the NMR signals is depicted for **A**.

The common fragmentations are shown in Tables 11-13. Abundant molecular ion peaks were seen for compounds **18–20**, except for **19** and *o*-Cl-substituted **18f**. Compounds **21** gave weak molecular ions, caused by the ready loss of *o*-Cl. Loss of substituent R[•] was also very strong for *o*-OMe substituted **18d**. Various fragmentations related to CO groups were observed. CO loss from the molecular ion was found for **18** and **19**. For the 6-benzyl-substituted pyrimidinediones **20**, the ion [M-CO]⁺⁺ co-existed with [M-C₂H₄]⁺⁺ with the same nominal mass, with the *p*-Cl derivative **20h** having the most [M-C₂H₄]⁺⁺ and the *o*-OMe derivative **20d** the most [M-CO]⁺⁺; generally, the compounds with electron-accepting substituents (**20f–h**) slightly favored C₂H₄ loss, whereas compounds with electron-donating substituents favored CO loss. For **20**, ions [M-HCO]⁺ were detected, co-existing with [M-C₂H₅]⁺. However, [M-HCO]⁺ was always preferred to [M-C₂H₅]⁺. CO or HCO[•] loss was not detected for **21**.

The ion [M-COCHCO]⁺⁺ (or [M-COCCOH]⁺⁺) and/or its complementary ion at *m/z* 69 was present in the spectra of compounds **18** and **19**. Also losses of CH_{1.3}CO^(•) too were detected. Losses of substituent R[•] and C₃O₂ from the molecular ion were seen for *o*-substituted compounds. The ion C₉H₁₀N₃⁺ formed at *m/z* 160 was observed for **18b** (RA 4%), **18d** (30.5%) and **18f** (33%) and also for **18a** (4%). For **19**, carbon suboxide C₃O₂ was lost after the loss of C₇H₇[•], i.e. tropylium radical, leading to the ion C₃H₆N₃⁺ (RA 4%). The tropylium ion C₇H₇⁺ also formed the base peak for **19**. For compounds **20**, a route [M-C₆H₅-C₃O₂]⁺ requiring skeletal rearrangements was confirmed. For **20a–e**, an interesting fragmentation was the direct loss of C₁₀H₈O₂, i.e. (CO)₂CHCH₂C₆H₅ or C₁₀H₇O₂[•]. For **20**, fragmentations involving the loss of the moiety (CO)CHCH₂C₆H₅ and (±H) (i.e. C₉H_{7.9}O^(•)) from the molecular ion were seen. For compounds **21** similar losses of neutral fragments C₉H_{6.8}OCl^(•) were detected, the precursor ions being [M-Cl-C₆H₄]⁺ or [M-C₆H₄Cl]⁺.

Table 11. Common ions, m/z (RAs mostly $\geq 4\%$), for **18a–h** and **19**. RAs are isotope-corrected for ^{13}C , **18b, d** are renormalized. RAs are rounded to the nearest half per cent.

		m/z (% RA)									
M^{+}	M^{+}	$[\text{M}-\text{CO}]^{+}$	$[\text{M}-\text{CO}]^{+}$	$[\text{M}-\text{CHCO}]^{+}$	$[\text{M}-\text{CH}_2\text{CO}]^{+}$	$[\text{M}-\text{CH}_3\text{CO}]^{+}$	$[\text{M}-\text{COCHCO}]^{+}$	$[\text{M}-\text{R}]^{+}$	$[\text{M}-\text{R}-\text{COCCO}]^{+}$		
18a	229(100)	228(6)	201(15.5)	188(60)	187(19)	186(20)	160(4)	228(6)	160(4)	160(4)	
18b	243(100)	242(52)	201(3)	202(24)	201(6)	200(16)	174(14)	228(9)	160(4)	160(4)	
18c	243(100)	242(7)	215(14)	202(54)	201(25)	200(18)	174(4)	–	160(1)	160(1)	
18d	259(100)	258(13)	231(3)	218(33.5)	217(13)	216(23)	190(4)	228(89)	160(30.5)	160(30.5)	
18e	259(100)	258(4)	231(8)	218(34)	217(30)	216(9.5)	–	228 (trace)	160(2)	160(2)	
18f	265(20)	264(2)	237(3)	224(15)	223(4)	222(9)	196(2)	228(100)	160(33)	160(33)	
	263(65)	262(2)	235(9)	222(48)	221(13)	220(26)	194(5)	–	–	–	
18g	265(30)	264(2)	237(6)	224(23)	223(7)	222(5)	196(1)	–	–	–	
	263(100)	262(5)	235(19)	222(74)	221(20)	220(16)	194(4)	–	–	–	
18h	265(30)	264(3)	237(5)	224(17)	223(8)	222(5)	196(1,8)	–	–	–	
	263(100)	262(5)	235(16)	222(54)	221(24)	220(14)	194(4)	–	–	–	
19	243(56)	242(14)	215(1)	202(3)	201(3)	200(3)	174(5)	$[\text{M}-\text{C}_7\text{H}_7]^{+}$	84(4)	84(4)	
								152(9)			

Table 12. Common ions, m/z (RAs mostly $\geq 4\%$), for **20a–h**. RAs are isotope-corrected for ^{13}C , **20a–c,f–h** are renormalized. RAs are rounded to the nearest half per cent.

	M^{++}	m/z (% RA)										
		[M–H] ⁺	[M–CO/C ₂ H ₄] ⁺⁺ ; [M–CO] ⁺⁺ : [M–C ₂ H ₄] ⁺⁺	[M–HCO/C ₂ H ₅] ⁺	[M–C ₆ H ₅] ⁺	[M–C ₆ H ₅ –CO] ⁺	[M–C ₉ H ₉ O] ⁺	[M–C ₉ H ₈ O] ⁺⁺ ; [M–C ₉ H ₉ O] ⁺	[M–C ₁₀ H ₇ O ₂] ⁺	[M–C ₁₀ H ₈ O ₂] ⁺⁺	[M–R] ⁺	C ₇ H ₇ ⁺ C ₆ H ₅ ⁺
20a	319(100)	318(17.5)	291(3), 1:1	290(9.5), 10:3	242(50)	214(12)	160(6)	188(17.5)	187(17)	159(2)	318(17.5)	91(32)
20b	333(100)	332(21)	305(1); 5:3	304(7), 6:1	256(45)	228(5)	174(7)	202(9.5)	201(10.5)	173(2)	318(2)	77(45.5)
20c	333(100)	332(21)	305(3); 3:4	304(8), 4:1	256(50)	228(10.5)	174(5)	202(16)	201(22)	173(1)	318(trace)	91(31)
20d	349(100)	348(18)	321(1); 5:1	320(4), 10:1	272(47)	244(5)	190(3)	218(8)	217(13.5)	159(1)	318(10)	91(17)
20e	349(100)	348(14)	321(4), 7:10	320(8.5), 6:1	272(45.5)	244(12)	190(4.5)	218(16.5)	217(24)	189(1.5)	318(trace)	91(26)
20f	355(25) 353(100)	354(8) 352(16.5)	327(1) 325(4); 4:5	326(2) 324(7), 2:1	278(13) 276(44)	250(3) 248(9)	194(5)	224(4)	223(4)	193(trace)	318(2)	91(26)
20g	355(25) 353(100)	354(6) 352(18)	327(1) 325(3); 2:3	326(2) 324(7.5), 2:1	278(13.5) 276(45)	250(3) 248(9)	194(5)	224(5)	223(5)	193(trace)	318(2)	91(23)
20h	355(28)	354(6)	327(1)	326(2)	278(13.5)	250(3)	194(4)	224(4.5)	224(4.5)	159(0.5)	318(2)	91(21)

Table 13. Common ions, m/z (RAs mostly $\geq 4\%$), for **21a–e,g,h**. RAs are isotope-corrected for ^{13}C . RAs are rounded to the nearest half per-cent.

M^+	m/z (% RA)									
	$[\text{M}-\text{Cl}]^+$	$[\text{M}-\text{HCl}]^{+*}$	$[\text{M}-\text{H}-\text{HCl}]^+$	$[\text{M}-\text{Cl}-\text{C}_6\text{H}_4]^{+*}$	$[\text{M}-\text{C}_9\text{H}_6\text{OCl}]^+$	$[\text{M}-\text{C}_9\text{H}_7\text{OCl}]^{+*}$	$[\text{M}-\text{C}_9\text{H}_8\text{OCl}]^+$	$\text{C}_7\text{H}_6\text{Cl}^+$	Other ions	
21a	318(100)	317(2.5)	316(4)	242(4)	188(3)	187(3)	186(2.5)	125(3)	$[\text{M}-\text{Cl}]^{2+}$: 158.5(3), 77(10)	
21b	332(100)	331(4)	330(3.5)	256(5)	202(3)	201(2)	200(3)	125(4)	118(4), 117(4), 91(10), 65(5)	
21c	332(100)	331(4)	330(6)	256(5)	202(5)	201(5)	200(2)	125(4)	$\text{C}_9\text{H}_6\text{OCl}^+$: 165(4), 120(4), 91: C_7H_7^+ (4) + $\text{C}_6\text{H}_5\text{N}^{+}(6)$, 65(4) $\text{C}_9\text{H}_8\text{N}_3\text{O}^+$: 174(3.5), 120: $\text{C}_7\text{H}_6\text{NO}^+(5)$, 77(5)	
21d	348(100)	347(3)	346(4)	272(4.5)	218(2.5)	217(3)	216(2.5)	125(6.5)	136(4.5), 77(5)	
21e	348(100)	347(3.5)	346(5.5)	272(5)	218(5)	217(6)	216(2)	125(4.5)	111(4.5)	
21g	389(1)	353(2) ^a	352(-) ^b	278(1)	224(1)	223(1)	222(0.5)	125(6)		
	387(1)	352(100)	350(4)	276(3)	222(3.5)	221(2.5)	220(2)			
21h	389(1)	354(30)	353(5) ^a	278(1)	224(1)	223(1)	222(0.5)	125(6)	318(3.5), 111(5.5), 75(5)	
	387(1.5)	352(100)	350(6)	276(4)	222(4)	221(3.5)	220(2)			

^aCalculated value after removal of ^{13}C isotopic peak.^bImpossible to resolve $[\text{M}-\text{H}-\text{HCl}]^+$ with ^{37}Cl from $[\text{M}-\text{Cl}]^+$ with ^{35}Cl .

The formation of $[M-OH]^+$ was detected only for compounds **20a–h**, but their RAs were low. The OH and HCO[•] losses may indicate the presence of the enol tautomer in **20**, in contrast with 8-aryl-3,4-dioxo-2H,8H-6,7-dihydroimidazo[2,1-*c*][1,2,4]triazines (**18a–j**) where the keto form was indicated by the lack of $[M-OH]^+$ and $[M-HCO]^+$. Similar fragmentations, involving the losses of $CH_{1.3}CO^{(+)}$ (**18** and **19**), $C_9H_{7.9}O^{(+)}$ (**20**), and $C_9H_6.8OCl^{(+)}$ (**21**), which require the migration of H-atoms, may indicate different tautomeric forms.

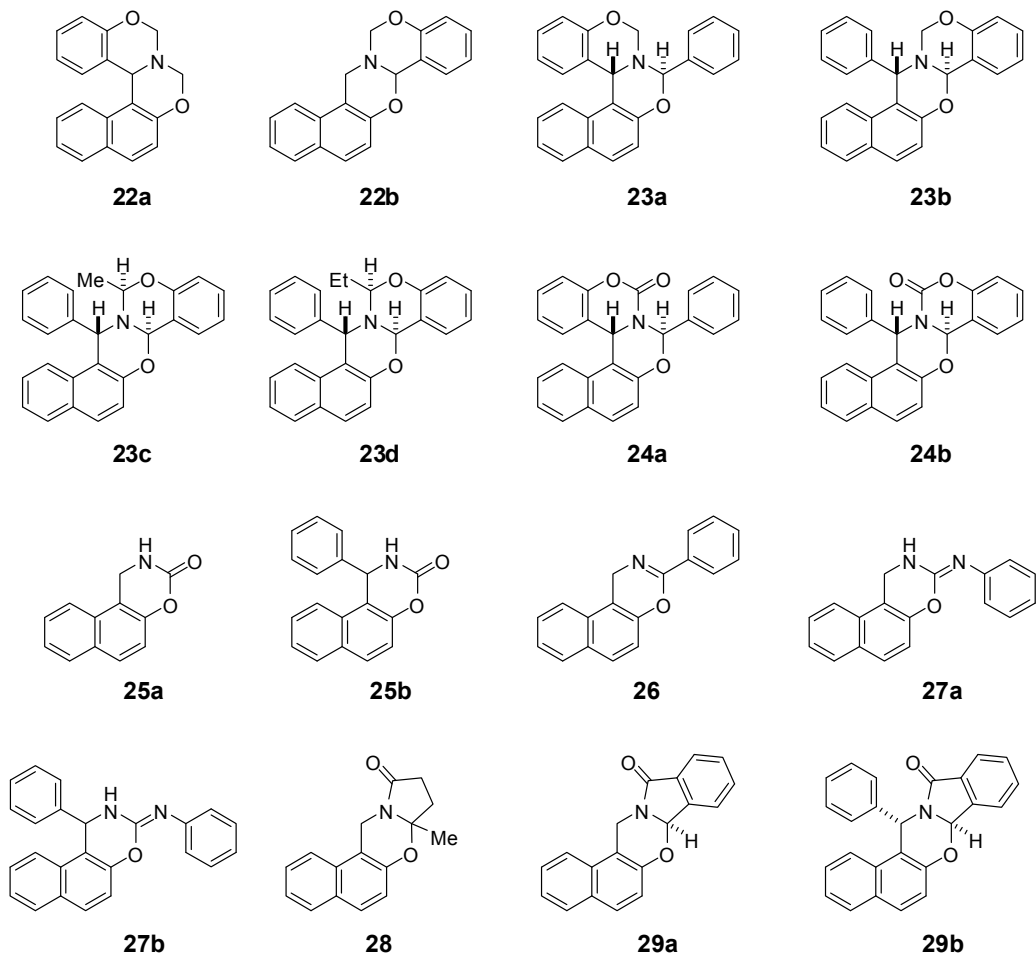
The ¹H and ¹³C NMR spectra of **18a,d,g**, **19**, **20d,g** and **21d,g**, measured in DMSO-*d*₆ solution at 298 K, show the presence of the 5-OH or 7-OH form, but not the dioxo form. The weak NOESY correlation between the OH peak and the 1-Ar substituent indicates that either 7-OH-5-oxo form or the spectral average of 7-OH and 5-OH forms prevails if the interconversion is fast on the NMR time scale). Only for compound **19** was a small amount of dioxo-form present, i.e. 5% of that of the OH form, based on the integrated intensities.

For **3a–j**, the predominance of the keto form was supported by fragmentations involving the losses of CO and COCO but not those of OH or HCO. Similarly, for **18–21** no fragmentations related to the Ar group migration were found. In conclusion, in view of the fragmentations requiring H-migrations involving the CO groups, and also the presence of the ions $[M-OH]^+$ and/or $[M-HCO]^+$, it appears that some amount of enol is present for **18–21**. This is most clearly seen for **18d**, **19** and **20**. In comparison with crystallographic and NMR methods, it can be concluded that the intermolecular H-bonding in the enol form is the main stabilizing effect, which is lost in the gas phase.

4.5 Naphthoxazine, naphthpyrrolo-oxazinone and naphthoxazino-benzoxazine derivatives 22–29 [V]

4.5.1 General fragmentations

The structures of **22–29** are presented in Scheme 11, and the names in Table 14.

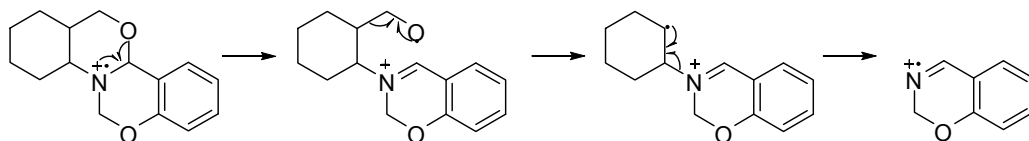


Scheme 11. Naphthoxazinobenzoxazines (**22a**, **22b**, **23a–d**, and **24a,b**), naphth-oxazines (**25a,b**, **26** and **27a,b**) and naphthpyrrolo-oxazinones (**28** and **29a,b**).

Table 14. The names of compounds **22–29**

22a	Naphth[1',2':5,6][1,3]oxazino[3,4- <i>c</i>][1,3]benzoxazine
22b	Naphth[1',2':5,6][1,3]oxazino[3,2- <i>c</i>][1,3]benzoxazine
23a	(8 <i>R</i> *,15 <i>bS</i> *)-8-Phenylnaphth[1',2':5,6][1,3]oxazino[3,4- <i>c</i>][1,3]benzoxazine
23b	(7 <i>aR</i> *,15 <i>S</i> *)-15-Phenyl-7 <i>aH</i> ,13 <i>H</i> ,15 <i>H</i> -naphth[1',2':5,6][1,3]oxazino[3,2- <i>c</i>][1,3]benzoxazine
23c	(7 <i>aR</i> *,13 <i>R</i> *,15 <i>S</i> *)-13-Methyl-15-phenyl-7 <i>aH</i> ,13 <i>H</i> ,15 <i>H</i> -naphth[1',2':5,6][1,3]oxazino[3,2- <i>c</i>][1,3]benzoxazine
23d	(7 <i>aR</i> *,13 <i>R</i> *,15 <i>S</i> *)-13-Ethyl-15-phenylnaphth[1',2':5,6][1,3]oxazino[3,2- <i>c</i>][1,3]benzoxazine
24a	(8 <i>R</i> *,15 <i>bS</i> *)-8-Phenylnaphth[1',2':5,6][1,3]oxazino[3,4- <i>c</i>][1,3]benzoxazin-10-one
24b	(7 <i>aR</i> *,15 <i>S</i> *)-15-Phenylnaphth[1',2':5,6][1,3]oxazino[3,2- <i>c</i>][1,3]benzoxazin-13-one
25a	2,3-Dihydro-1 <i>H</i> -naphth[1,2- <i>e</i>][1,3]oxazin-3-one
25b	1-Phenyl-2,3-dihydro-1 <i>H</i> -naphth[1,2- <i>e</i>][1,3]oxazin-3-one
26	3-Phenyl-1 <i>H</i> -naphth[1,2- <i>e</i>][1,3]oxazine
27a	3-Phenylimino-2,3-dihydro-1 <i>H</i> -naphth[1,2- <i>e</i>][1,3]oxazine
27b	1-Phenyl-3-Phenylimino-2,3-dihydro-1 <i>H</i> -naphth[1,2- <i>e</i>][1,3]oxazine
28	7 <i>a</i> -Methyl-8,9-dihydro-7 <i>aH</i> ,10 <i>H</i> ,12 <i>H</i> -naphth[1,2- <i>e</i>]pyrrolo[2,1- <i>b</i>][1,3]oxazin-10-one
29a	7 <i>aH</i> ,12 <i>H</i> ,14 <i>H</i> -Naphth[1',2':5,6][1,3]-oxazino[2,3- <i>a</i>]isoindol-12-one
29b	(7 <i>aR</i> *,14 <i>S</i> *)-14-Phenyl-7 <i>aH</i> ,12 <i>H</i> ,14 <i>H</i> -naphth[1',2':5,6][1,3]oxazino[2,3- <i>a</i>]isoindol-12-one

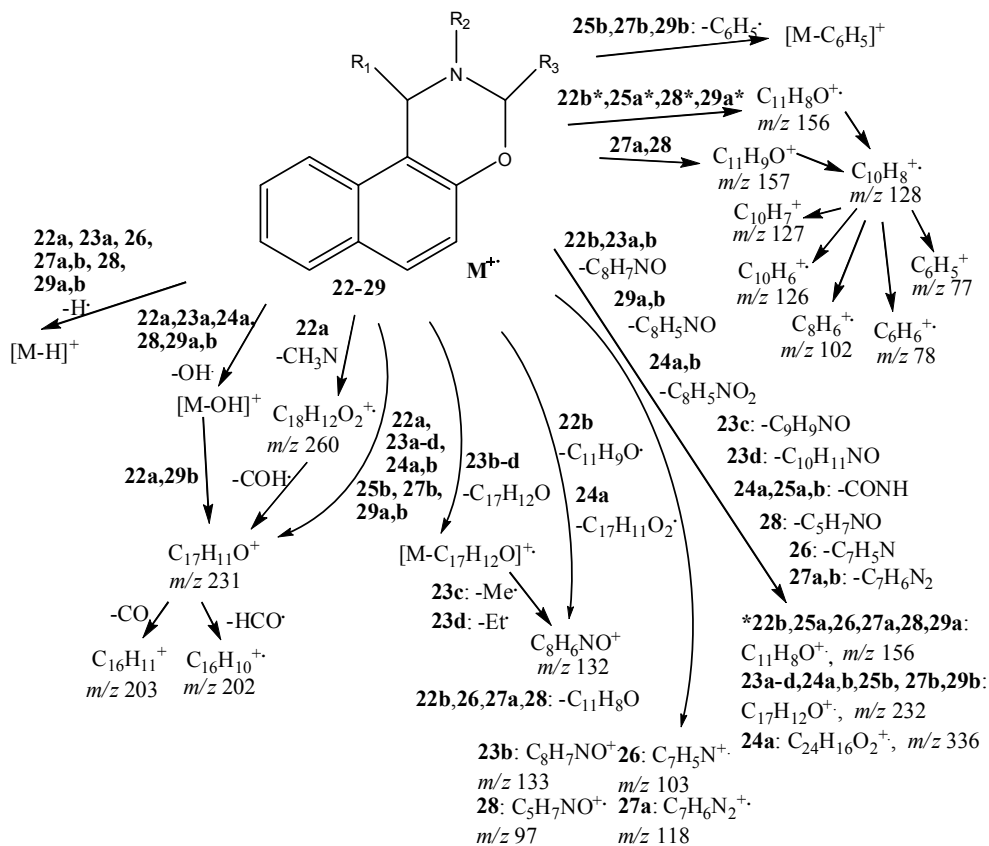
The 1,3-oxazine ring has been widely studied for ring-chain tautomeric equilibria. The compounds studied, **22–29**, cannot exhibit ring-chain tautomerism, but mass spectrometric fragmentations involving ring openings are possible, such as the one observed for 3,1-benzoxazino[1,2-*c*]-[1,3]benzoxazines (Scheme 12) [137].



Scheme 12. An example of the fragmentation of 3,1-benzoxazino[1,2-*c*]-1,3-benzoxazine involving ring opening.

Naphthoxazine (**22a,b**, **23a–d** and **24a,b**), naphthpyrrolo-oxazinone (**25a,b**, **26** and **27a,b**) and naphthoxazinobenzoxazine (**28** and **29a,b**) derivatives were studied to screen regioisomeric effects. The effects of functional groups (CO and alkyl groups and phenylimino groups) were also investigated [V]. Three regioisomeric pairs were available: **22a/b**, **23a/b** and **24a/b**. The compounds **22a,b**, **24a**, **23b,c** and **29b** have been subjected to NMR spectroscopy, molecular modeling and geometry optimization [123,124].

The general fragmentations are shown in Scheme 13 and the common ions in Table 15. The compounds derived from the Betti base 1-(α -aminobenzyl)-2-naphthol (**22a**, **23b–d**, **24a,b**, **25b**, **27b**, **29b**) had the base peak at m/z 231 ($C_{17}H_{11}O^+$), which also gave a medium strong peak for **23a**. The molecular ion formed the base peak for **23a**, **28** and **29a**. For **26**, the base peak was the ion $C_{11}H_8O^+$, and for **27a** it was $C_{11}H_9O^+$. **22b** and **25a** had the base peak at m/z 128 ($C_{10}H_8^+$). The latter radical cation was abundant for 1-aminomethyl-2-naphthol derivatives (**22b**, **25a**, **26**, **27a**, **28** and **29a**), and was obtained via the loss of CO from $C_{11}H_8O^+$.



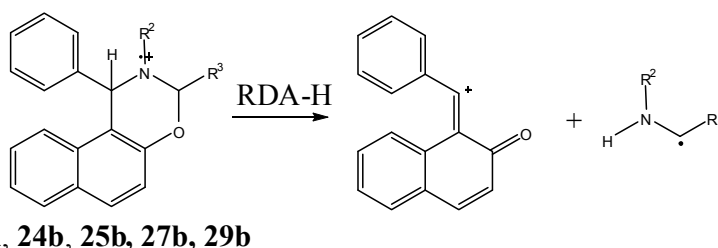
Scheme 13. The general fragmentation routes of compounds 22–29.

Table 15. Common ions for **22–29** and their RAs m/z (% RA). RAs are corrected for ^{13}C isotopes and those of **22b**, **25a**, **27a** and **29a** have been renormalized. RAs are rounded to the nearest half per cent.

Compound	M ⁺	m/z (% RA)									
		[M – H] ⁺	[M – OH] ⁺	[M – CONH] ⁺	[M – CONH ₂] ⁺	C ₁₇ H ₁₂ O ⁺	C ₁₇ H ₁₁ O ⁺	C ₁₆ H ₁₁ ⁺	C ₁₆ H ₁₀ ⁺	C ₁₁ H ₉ O ⁺	C ₁₀ H ₈ ⁺
22a	289(82.5)	288(32.5)	272(33)	-	232(1)	231(100)	203(2)	202(8)	-	128(1.5)	
22b	289(6)	-	-	-	-	-	-	-	157(2.5)	128(100)	
23a	365(100)	364(4)	348(67.5)	-	232(3)	231(27)	202(8)	202(8)	-	-	
23b	365(5.5)	-	-	-	232(23)	231(100)	203(3)	202(21)	-	-	
23c	379(3)	-	-	-	232(22)	231(100)	203(3)	202(22)	-	-	
23d	393(2.5)	-	-	-	232(24)	231(100)	203(3)	202(22)	-	-	
24a	379(36.5)	-	362(4)	336(9)	232(12)	231(100)	202(9)	202(9)	-	-	
24b	379(10.5)	-	-	-	232(24)	231(100)	203(3)	202(15)	-	-	
25a	199(46)	-	-	156(96)	-	-	-	-	157(4)	128(100)	
				155(4)					156(96)		
25b	275(31)	-	-	232(19)	232(19)	231(100)	203(3)	202(14)	-	-	
				231(100)							
26	259(54)	258(2)	-	-	-	-	203(3)	202(14)	-	128(70)	
27a	274(68)	273(32)	-	-	-	-	-	-	156(100)	128(76)	
27b	350(29)	349(4.5)	-	-	232(16)	231(100)	203(3)	202(15)	156(40)	128(2)	

For **23b–d**, **24b**, **25b**, **27b** and **29b** the mechanism for the formation of the ion $C_{17}H_{11}O^+$ at m/z 231 and a nitrogen radical is presented in Scheme 14. The fragmentation corresponds to an RDA-H and it is exceptional since the charge does not remain on the nitrogen. For **22a**, **23a** and **24a**, however, the fragmentation mechanism is more complicated, because it requires a cleavage of a benzo-bound oxygen bond. For **22a**, **23a** and **24**, an abundant ion $[M-C_{17}H_{11}O_2]^+$ is also formed (Table 16, p. 86), i.e. the ion containing the nitrogen has a positive charge. For **23b–d** a nitrogen radical cation $[M-C_{17}H_{12}O]^+$ was also formed, although the RAs were low.

For **29b**, $C_{17}H_{11}O^+$ was also formed by a loss of C_8H_5N from $[M-OH]^+$; for **22a**, a minor route to $C_{17}H_{11}O^+$ consisted in C_2H_3N loss from $[M-OH]^+$. For **22a**, the loss of COH^{\bullet} from $[M-CH_3N]^+$ gave the ion $C_{17}H_{11}O^+$, as confirmed by B^2/E scans.

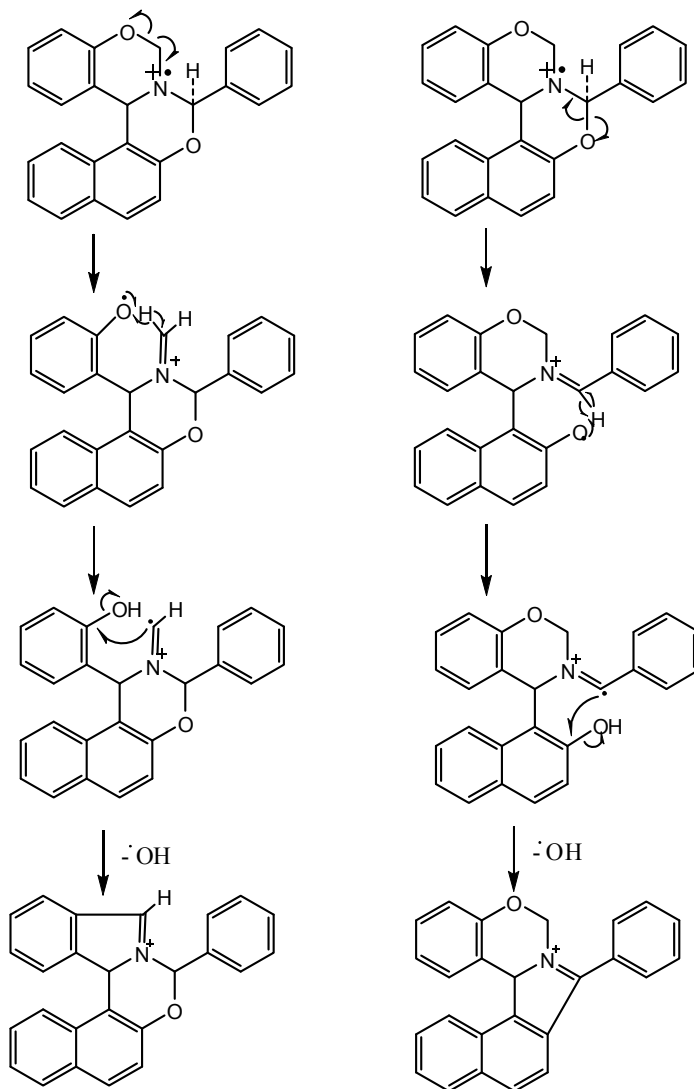


Scheme 14. The formation of $C_{17}H_{11}O^+$ from **23b–d**, **24b**, **27b** and **29b**.

The ion $C_{17}H_{11}O^+$ (**22a**, **23a–d**, **24a,b**, **25b**, **27b** and **29b**) at m/z 231 can lose CO and HCO^{\bullet} , the product ions being $C_{16}H_{11}^+$ and $C_{16}H_{10}^{+\bullet}$, respectively. $C_{11}H_8O^+$ (**22b**, **25a**, **26**, **27a**, **28** and **29a**) gave analogously the ions $C_{10}H_8^{+\bullet}$ and $C_{10}H_7^+$.

Very weak CO loss was detected only for compounds **28** and **29a**. For **22a**, **23a**, **24a**, **28**, **29a**, and **29b**, the ion $[M-OH]^+$ had RAs between 4 and 67.5%, being most abundant for **22a**, **23a**, **28** and **29a**. This fragmentation requires H-migration and ring opening, and solving the exact mechanism would require deuterium labeling. Suggested mechanisms for OH^{\bullet} loss from **23a** are presented in Scheme 15. For **23a**, the B/E scans of $[M-OH]^+$

gave no significant signals; the ion therefore appears to be unusually stable, the positive charge probably being stabilized by aromatic groups.



Scheme 15. Possible ring openings of **23a** and the consequent OH loss.

4.5.2 Comparison of regioisomers

22a–24a are derivatives of 1-(α -aminobenzyl)-2-naphthol, while **22b–24b** are derivatives of 1-aminomethyl-2-naphthol, the mass spectra of these regioisomeric pairs were

expected to be very different. The ions useful for differentiating the regioisomers **22a–24a** vs **22b–24b** are listed in Table 16.

Table 16. Ions useful for differentiating regioisomeric pairs (**22–24**)a/b and their RAs.

Ion	22a	22b	23a	23b	24a	24b
M ⁺	82.5	6	100	5.5	36.5	10.5
[M–OH] ⁺	33	-	67.5	-	4	-
C ₁₇ H ₁₁ O ₂ ⁺	22	-	6	-	13	-
C ₁₆ H ₁₀ O ⁺	11	-	6	-	7	-
C ₁₅ H ₉ ⁺	19	-	6	-	10	-
C ₈ H ₇ NO ⁺	52	-	14	-	-	-
C ₁₇ H ₁₁ O ⁺	100	-	27	100	100	100
C ₁₀ H ₈ ⁺	1.5	100	-	-	-	-
C ₈ H ₆ NO ⁺	-	25	-	7	52	-
C ₇ H ₅ O ⁺	-	13	-	5	5	-
C ₆ H ₅ ⁺	-	20	-	6	18	-

Also only for **23a**: C₈H₈N⁺ (77) and C₇H₇⁺ (44)

The formation mechanism of [M–OH]⁺ may be different for **22a**, **23a** and **24a**. For **22a** and **23a** the OH loss may involve ring opening (Scheme 15). The formation of the ion [M–OH]⁺ from **24a** may be due to the geometry since the tertiary α -hydrogen vicinal to Ph group can migrate to the CO oxygen (Figure 39). The formation of the ions C₇H₅O⁺ and C₁₇H₁₁O₂⁺ may be affected by the *boat* form of the benzo-bound oxazine ring. On the other hand the tertiary α -H migration is unfavorable for **24b** (Figure 40). It should be noted that the configuration of the H-atoms in the calculated structure corresponding to the global energy minimum for **24a** in Ref. [124] was incorrect; hence the structure in Figure 39 was established by using MM2 minimum energy optimization.

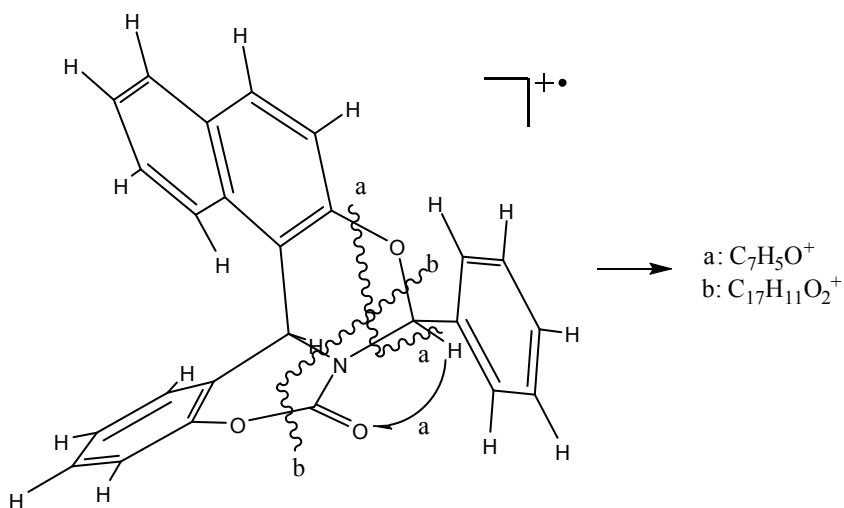


Figure 39. Suggested formation of ions $\text{C}_7\text{H}_5\text{O}^+$ (a) and $\text{C}_{17}\text{H}_{11}\text{O}_2^+$ (b) from **24a**. Structure was optimized by using MM2 minimum energy calculations.

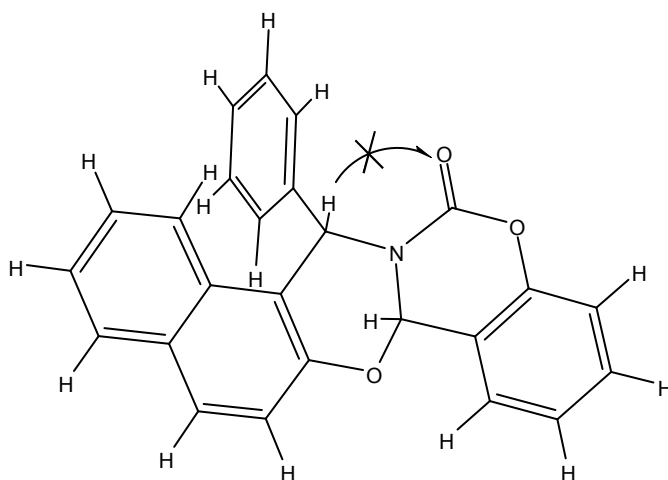


Figure 40. MM2 optimized minimum energy structure for **24b**. The migration of H-atom to CO oxygen is not favorable.

4.5.3 Effect of substituents

Me- (**23c**) and Et-substituted (**23d**) compounds yielded very similar spectra. The fragments $\text{C}_9\text{H}_9\text{NO}^{+\bullet}$ and $\text{C}_{10}\text{H}_{11}\text{NO}^{+\bullet}$ were formed exclusively from **23c** or **23d**, respectively. These ions also lost Me^\bullet or Et^\bullet and the product ion $\text{C}_8\text{H}_6\text{NO}^+$ was more

abundant for **23d**. The spectra of **25a** and its Ph analog **25b** differed as expected. Accordingly, for **25a** the base peak was given by the ion $C_{10}H_8^{++}$ and for **25b** by the ion $[M-CONH_2]^+$, i.e. $C_{17}H_{11}O^+$. For **25a** the RA of $[M-CONH_2]^+$ was only 4%, but that of $[M-CONH]^{++}$ was 96%.

Compound **27a** furnished an abundant ion $[M-H]^+$ and its Ph analog **27b** an abundant ion $[M-Ph]^+$, both giving weak ions $[M-HNPh]^+$. However, **27a** did not give the ion $[M-Ph]^+$, which would require the cleavage of the Ph-N bond, therefore for **27b** an α cleavage of the Ph-C bond explains the relatively abundant Ph \cdot loss.

4.5.4 Fragmentations of 1-(α -aminobenzyl)-2-naphthol and 1-aminomethyl-2-naphthol derivatives

The ions useful for identifying 1-(α -aminobenzyl)-2-naphthol (**22a**, **23b-d**, **24a,b**, **25b**, **27b** and **29b**) and 1-aminomethyl-2-naphthol (**22b**, **25a**, **26**, **27a**, **28** and **29a**) derivatives are listed in Table 17. The ions $C_{17}H_{12}O^{++}$, $C_{17}H_{11}O^+$, $C_{11}H_8O^{++}$ and $C_{17}H_{11}O_2^+$ and the complementary ions $[M-C_{17}H_{12}O]^{++}$, $[M-C_{11}H_8O]^+$ and $[M-C_{17}H_{11}O_2]^+$ were formed logically from the structures studied. For **24b**, **25a,b**, **27b** and **29a,b** (i.e. the structures with CO or imino substituents, except **28**), the complementary ions were not seen.

Table 17. RAs of ions $C_{17}H_{12}O^{2+}$, $C_{17}H_{11}O^+$, $C_{11}H_8O^{2+}$ and $C_{17}H_{11}O_2^+$ and their complementary ions for 22–29.

Ion	22a	22b	23a	23b	23c	23d	24a	24b
$C_{17}H_{12}O^{2+}$	1	-	3	23	22	24	12	24
$C_{17}H_{11}O^+$	100	-	27	100	100	100	100	100
$C_{11}H_8O^+$	-	51	-	-	-	-	-	-
$C_{17}H_{11}O_2^+$	22	-	6	-	-	-	13	-
$[M-C_{17}H_{12}O]^{2+}$	-	-	-	14	11	6	-	-
$[M-C_{17}H_{11}O_2]^+$	78	-	77	-	-	-	52	-
$[M-C_{11}H_8O]^+$	-	52	-	-	-	-	-	-

Ion	25a	25b	26	27a	27b	28	29a	29b
$C_{17}H_{12}O^{2+}$	-	19	-	-	16	-	2	14
$C_{17}H_{11}O^+$	96	100	100	40	100	72	26.5	100
$C_{11}H_8O^+$	-	-	-	-	-	-	-	-
$C_{17}H_{11}O_2^+$	-	-	-	-	2	-	-	-
$[M-C_{17}H_{12}O]^{2+}$	-	-	-	-	-	-	-	-
$[M-C_{17}H_{11}O_2]^+$	-	-	-	-	-	-	-	-
$[M-C_{11}H_8O]^+$	-	-	5	15	-	28	-	-

5. CONCLUSIONS

The EIMS revealed linear correlations of the Hammett σ constants and the RAs and/or % TICs of the ions for variously substituted 2-phenacylpyridines **1a–n** and 2-phenacylquinolines **2a–h**. The substituents therefore clearly affected the fragmentations.

The strongest electron donors presumably favor form **K**, while the electron acceptors favor form **O** (**1a–n**) or **E** (**2a–h**) as in solution or in the solid state. The OH loss is expected to occur from form **E** or **O**. The increasing RAs of the molecular ion and $[M-H]^+$ may indicate the increase of forms **E** and **O**, because the molecular ion is often more abundant for enol than for keto tautomers. Besides intramolecular H-bonds, the **E** or **O** tautomers are possibly stabilized by the resonance effect of the Ph ring substituents.

For **1a–n** and **2a–h** the % TIC of $ArCO^+$ appeared to be an indicator for form **K**, as were those of $[M-Ar]^+$ for forms **E** and **O**. The losses of CO and HCO^\bullet also seemed to be related to forms **E** and **O**. $[M-CO]^{++}$ correlated with the Hammett σ constants for **1a–h**, but not for **2a–h**; this may be caused by the different conjugation of forms **O** and **E**.

For dioxoimidazotriazines **3a–j** and pyrimidinediones **18–21**, the tautomerism was not clear. For **3a–j** and **18–21**, the substituents had only minor effects on the ion RAs. For **3a–j**, the lack of OH loss and the fragmentations involving the losses of CO and COCO show that the amido form predominates in the gas phase, though the fragmentations involving the loss of HOCN may indicate a small amount of the enol form. On the other hand, **18–21** exhibit $[M-OH]^+$ peaks and many of the observed fragmentations require H-migrations; thus at least a small amount of the enol form appears to be present.

For pyrrolo- and isoindoloquinazolinones **4–17**, the geometries of the molecules affected the fragmentations. Stereospecific fragmentations were observed most clearly for stereoisomeric pairs **5,6** and **10,11**. However, the RDA-related fragmentations were non-stereospecific, indicating a stepwise mechanism, the first step possibly involving the CO group-induced ring opening.

Conclusions

Naphthoxazine derivatives **22–29** displayed some regiospecific fragmentations, which were useful for differentiating regioisomers with the same nominal mass. The regiospecific pairs (**22–24**)**a/b** could be clearly distinguished by using the RAs of the ions M^{+} , $[M-OH]^+$, $C_{17}H_{11}O_2^+$, $C_{16}H_{10}O^+$ and $C_{15}H_9^+$. The compounds derived from 1-(α -aminobenzyl)-2-naphthol generally gave a strong peak at m/z 231 ($C_{17}H_{11}O^+$), while the 1-aminomethyl-2-naphthol derivatives exhibited an ion at m/z 156 ($C_{11}H_8O^+$) instead. This is useful for identifying regioisomeric compounds with the same nominal masses.

6. REFERENCES

- [1] Fessenden RJ, Fessenden JS, Logue MW. "Organic Chemistry 6th edition", Brooks/Cole Publishing Company, USA, 1998, p. 578.
- [2] Watson JD, Crick FHC. "Molecular Structure of Nucleic Acids: A Structure for Deoxyribose Nucleic Acid", *Nature*, 1953; **171**: 737–738.
- [3] Watson JD. "The Double Helix", Penguin Books, New York, USA, 1968.
- [4] Terent'ev PB, Kalandarishvili AG. "Application of Mass Spectrometry for the Analysis of Organic Tautomeric Compounds", *Mass Spectrom. Rev.*, 1996; **15**: 339–363.
- [5] Pullman B, Berthod H, Dreyfus M. "Amine-Imine Tautomerism in Adenines", *Theoret. Chim. Acta (Berl.)*, 1969; **15**: 265–268.
- [6] Imperiali B, O'Connor SE, Hendrickson T, Kellenberger C. "Chemistry and biology of asparagine-linked glycosylation", *Pure Appl. Chem.*, 1999; **71**: 777–787.
- [7] Daniels M. "Tautomerism of Uracil and Thymine in Aqueous Solution: Spectroscopic Evidence", *Proc. Nat. Acad. Sci. USA*, 1972; **69**: 2488–2491.
- [8] Allegretti PE, de las Mercedes Schiavoni M, Castro EA, Furlong JJP. "Tautomeric Equilibria Studies by Mass Spectrometry", *Nature Precedings*, 2008: <<http://hdl.handle.net/10101/npre.2008.1842.1>>
- [9] Minkin VI, Garnovskii DG, Elguero J, Katritzky AR, Denisko OV. "The tautomerism of heterocycles: Five-membered rings with two or more heteroatoms", *Adv. Heterocycl. Chem.*, 2000; **76**: 157–323.

- [10] Alkorta I and Elguero J. “Theoretical estimation of the annular tautomerism of indazoles”, *J. Phys. Org. Chem.*, 2005; **18**: 719–724.
- [11] Lindsay Smith JR, Sadd JS. “Isomerism of 1- and 2-(N,N-disubstituted aminomethyl)benzotriazoles. Investigation by nuclear magnetic resonance spectroscopy”, *J. Chem. Soc., Perkin Trans. I.*, 1975; **12**: 1181–1184.
- [12] Lutsenko IF. “O- and C-isomeric organoelement derivatives of keto-enol systems: rearrangements and elementotropism”, *Pure Appl. Chem.*, 1972; **30**: 409–426.
- [13] Alkorta I, Goya P, Elguero J, Singh SP. “A simple approach to the tautomerism of aromatic heterocycles. A Review”, *Natl. Acad. Sci. Lett.*, 2007; **30**: 139–159.
- [14] Shurukhin YV, Klyuev NA, and Grandberg II. “Similarities Between Thermolysis And Mass Spectrometric Fragmentation Of Tetrazoles (Review)”, *Chem. Heterocycl. Comp.*, 1985; **21**: 605–620.
- [15] a) Juhász M, Lázár L, Fülöp F. “Substituent effects in the ring-chain tautomerism of 4-alkyl-2-aryl substituted oxazolidines and tetrahydro-1,3-oxazines”, *J. Heterocycl. Chem.*, 2007; **44**: 1465–1473.
- b) Juhász M, Fülöp F, Pihlaja K. “Substituent effects on the gas-phase ring-chain tautomerism of 3,4,5,6-tetrahydro-2H-1,3-oxazines”, *Rapid Commun. Mass Spectrom.*, 2007; **21**: 3701–3710.
- c) Pihlaja K, Juhász M, Kivelä H, Fülöp F. “Substituent effects on the ring-chain tautomerism of some 1,3-oxazolidine derivatives”, *Rapid Commun. Mass Spectrom.*, 2008; **22**: 1510–1518.
- d) Vainiotalo P, Ronkanen S, Fülöp F, Pihlaja K. “Gas-Phase Ring-Chain Tautomerism in 1,3-oxazolidines”, *Tetrahedron*, 1990; **46**: 3683–3692.
- e) Vainiotalo P, Fulöp F, Pihlaja K. “Gas-phase Ring-chain Tautomerism in 1,3-Oxazines. Does it exist?“, *Org. Mass Spectrom.*, 1991; **26**: 438–442.

- f) Vainiotalo P, Fulöp F, Bernath G, Pihlaja K “Mass Spectrometric Intramolecular Cyclization Reactions of Some 2-N-Phenyliminoperhydro-1,3-oxazines”, *J. Heterocyclic Chem.*, 1989; **26**: 1453–1459.
- g) Vainiotalo P, Savolainen P-L, Ahlgrén M, Mälkönen PJ, Vepsäläinen J. ”Identification of the Condensation Products of 1,2- and 1,3-Amino Alcohols with Keto Esters by NMR Spectroscopy, Mass Spectrometry and X-Ray Crystallography Studies. Open or Ring Forms?”, *J. Chem. Soc., Perkin Trans. 2*, 1991; **5**: 735–741.
- [16] Cope AC, Haven Jr AC, Ramp FL, Trumbull ER. “Cyclic Polyolefins. XXIII. Valence Tautomerism of 1,3,5-Cycloöctatriene and Bicyclo [4.2.0]octa-2,4-diene”, *J. Am. Chem. Soc.*, 1952; **74**: 4867–4871.
- [17] Doering W von E, Roth W. “A rapidly reversible degenerate Cope rearrangement Bicyclo[5.1.0]octa-2,5-diene”, *Tetrahedron*, 1963; **19**: 715–737.
- [18] Ault A. “The Bullvalene Story. The Conception of Bullvalene, a Molecule That Has No Permanent Structure”, *J. Chem. Educ.*, 2001; **78**: 924–927.
- [19] Schröder G. “Preparation and Properties of Tricyclo[3,3,2,0^{4,6}]deca-2,7,9-triene (Bullvalene)”, *Angew. Chem., Int. Ed. Eng.*, 1963; **2**: 481–482.
- [20] Postovskii I Ya, Bednyagina NP, Senyavina LB, Sheinker Yu N. “Study of the azide-tetrazole tautomerism by means of infrared spectroscopy” *Izvestiya Akademii Nauk SSSR, Seriya Fizicheskaya*, 1962; **26**: 1298–1300.
- [21] Klyuev NA, Adanin VM, Postovskii I Ya, Azev Yu A. “Mass-spectrometric study of azido-tetrazole tautomerism in the pyrimido-as-triazine series”, *Chem. Heterocyc. Comp.*, 1983; **19**: 451–453.
- [22] a) Kolehmainen E, Ośmiałowski B, Krygowski TM, Kauppinen R, Nissinen M, Gawinecki R. “Substituent and temperature controlled tautomerism: multinuclear

magnetic resonance, X-ray, and theoretical studies on 2-phenacylquinolines”, *J. Chem. Soc., Perkin Trans. 2*, 2000; **6**: 1259–1266.

b) Dewar MJS, Zoebisch EG, Healy EF, Stewart JJP. “Development and use of quantum mechanical molecular models. 76. AM1: a new general purpose quantum mechanical molecular model”, *J. Am. Chem. Soc.*, 1985; **107**: 3902–3909.

[23] Kolehmainen E, Ośmiałowski B, Nissinen M, Kauppinen R, Gawinecki R. “Substituent and temperature controlled tautomerism of 2-phenacylpyridine: the hydrogen bond as a configurational lock of (*Z*)-2-(2-hydroxy-2-phenylvinyl)pyridine”, *J. Chem. Soc., Perkin Trans. 2*, 2000; **11**: 2185–2191.

[24] Gawinecki R, Ośmiałowski B, Kolehmainen E and Kauppinen R. “Long-range substituent and temperature effect on prototropic tautomerism in 2-(acylmethyl)quinolines”, *J. Phys. Org. Chem.*, 2001; **14**: 201–204.

[25] Gawinecki R, Kuczek A, Kolehmainen E, Osmiałowski B, Krygowski TM, Kauppinen R. “Influence of Bond Fixation in Benzo-Annulated N-Salicylideneanilines and Their ortho-C(=O)X Derivatives (X = CH₃, NH₂, OCH₃) on Tautomeric Equilibria in Solution”, *J. Org. Chem.*, 2007; **72**: 5598–5607.

[26] Sztanke K, Fidecka S, Kędzierska E, Karczmarzyk Z, Pihlaja K, Matosiuk D. “Antinociceptive activity of new imidazolidine carbonyl derivatives. Part 4. Synthesis and pharmacological activity of 8-aryl-3,4-dioxo- 2*H*, 8*H*-6,7 -dihydroimidazo[2,1-*c*][1,2,4]triazines”, *Eur. J. Med. Chem.*, 2005; **40**: 127–134.

[27] Emsley J, Freeman NJ. “β-diketone interactions : Part 5. Solvent effects on the keto ⇌ enol equilibrium”, *J. Mol. Struct.*, 1987; **161**: 193–204.

[28] Yoshida Z, Ogoshi H, Tokumitsu T. “Intramolecular hydrogen bond in enol form of 3-substituted-2,4-pentanedione”, *Tetrahedron*, 1970; **26**: 5691–5697.

- [29] Simmons T, Love RF, Kreuz KL, "The Structure of α -Nitro Ketones", *J. Org. Chem.*, 1966; **31**: 2400–2401.
- [30] Fontana A, De Maria P, Siani G, Pierini M, Cerritelli S, Ballini R. "Equilibrium Constants for Ionisation and Enolisation of 3-Nitrobutan-2-one", *Eur. J. Org. Chem.* 2000; **8**: 1641–1646.
- [31] Carey ARE, Eustace S, More O'Ferrall RA, Murray BA. "Keto-enol and imine-enamine tautomerism of 2-, 3-, and 4-phenacylpyridines", *J. Chem. Soc., Perkin Trans. 2*, 1993; **11**: 2285–2296.
- [32] Katritzky AR, Kucharska HZ, Rowe JD. "Potentially tautomeric pyridines. VI. 2-, 3-, and 4-Phenacylpyridines", *J. Chem. Soc.*, 1965; 3093–3096.
- [33] More O'Ferrall RA, Murray A, "1H and 13C NMR spectra of α -heterocyclic ketones and assignment of keto, enol and enamionone tautomeric structures", *J. Chem. Soc., Perkin Trans. 2*, 1994; **12**: 2461–2470.
- [34] Gawinecki R, Kolehmainen E, Loghmani-Khouzani H, Osmiałowski B, Lovász T and Rosa P. "Effect of π -electron delocalization on tautomeric equilibria - benzoannulated 2-phenacylpyridines", *Eur. J. Org. Chem.* 2006, **12**, 2817–2824.
- [35] Greenhill JV, Loghmani-Khouzani H, Maitland DJ. "Tautomerism in ketomethyl quinolines. Part 3. 4-Ketomethylquinolines", *Can. J. Chem.*, 1991; **69**: 696–701.
- [36] Hammett LP. "The Effect of Structure upon the Reactions of Organic Compounds. Benzene Derivatives", *J. Am. Chem. Soc.*, 1937; **59**: 96–103.
- [37] Taft Jr RW. "Polar and Steric Substituent Constants for Aliphatic and *o*-Benzoate Groups from Rates of Esterification and Hydrolysis of Esters", *J. Am. Chem. Soc.*, 1952; **74**: 3120–3128.

- [38] Taft Jr RW, Lewis IC. "The General Applicability of a Fixed Scale of Inductive Effects. II. Inductive Effects of Dipolar Substituents in the Reactivities of *m*- and *p*-Substituted Derivatives of Benzene", *J. Am. Chem. Soc.*, 1958; **80**: 2436–2443.
- [39] Taft Jr RW, Lewis IC. "Evaluation of Resonance Effects on Reactivity by Application of the Linear Inductive Energy Relationship-IV. Hyperconjugation Effects of Para-alkyl Groups", *Tetrahedron*, 1959; **5**: 210–232.
- [40] Taft Jr RW, Lewis IC. "Evaluation of Resonance Effects on Reactivity by Application of the Linear Inductive Energy Relationship. V. Concerning a σ_R Scale of Resonance Effects", *J. Am. Chem. Soc.*, 1959; **81**: 5343–5352.
- [41] Carey FA, Sundberg RJ. "Structural Effects on Stability and Reactivity" in "Advanced organic chemistry Part A: Structure and Mechanisms, 5th edition", Springer Science, USA, 2007, p. 253–388.
- [42] Wilcox CF, Leung C. "Transmission of Substituent Effects. Dominance of Field Effects", *J. Am. Chem. Soc.*, 1968; **90**: 336–341.
- [43] Dewar MJS, Marchand AP. "Substituent Effects. V. Further Evidence Concerning the Nature of the Inductive Effect", *J. Am. Chem. Soc.*, 1966; **88**: 354–358.
- [44] Liotta CL, Fisher WF, Greene Jr GH, and Joyner BL. "Mechanism of Transmission of Nonconjugative Substituent Effects. IV. Analysis of the Dissociation Constants of 6-Substituted Spiro [3.3] heptane-2-carboxylic Acids", *J. Am. Chem. Soc.*, 1972; **94**: 4891–4897.
- [45] Roberts JD, Moreland Jr WT. "Electrical Effects of Substituent Groups in Saturated Systems. Reactivities of 4-Substituted Bicyclo [2.2.2]octane-1-carboxylic Acids", *J. Am. Chem. Soc.*, 1953; **75**: 2167–2173.

- [46] Grob CA, Schlageter MG. "The Derivation of Inductive Substituent Constants from pKa Values of 4-Substituted Quinuclidines. Polar effects. Part I" *Helv. Chim. Acta.*, 1976; **59**: 264–276.
- [47] Hansch C, Leo A, Taft RW. "A Survey of Hammett Substituent Constants and Resonance and Field Parameters", *Chem. Rev.*, 1991; **97**: 165–195.
- [48] Swain CG, Lupton Jr EC. "Field and resonance components of substituent effects", *J. Am. Chem. Soc.*, 1968; **90**: 4328–4337.
- [49] Taft RW, Topsom RD. "The Nature and Analysis of Substituent Electronic Effects", *Prog. Phys. Org. Chem.*, 1987; **16**: 1–83.
- [50] Brown HC, Okamoto Y. "Electrophilic Substituent Constants", *J. Am. Chem. Soc.*, 1958; **80**: 4979–4987.
- [51] Seydel JK. "Prediction of in Vitro Activity of Sulfonamides, Using Hammett Constants or Spectrophotometric Data of the Basic Amines for Calculation", *Mol. Pharmacol.*, 1966; **2**: 259–265.
- [52] Sharma P, Sharma S, Rane N. "Synthesis and in vitro antimicrobial activities of 2-hydroxy-6-methyl-7-(arylamino)-1,7-dihydropurin-8-ones", *Bioorg. Med. Chem.*, 2004; **12**: 3135–3139.
- [53] Fukuto TR, Metcalf RL. "Pesticidal Activity And Structure: Structure and Insecticidal Activity of Some Diethyl Substituted Phenyl Phosphates", *J. Agr. Food Chem.*, 1956; **4**: 930–935.
- [54] a) Hansch C. "A Quantitative Approach to Biochemical Structure-Activity Relationships", *Acc. Chem. Res.*, 1969; **2**: 232–239.

b) Leo A, Hansch C, Elkins D. "Partition coefficients and their uses", *Chem. Rev.* 1971; **71**: 525–616.

[55] Kohen A, Klinman JP. "Enzyme Catalysis: Beyond Classical Paradigms", *Acc. Chem. Res.*, 1998; **31**: 397–404.

[56] Watson JD, Crick FHC. "Genetical implications of the structure of deoxyribonucleic acid", *Nature*, 1953; **171**: 964–967.

[57] Topal MD, Fresco JR. "Complementary base pairing and the origin of substitution mutations", *Nature*, 1976; **263**: 285–289.

[58] Harris VH, Smith CL, Cummins WJ, Hamilton AL, Adams H, Dickman M, Hornby DP, Williams DM. "The Effect of Tautomeric Constant on the Specificity of Nucleotide Incorporation during DNA Replication: Support for the Rare Tautomer Hypothesis of Substitution Mutagenesis", *J. Mol. Biol.*, 2003; **326**: 1389–1401.

[59] Podolyan Y, Gorb L, Leszczynski J. "Rare Tautomer Hypothesis Supported by Theoretical Studies: Ab Initio Investigations of Prototropic Tautomerism in the *N*-Methyl-P Base", *J. Phys. Chem. A*, 2005; **109**: 10445–10450.

[60] Fedor LR. "Acid-catalyzed hydrolysis of (R)-C[(1-methyl-3-oxo-1-butenyl)amino]-3-isoxazolidinone, prodrug of cycloserine", *Int. J. Pharm.* 1984; **22**: 197–205.

[61] Murakami T, Yata N, Tamauchi H, Nakai J, Yamazaki M, Kamada A. "Studies on absorption promoters for rectal delivery preparations. I. Promoting efficacy of enamine derivatives of amino acids for the rectal absorption of β -lactam antibiotics in rabbits." *Chem. Pharm. Bull.*, 1981; **29**: 1998–2004.

- [62] Garro JC, Manzanares GD, Zamarbide GN, Ponce CA, Estrada MR, Jáuregui EA. “Geometrical isomerism, tautomerism and conformational charges of 2-propenal-3-amine in its neutral and protonated forms” *J. Mol. Struct. (Theochem)* 2001; **545**: 17–27.
- [63] Scott KR, Edafiogho IO, Richardson EL, Farrar VA, Moore JA, Tietz EI, Hinko CN, Chang H, El-Assadi A, Nicholson JM. “Synthesis and anticonvulsant activity of enaminones. 2. Further structure-activity correlations” *J. Med. Chem.*, 1993; **36**: 1947–1955.
- [64] Edafiogho IO, Hinko CN, Chang H, Moore JA, Mulzac D, Nicholson JM, Scott KR. “Synthesis and anticonvulsant activity of enaminones”, *J. Med. Chem.* 1992; **35**: 2798–2805.
- [65] Beckett AH, Kerridge KA, Clark PM, Smith WG. “Preparation and antibacterial activity of 2-phenacylpyridine and related ketones.” *J. Pharm. Pharmacol.*, 1955; **7**: 717–730.
- [66] Bell IM, Erb JM, Freidinger RM, Gallicchio SN, Guare JP, Guidotti MT, Halpin RA, Hobbs DW, Homnick CF, Kuo MS, Lis EV, Mathre DJ, Michelson SR, Pawluczyk JM, Pettibone DJ, Reiss DR, Vickers S, Williams PD, Woyden CJ. “Development of Orally Active Oxytocin Antagonists: Studies on 1-(1-{4-[1-(2-Methyl-1-oxidopyridin-3-ylmethyl)piperidin-4-yl]oxy}-2-methoxybenzoyl}piperidin-4-yl)-1,4-dihydrobenz[*d*][1,3]oxazin-2-one (L-372,662) and Related Pyridines”. *J. Med. Chem.*, 1998; **41**: 2146–2163.
- [67] Epifano F, Genovese S, Curini M. “Ytterbium triflate catalyzed synthesis of β -enaminones”, *Tetrahedron Lett.*, 2007; **48**: 2717–2720 and references cited therein.
- [68] Matosiuk D, Fidecka S, Antkiewicz-Michaluk L, Dybala I, Koziol AE. “Synthesis and pharmacological activity of new carbonyl derivatives of 1-aryl-2-iminoimidazolidine

Part 3. Synthesis and pharmacological activity of 1-aryl-5,6(1H)dioxo-2,3-dihydroimidazo[1,2-a]imidazoles”, *Eur. J. Med. Chem.*, 2002; **37**: 845–853.

[69] Sztanke K, Pasternak K, Rzymowska J, Sztanke M, Kandefer-Szerszeń M, Dybała I, Koziół AE. “Identification of antitumour activity of novel derivatives of 8-aryl-2,6,7,8-tetrahydroimidazo[2,1-c][1,2,4]triazine-3,4-dione and 8-aryl-4-imino-2,3,7,8-tetrahydroimidazo[2,1-c][1,2,4]triazin-3(6H)-one” *Bioorg. Med. Chem.*, 2007; **15**: 2837–2849.

[70] Rzadkowska M, Szacon E, Fidecka S, Kedzierska E, Matosiuk D. “Nowe pochodne 1-arylo-5,7 (1H) diokso-2,3-dihydroimidazo[1,2-a]pirymidyny i spos`b ich wytwarzania” PL Patent Appl. 2004; 366270.

[71] Wysocki W, Matosiuk D, Karczmarzyk Z, Rzadkowska M, Urbanczyk-Lipkowska Z. “6-Benzyl-7-hydroxy-1-(2-methoxyphenyl)-2,3-dihydro-1H,7H-imidazo[1,2-a]pyrimidin-5-one”, *Acta Crystallogr. E*, 2006; **E62**: o2548–o2550.

[72] Houlihan WJ. “1,2,3,3a,4,5-Hexahydropyrrolo[1,2-a]quinazolin-5-one and 1,2,3,4,5,6-hexahydro-4aH-pyrido[1,2-a]quinazoline-1,6-dione antihypertensives”, Patent Application, 1969; US 64-409949 19641109.

[73] Houlihan WJ. “Central nervous system active isoindoloquinazolines”, US Patent Application, 1970; US 66-591694 19661103.

[74] Tate JT, Lozier WW. “The dissociation of nitrogen and carbon monoxide by electron impact”, *Phys. Rev.*, 1932; **39**: 254–269.

[75] Lester GR. “Theory of mass spectra” *Brit. J. Appl. Phys.*, 1963; **14**: 414–421.

[76] a) de Hoffmann E, Stroobant V. “Mass Spectrometry Principles and Applications. Second Edition”, John Wiley & Sons Ltd, Chichester, Great Britain 2001, pp. 207–237.

b) Rosenstock HM, Wallenstein MB, Wahrhaftig AL, Henry Eyring H. "Absolute Rate Theory for Isolated Systems and the Mass Spectra of Polyatomic Molecules", *Proc. Nat. Acad. Sci.*, 1952; **38**: 667–678.

[77] Marcus RA. "Unimolecular dissociations and free radical recombination reactions", *J. Chem. Phys.*, 1952; **20**: 359–364.

[78] Stevenson DP. "Ionization and dissociation by electronic impact. The ionization potentials and energies of formation of sec.-propyl and tert.-butyl radicals. Some limitations on the method", *Discuss. Faraday Soc.*, 1951; **10**: 35–45.

[79] McLafferty FW. "Interpretation of Mass Spectra, Third Edition", University Science Books, USA, 1980. a) pp. 45-74; b) pp. 155–175.

[80] Sparkman OD. "Mass Spec Desk Reference. Second Edition" Global View Publishing, Pittsburgh, Pennsylvania 2006. p. 37.

[81] a) Bruins AP, Jennings KR, Evans S. "The observation of metastable transitions in a double-focussing mass spectrometer using a linked scan of the electric sector and magnetic sector fields." *Int. J. Mass Spectrom. Ion Phys.*, 1978; **26**: 395–404.

b) Veith HJ. "Mass analysed collisional activation mass spectra of organic salt cations produced by field desorption linked magnetic and electric field scanning" *Org. Mass Spectrom.*, 1978; **13**: 280–283.

[82] a) Shchapin I Yu, Feldman VI, Belevskii VN, Khoroshutin AV, Boblyyova AA. "Ion-molecule reactions and thermal isomerization of tricyclo[4.3.0.0^{3,7}]nona-4,8-diene radical cations to tricyclo[4.2.1.0^{4,9}]nona-2,7-diene radical cations in a γ -irradiated frozen Freon matrix" *Radiat. Phys. Chem.*, 1999; **55**: 559–563.

b) Stirk KM, Kiminkinen LKM, and Kenttämäa HI. "Ion-Molecule Reactions of Distonic Radical Cations", *Chem. Rev.*, 1992; **92**: 1649–1665.

- [83] a) Falick AM. In Applications of Mass Spectrometry to Organic Stereochemistry, Splitter JS, Tureček F (eds), VCH Publishers, Inc.: New York, 1994; p. 28.
- b) Beckey HD. “A new rule concerning comparative interpretation of electron impact and field ionization mass spectra”, *Int. J. Mass Spectrom. Ion Phys.*, 1968; **1**: 93–97.
- c) Beckey HD, Hey H, Levsen K, Tenschert G. “Study of the kinetics of fast unimolecular decomposition processes and of organic rearrangement reactions by field ionization mass spectrometry”, *Int. J. Mass Spectrom. Ion Phys.*, 1969; **2**: 101–123.
- [84] a) McLafferty FW, “Mass Spectrometric Analysis Broad Applicability to Chemical Research” *Anal. Chem.*, 1956; **28**: 306–316.
- b) Kingston DGI, Bursley JT, Bursley MM, “Intramolecular hydrogen transfer in mass spectra. II. McLafferty rearrangement and related reactions” *Chem. Rev.*, 1974; **74**: 215–242.
- [85] Winkler J, Grützmaier H-F. “Zum Mechanismus massenspektrometrischer Fragmentierungsreaktionen-II: Methoxygruppenwanderungen und Ringfragmentierungen in den Massenspektren der Methylather cyclischer Polyalkohole”, *Org. Mass. Spectrom.*, 1970; **3**: 1117-1138.
- [86] Bowie JH, Williams DH, Lawesson SO, Schroll G. “Studies in Mass Spectrometry. IX.¹ Mass Spectra of β -Diketones” *J. Org. Chem.*, 1966; **31**: 1384–1390.
- [87] Grützmaier H-F, Masur M. “Loss Of CO From The Molecular Ions of 2,2-Dimethyl-3,5-Hexandione”, *Org. Mass Spectrom.*, 1988; **23**: 223–227.
- [88] Wang X, Holmes JL. “The unexpected decarbonylation of ionized 2,3-pentanedione and related diketones”, *Int. J. of Mass Spectrom.*, 2006; **249–250**: 222–229.
- [89] a) Linstrom PJ, Mallard WG, Eds. *NIST Chemistry Webbook*, NIST Standard Reference Database Number 69, January 2009, National Institute of Standards and Technology, Gaithersburg MD, 20899 (<http://webbook.nist.gov>).

b) Beynon JH, Lester GR, Williams AE. "Some Specific Molecular Rearrangements in the Mass Spectra of Organic Compounds", *J. Phys. Chem.*, 1959; **63**: 1861–1868.

c) Russell DH, Gross ML, Nibbering NMM. "Keto-Enol Tautomerism of Gas-Phase Ions. Structure of Reactive C₆H₆O Radical Cations", *J. Am. Chem. Soc.*, 1978; **100**: 6133–6137.

[90] Tajima S, Tobita S, Mitani M, Akuzawa K, Sawada H, Nakayama M. "Loss of CO from the Molecular Ions of *o*-, *m*- and *p*-Anisoyl Fluorides, CH₃OC₆H₄COF, with Fluorine Atom Migration", *Org. Mass Spectrom.*, 1991; **26**: 1023–1026.

[91] Tajima S, Siang LF, Fujishige M, Nakajima S, Sekiguchi O. "Collision-induced dissociation spectra versus collision energy (collision-induced dissociation curve) using a quadrupole ion trap mass spectrometer. II. Loss of CO from ionized *o*-, *m* and *p*-anisoyl fluoride, CH₃OC₆H₄COF⁺" *J. Mass Spectrom.*, 2000; **35**: 1144–1146.

[92] Drewello T, Nikolaus Heinrich N, Wilfried P. M. Maas WPM, Nibbering NMM, Weiske T, Schwarz H. "Generation of the distonic ion CH₂NH₃⁺: nucleophilic substitution of the ketene cation radical by ammonia and unimolecular decarbonylation of ionized acetamide", *J. Am. Chem. Soc.*, 1987; **109**: 4810–4818.

[93] Tobita S, Ogino K, Ino S, Tajima S. "On the mechanism of CO loss from the metastable molecular ion of dimethyl malonate", *Int. J. Mass Spectrom. Ion Process.*, 1988; **85**: 31–42.

[94] Audier HE, Dupin JF, Fétizon M, Hoppilliard T. "Mass Spectra of Aromatic Epoxides: Cases of Alkyl and Aryl Migration", *Tetrahedron Lett.*, 1966; **7**: 2077–2081.

[95] Fetizon M, Henry Y, Aranda G, Audier H-E, De Luzes H. "Spectrometrie De Masse Des Epoxydes Phenyles-II", *Org. Mass Spectrom.*, 1974; **8**: 201–216.

- [96] Ardanaz C, Kavka J, Guidugli FH, Favretto D, Traldi P. “An Unexpected Methyl Loss Observed in Electron Ionization of Chalcones”, *Rapid Commun. Mass Spectrom.*, 1998; **12**: 139–143.
- [97] a) Ronayne J, Williams DW, Bowie JH. “Studies in Mass Spectrometry. XIX.1 Evidence for the Occurrence of Aromatic Substitution Reactions upon Electron Impact”, *J. Am. Chem. Soc.*, 1966; **88**: 4980–4984.
b) Ardanaz CE, Traldi P, Vettori U, Kavka J, Guidugli F. “The Ion-trap Mass Spectrometer in Ion Structure Studies. The Case of $[M-H]^+$ Ions from Chalcone”, *Rapid Commun. Mass Spectrom.*, 1991; **5**: 5–10.
- [98] a) Budzikiewicz H, Brauman JI, Djerassi C. “Massenspektrometrie und Ihre anwendung auf strukturelle und stereochemische Probleme—LXVII: Zum retro-Diels-Alder-zerfall organischer Moleküle unter Elektronenbeschuss”, *Tetrahedron*, 1965; **21**: 1855–1879.
b) Tureček F, Hanuš V. “Retro-Diels-Alder reaction in mass spectrometry”, *Mass Spectrom. Rev.*, 1984; **3**: 85–152.
- [99] Bohlmann F, Fischer C-H, Förster J, Mather W, Schwarz H. “Untersuchungen zum Einfluss der Stereochemie auf die Elektronenstossinduzierte “Retro-Diels-Alders”-Reaktion”, *Org. Mass Spectrom.*, 1975; **10**: 1141–1146.
- [100] Mandelbaum A. “Stereochemical Effects in the Retro-Diels-Alder Fragmentation” in *Applications of Mass Spectrometry to Organic Stereochemistry*, Edited by Splitter F, Tureček F. VCH Publishers Inc New York USA, 1994, pp. 299–324.
- [101] Pihlaja K, Ovcharenko VV, Stájer G. “Stereospecific Fragmentation Processes in Cycloalkane/Cycloalkene-Fused Isomers of Saturated Pyrrolo[2,1-*b*][1,3]oxazin-6-one Derivatives”, *J. Am. Soc. Mass Spectrom.*, 1999; **10**: 393–401.

- [102] Denekamp C, Weisz A, Mandelbaum A. “Stereospecificity and Concertedness of Retro-Diels-Alder Fragmentation in Some Diester Systems Upon Chemical Ionization”, *J. Mass Spectrom.*, 1996; **31**: 1028–1032.
- [103] Eguchi S. “Hydrogen Transfer in the Retro Diels-Alder Fragmentation of Oxygen-Containing Heterocyclic Compounds. II – Chromones”, *Org. Mass Spectrom.*, 1979; **14**: 345–349.
- [104] Morlender-Vais N, Mandelbaum A. “Stereospecific Retro-Diels–Alder Fragmentation of Stereoisomeric 3-Methoxy- and 3,6-Dialkoxytricyclo [6.2.2.0^{2,7}] dodeca-9-enes upon Electron Ionization”, *J. Mass Spectrom.*, 1998; **33**: 229–241.
- [105] Ovcharenko VV, Pihlaja K, Stájer G. “Stereospecific Fragmentations in the Mass Spectra of Stereoisomeric Isoindoloquinazolines”, *J. Am. Soc. Mass Spectrom.*, 2003; **14**: 1049–1056.
- [106] Schamp N, Vandewalle M. “Organic mass spectrometry. I. Acyclic 1,3-diketones”, *Bull. Soc. Chim. Belges*, 1966; **75**: 539–550.
- [107] Vandewalle M, Schamp N, De Wilde H. “Studies in organic mass spectrometry. III. 1,3-Cyclohexanediones”, *Bull. Soc. Chim. Belges*, 1967; **76**: 111–122.
- [108] Vandewalle M, Schamp N, De Wilde H. “Studies in organic mass spectrometry. IV. Fragmentation of 2-alkyl-1,3-cyclohexanediones”, *Bull. Soc. Chim. Belges*, 1967; **76**: 123–132.
- [109] Bowie JH, Grigg R, Lawesson SO, Schroll G, Williams DH. “Rearrangement reactions of some simple ketones and esters upon electron impact”, *Chem. Commun.*, 1965; **17**: 403.

- [110] Zamir L, Jensen BS, Larsen E. "An Investigation Of Tautomeric Equilibria By Means Of Mass Spectrometry", *Org. Mass Spectrom.*, 1969; **2**: 49–61.
- [111] Wood KV, McLuckey SA, Cooks RG. "The effect of ion source temperature on the fragmentation of 2-pentanone", *Org. Mass Spectrom.*, 1986; **21**: 11–14.
- [112] Allegretti PE, Schiavoni MM, Di Loreto HE, Furlong JJP, Della Védova CO. "Separation of keto-enol tautomers in β -ketoesters: a gas chromatography-mass spectrometric study", *J. Mol. Struct.*, 2001; **560**: 327–335.
- [113] Levsen K, Schwarz H. "Gas-phase chemistry of collisionally activated ions", *Mass Spectrom. Rev.*, 1983; **2**: 77–148.
- [114] Allegretti PE, Gavernet L, Castro EA, Furlong JJP. "Spectrometric and theoretical evidences for the occurrence of tautomeric structures of selected ketones", *J. Mol. Struct. (Theochem.)*, 2000; **532**: 139–142.
- [115] Allegretti PE, Castro EA, Furlong JJP. "Tautomeric equilibrium of amides and related compounds: theoretical and spectral evidences", *J. Mol. Struct. (Theochem.)*, 2000; **499**: 121–126.
- [116] Allegretti PE, Cortizo MS, Guzmán C, Castro EA, Furlong JJP. "Tautomerism of lactones and related compounds. Mass spectrometric data and theoretical calculations", *ARKIVOC*, 2003; (x): 24–31.
- [117] a) MacLeod JK, Thomson JB, Djerassi C. "Mass spectrometry in structural and stereochemical problems—CXXII Possible operation of tautomerism before and after electron-impact induced fragmentation of molecular ions" *Tetrahedron*, 1967; **23**: 2095–2103.

b) Budzikiewicz H, Fenselau C, Djerassi C. "Mass spectrometry in structural and stereochemical problems—XCII: Further studies on the McLafferty rearrangement of aliphatic ketones", *Tetrahedron*, 1966; **22**: 1391–1398.

[118] Uggerud E, Drewello T, Schwarz H, Nadler EB, Biali SE, Rappoport Z. "The Gas-Phase Ion Chemistry Of Crowded, Triaryl-Substituted Keto/Enol Pairs", *Int. J. Mass Spectrom. and Ion Process.*, 1986; **71**: 287–302.

[119] Goldberg NN, Barkley LB, Lewine R. "The Synthesis of Heterocyclic Nitrogen-containing Ketones. I. Ketones Derived from 2-Picoline", *J. Am. Chem. Soc.*, 1951; **73**: 4301–4303.

[120] Beckett AH, Kerridge KA. "Some alkyl and acyl derivatives of 2-phenacylpyridine", *J. Chem. Soc.*, 1954: 2948–2951.

[121] Sztanke K, Matosiuk D, Fidecka S. "Preparation of new 3-hydroxy-4-oxo-8-aryl-7,8-dihydro-6H-imidazo[2,1-c][1,2,4]triazines as antinociceptive agents." PL196752 (B1), 20080131 Patent written in Polish (2008). Application: PL 2003-361373 20030721.

[122] Sohár P, Csámpai A, Szabó AE, Stájer G. "Preparation and structure of pyrrolo- and isoindoloquinazolinones", *J. Mol. Struct.*, 2004; **694**: 139–147.

[123] Szatmári I, Hetényi A, Lázár L, Fülöp F. "Transformation reactions of the Betti base analog aminonaphthols", *J. Heterocyclic Chem.*, 2004; **41**: 367–373.

[124] Heydenreich M, Koch A, Klod S, Szatmári I, Fülöp F, Kleinpeter E. "Synthesis and conformational analysis of naphth[1',2':5,6][1,3]oxazino[3,2-c][1,3]benzoxazine and naphth[1',2':5,6][1,3]oxazino[3,4-c][1,3]benzoxazine derivatives", *Tetrahedron*, 2006; **62**: 11081–11089.

- [125] Fukata G, O'Brien C, More O'Ferrall RA. "Enamine–imine tautomerism of benzyl- and phenacyl-quinolines", *J. Chem. Soc., Perkin Trans. 2* 1979; **6**: 792–795.
- [126] Bursley MM, McLafferty FW. "Substituent Effects in Unimolecular Ion Decompositions. II. A Linear Free Energy Relationship between Acyl Ion Intensities in the Mass Spectra of Substituted Acylbenzenes^{1,2}", *J. Am. Chem. Soc.*, 1966; **88**: 529–536.
- [127]. Salman RS, Saleh NAI. "Mass Spectral Study of Tautomerism in Some Schiff Bases", *Spectros. Lett.*, 1998; **31**: 1179–1189.
- [128]. Salman RS, Kamounah FS. "Mass Spectral Study of Tautomerism in Some 1-Hydroxy-2-naphthaldehyde Schiff Bases", *Spectros. Lett.*, 2002; **35**: 327–335.
- [129] Holmes JL, Lossing FP. "Gas-phase heats of formation of keto and enol ions of carbonyl compounds", *J. Am. Chem. Soc.* 1980; **102**: 1591–1595.
- [130] Zakrzewska A, Gawinecki R, Kolehmainen E, Ośmiałowski B. "¹³C-NMR Based Evaluation of the Electronic and Steric Interactions in Aromatic Amines", *Int. J. Mol. Sci.* 2005; **6**: 52–62.
- [131] Pihlaja K, Ovcharenko VV, Stájer G. "Stereospecific Fragmentation Processes in Cycloalkane/Cycloalkene-Fused Isomers of Saturated Pyrrolo[2,1-*b*][1,3]oxazin-6-one Derivatives", *J. Am. Soc. Mass Spectrom.*, 1999; **10**: 393–401.
- [132] Pihlaja K, Himottu M, Fülöp F, Huber I, Bernáth G, Ovcharenko V, "Stereochemical Effects in the Electron Ionization Mass Spectra of Cycloalkane-(alkene)-fused 2,3-Dihydro-5*H*-thiazolo[3,2-*a*]pyrimidine-5-ones and 3,4-Dihydro-2*H*,6*H*-pyrimido[2,1-*b*]thiazin-6-ones", *Rapid Comm. Mass Spectrom.*, 1996; **10**: 721–726.

[133] Khoury PR, Goddard JD, Tam W. “Ring strain energies: substituted rings, norbornanes, norbornenes and norbornadienes”, *Tetrahedron*, 2004; **60**: 8103–8112.

[134] Weisz A, Mandelbaum A. “One and two hydrogen atom migrations in the retro-Diels-Alder fragmentation of norbornene and bicyclo [2.2.2] octene derivatives under electron impact”, *Org. Mass Spectrom.*, 1989; **24**: 37–40.

[135] Partanen T, Vainiotalo P, Stájer G, Bernáth G, Pihlaja K. “Electron Impact and Chemical Ionization Mass Spectra of Norbornane/ene di-*exo* and di-*endo*-fused 1,3-oxazin-2(1*H*)-ones and 1,3-oxazine-2(1*H*)-thiones”, *Org. Mass Spectrom.*, 1990; **25**: 615–619.

[136] Mandelbaum A, Weisz A, Karpati A. “Non-stereospecific hydrogen migrations accompanying Retro-Diels-Alder fragmentations in some adducts of cyclopentadiene and 1,3-cyclohexadiene under electron impact”, *Int. J. Mass Spectrom. Ion Phys.* 1983; **47**: 415–418.

[137] Joutsiniemi K, Vainiotalo P, Pihlaja K, Lázár L, Fülöp F, Bernáth G. “Electron Ionization Mass Spectrometry of Some Substituted, Stereoisomeric, Partly Saturated 1,3- and 3,1-Benzoxazino-1,3-benzoxazines“, *Rapid Comm. Mass Spectrom.*, 1995; **9**: 1035–1037.